AD-A156 469 FIBER OPTIC GRADIENT HYDROPHONE CONSTRUCTION AND CALIBRATION FOR SEA TRIAL(U) NAVAL POSTGRADUATE SCHOOL MONTEREY CA G E MACDONALD MAR 85 1/2

UNCLASSIFIED F/G 17/1 NL

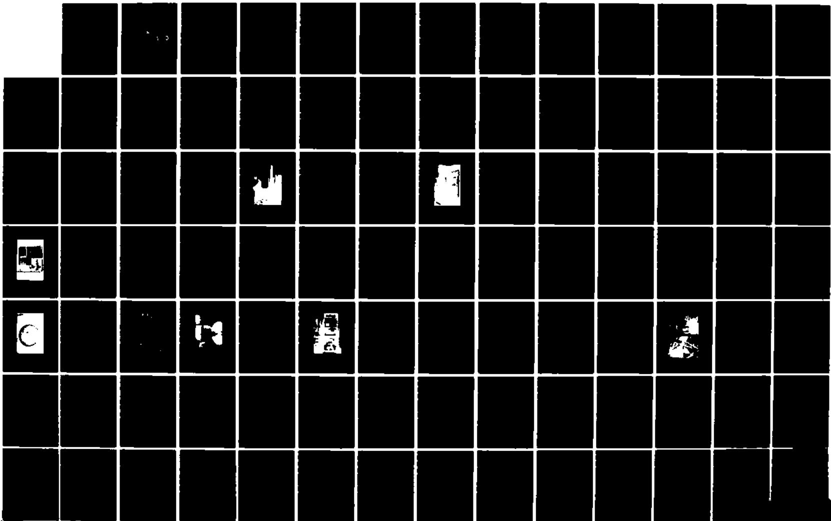

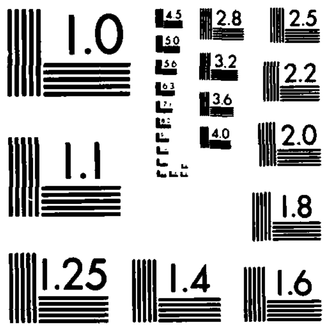

MICROCOPY RESOLUTION TEST CHART
NATIONAL BUREAU OF STANDARDS-1963-A

AD-A156 469

NAVAL POSTGRADUATE SCHOOL

Monterey, California

DTIC
S ELECTE D
JUL 1 1 1985
G

THESIS

FIBER OPTIC GRADIENT HYDROPHONE
CONSTRUCTION AND CALIBRATION FOR SEA TRIAL

by

Glenn E. MacDonald

March 1985

Thesis Advisor: S. L. Garrett

DTIC FILE COPY

Approved for public release; distribution unlimited

85 6 19 023

DISCLAIMER NOTICE

THIS DOCUMENT IS BEST QUALITY PRACTICABLE. THE COPY FURNISHED TO DTIC CONTAINED A SIGNIFICANT NUMBER OF PAGES WHICH DO NOT REPRODUCE LEGIBLY.

UNCLASSIFIED

SECURITY CLASSIFICATION OF THIS PAGE (When Data Entered)

REPORT DOCUMENTATION PAGE		READ INSTRUCTIONS BEFORE COMPLETING FORM
1. REPORT NUMBER	2. GOVT ACCESSION NO. AD-A156	3. RECIPIENT'S CATALOG NUMBER 469
4. TITLE (and Subtitle) Fiber Optic Gradient Hydrophone Construction and Calibration for Sea Trial		5. TYPE OF REPORT & PERIOD COVERED Master's Thesis March 1985
		6. PERFORMING ORG. REPORT NUMBER
7. AUTHOR(s) Sean T. McDonald		8. CONTRACT OR GRANT NUMBER(s)
9. PERFORMING ORGANIZATION NAME AND ADDRESS Naval Postgraduate School Monterey, California 93943		10. PROGRAM ELEMENT, PROJECT, TASK AREA & WORK UNIT NUMBERS
11. CONTROLLING OFFICE NAME AND ADDRESS Naval Postgraduate School Monterey, California 93943		12. REPORT DATE March 1985
		13. NUMBER OF PAGES 124
14. MONITORING AGENCY NAME & ADDRESS (if different from Controlling Office)		15. SECURITY CLASS. (of this report)
		15a. DECLASSIFICATION/DOWNGRADING SCHEDULE

16. DISTRIBUTION STATEMENT (of this Report)

Approved for public release; distribution unlimited

17. DISTRIBUTION STATEMENT (of the abstract entered in Block 20, if different from Report)

18. SUPPLEMENTARY NOTES

19. KEY WORDS (Continue on reverse side if necessary and identify by block number)

Fiber optic sensor; hydrophone; acoustic hydrophone; Mach-Zehnder interferometer; pressure gradient hydrophone; interferometric sensor; directional dipole hydrophone.

20. ABSTRACT (Continue on reverse side if necessary and identify by block number)

A Mach-Zehnder interferometric fiber optic gradient hydrophone, for operation at 632.8 nm wavelength, was designed and constructed for testing in the laboratory. Two individual fiber optic hydrophone sensing coils with [illegible] of fiber each were wound and potted on an open mandrel and their respective sensitivities were measured. They then were mounted on a rigid bar, separated by [illegible], to form a gradient hydrophone. The sensitivity of the [illegible] was obtained in a calibrator which allowed the

DD FORM 1 JAN 73 1473 EDITION OF 1 NOV 65 IS OBSOLETE

S/N 0102-LF-014-6601

UNCLASSIFIED

SECURITY CLASSIFICATION OF THIS PAGE (When Data Entered) coil pair to be rotated 360°.

Since the laboratory interferometric system was too large to be used in the sea trial tests, a second interferometric system, operating at [illegible] nm wavelength, using diode lasers was designed and constructed. This was mounted in an experimental apparatus designed and constructed for sea trial. A sea trial of a standard Navy type [illegible] hydrophone was conducted to test the effectiveness of the experimental apparatus. The results of the laboratory tests are summarized and discussed and recommendations for further studies are presented.

Accession For	
NTIS GRA&I	X
DTIC TAB	☐
Unannounced	☐
Justification	
By	
Distribution/	
Availability Codes	
Dist	Avail and/or Special
A/1	

Approved for Public Release, Distribution Unlimited.

Fiber Optic Gradient Hydrophone Construction and Calibration for Sea Trial

by

Glenn E. MacDonald
Lieutenant, United States Navy
B.S.M.E., University of Mississippi, 1978

Submitted in partial fulfillment of the requirements for the degree of

MASTER OF SCIENCE IN SYSTEMS TECHNOLOGY

(Antisubmarine Warfare)

FROM THE

NAVAL POSTGRADUATE SCHOOL
March 1985

Author ______________________________
Glenn E. MacDonald

Approved by: ______________________________
Steven L. Garrett, Thesis Advisor

____
Edward F. Carome, Co-Advisor

____
Robert N. Forrest, Chairman, Antisubmarine Warfare Academic Group

____
David A. Schrady, Academic Dean

ABSTRACT

A Mach-Zehnder interferometric fiber optic gradient hydrophone, for operation at 632.8 nm wavelength, was designed and constructed for testing in the laboratory. Two individual fiber optic hydrophone sensing coils with 10 m of fiber each were wound and potted on an epoxy mandrel and their respective sensitivities were obtained. They then were mounted on a rigid bar, separated by 10 cm, to form a gradient hydrophone. The sensitivity of the this arrangement then was obtained in a calibrator which allowed the coil pair to be rotated 360 deg.

Since the laboratory interferometric system was too large to be used in the sea trial tests, a second interferometric system, operating at 830 nm wavelength, using diode lasers was designed and constructed. This was mounted in an experimental apparatus designed and constructed for sea trial. A sea trial of a standard Navy type DIFAR hydrophone was conducted to test the effectiveness of the experimental apparatus. The results of the laboratory tests are summarized and discussed and recommendations for further studies are presented.

TABLE OF CONTENTS

I. INTRODUCTION 12
A. BACKGROUND 12
B. PURPOSE OF STUDY 13
C. FORMAT OF REPORT 14
II. THEORY 18
A. CONVENTIONAL GRADIENT HYDROPHONE 18
B. CALIBRATION OF GRADIENT HYDROPHONE 23
C. FIBER OPTIC ACOUSTIC SENSOR CONCEPTS 24
III. EXPERIMENTAL APPARATUS 28
A. ACOUSTIC CALIBRATOR 28
B. 632.8 nm INTERFEROMETRIC SYSTEM 30
1. Laser Source 33
2. Fiber Specifications 33
3. Couplers 35
4. Piezoelectric Phase Shifter 36
5. Polarization Controller 36
6. Photodetector 36
C. 830 nm INTERFEROMETRIC SYSTEM 37
1. Laser Source 37
2. Fiber Specifications 44
3. Couplers 45
a. Coupler 2X2 45
b. Coupler 3X3 45

4. Photodetector 46

D. FIBER PREPARATION AND SPLICING 46

E. MANDREL CONSTRUCTION 49

F. GRADIENT SENSOR CONSTRUCTION 51

1. Red Gradient Hydrophone 51

2. Infrared Gradient Hydrophone 54

G. INSTRUMENTATION AND DATA ACQUISITION SYSTEM . . 57

1. Computer HP-85F 57

2. Sythesizer/Function Generator HP-3325A . . . 57

3. Spectrum Analyzer HP-3582A 60

4. Oscilloscope COS5060 60

5. Digital Multimeter HP-3478A 61

6. Bipolar Power Amplifier POW35-1A 61

7. Digital Multimeter HP-3456A 61

8. Standard Hydrophone LC-10 62

9. Transducer J-11 62

H. SEA TRIAL EXPERIMENTAL APPARATUS 62

IV. EXPERIMENTAL PROCEDURE AND RESULTS 69

A. INTERFEROMETER CHARACTERISTICS 69

B. BESSEL FUNCTION REPONSE 75

C. CALIBRATOR CHARACTERISTICS 78

D. INDIVIDUAL SENSOR SENSITIVITY 85

E. GRADIENT SENSOR SENSITIVITY 89

F. ANALYSIS 94

G. DIFAR SEA TRIAL ANALYSIS 101

V. CONCLUSIONS AND RECOMMENDATIONS 108

APPENDIX A: DATA ACQUISITION PROGRAM 110
APPENDIX B: SINGLE SENSOR DATA 114
APPENDIX C: GRADIENT SENSOR DATA 116
APPENDIX D: DIFAR TRANSDUCER DATA 117
LIST OF REFERENCES 120
BIBLIOGRAPHY 122
INITIAL DISTRIBUTION LIST 123

LIST OF TABLES

I. Piezoelectric Sensitivity 74

II. Calibrator Speed of Sound 79

III. Standing Wave Acoustic Field for 683 Hz 80

IV. Bessel Function Maxima & Minima 87

V. Individual Fiber Optic Hydrophone Sensitivity . 89

VI. Gradient Hydrophone Dipole Data 95

LIST OF FIGURES

1.1. Fiber Optic Interferometric Hydrophone 15

1.2. Fiber Optic Interferometric Gradient Hydrophone . 16

2.1. Directivity Pattern of Pressure Gradient Hydrophone 19

2.2. Geometry Used in Deriving Sensing Characteristics of Acoustic Dipole (Pressure Gradient) 21

2.3. Pressure Distribution as Function of Distance from Null Pressure Point 22

3.1. Photograph of Acoustic Calibrator 29

3.2. Schematic of 632.8 nm Mach-Zehnder Interferometer 31

3.3. Photograph of 632.8 nm Interferomtric System . . 32

3.4. ITT Single-mode Fiber T-1601 34

3.5. Schematic of 830 nm Mach-Zehnder Interferometer . 38

3.6. Photograph of 830 nm Interferometric System . . . 39

3.7. Schematic of Laser Diode Power Supply 41

3.8. FU-21LD-54 Laser Diode Power Curve 42

3.9. FU-21LD-66 Laser Diode Power Curve 43

3.10. Representation of Proper and Improper Cleaves . . 48

3.11. Representation of Proper and Improper Fuse Alignments 50

3.12. Cross Section of Fiber Optic Mandrel 52

3.13. Photograph of a Fiber Optic Mandrel 53

3.14. Photograph of 632.8 nm Lradient Hydrophone . . . 55

3.15. Photograph of 830 nm Gradient Hydrophone 56

3.16. Photograph of Instrumentation Package 58

3.17. Block Diagram of Instrumentation System 59
3.18. Photograph of Sea Trial Apparatus 64
3.19. Schematic of Sea Trial Apparatus 65
3.20. Schematic of Quad-Amplifier Circuit 67
4.1. Block Diagram of Instrumentation System 70
4.2. Piezoelectric Phase Modulator Response 72
4.3. Piezoelectric Sensitivity Phase Modulator Frequency Reponse 73
4.4. Standing Wave Acoustic Field for 683 Hz 81
4.5. Standing Wave Acoustic Field for 517 Hz 82
4.6. Standing Wave Acoustic Field for 432 Hz 83
4.7. Standing Wave Acoustic Field for 218 Hz 84
4.8. Single Hydrophone Sensitivity at 517 Hz 86
4.9. Block Diagram of Instrumentation System 91
4.10. Fiber Optic Gradient Hydrophone Dipole Pattern . 96
4.11. Fiber Optic Gradient Hydrophone Dipole Pattern . 97
4.12. Fiber Optic Gradient Hydrophone Position in Calibrator 98
4.13. Depth Dependency 102
4.14. Block Diagram of Instrumentation Package . . . 104
4.15. DIFAR Cosine Dipole Pattern 105
4.16. DIFAR Sine Dipole Pattern 106
4.17. DIFAR Omni Dipole Pattern 107

ACKNOWLEDGEMENTS

I want to express my heartfelt gratitude to those who through assistance and encouragement made this project possible. First, to Drs. Edward F. Carome and Steven L. Garrett for their untiring efforts and patience so that this project could reach fruition. Also a special thanks to the crew of the R/V Acañia for the help and support for the sea trial part of the project. To the best machinist without whose untiring effort most of the equipment would not have been possible a special thanks to Bob Moeller. And to my wife, Madonna, for the special assistance in proof reading the report, a very special thanks.

I would like to dedicate this work to three very special people with love; my wife Madonna, my son Grant and my daughter Katrina, without whose support and love this work would not have been possible.

I. INTRODUCTION

A. BACKGROUND

The concept of light transmission in a dielectric medium, was first demonstrated before the Royal Society in 1854 by John Tyndell. Alexander Graham Bell, in 1880, proposed use of light waves for telecommunications [Ref.1]. At the birth of optical fiber technology, more than fifteen years ago, the light losses sustained in the fiber were close to 1000 dB/km [Ref.2]. By 1970, research in England had lowered this to 150 dB/km. In 1970, researchers in both the United States and Japan lowered the losses in optical fiber to 20 dB/km [Ref.3].

During the mid 1970's, advancements were made in material processing, fabrication of optical fibers, coupling devices, cables, sources and detectors. The loss in the single-mode optical fiber is now as low as to 0.01 dB/km. This is very close to the intrinsic loss expected, for pure SiO_2.

As technology matured it was found that optical fiber could be used as a transduction element as well as a transmitter of information. Various physical perturbations may be sensed, such as acoustic, magnetic, thermal, linear and rotational motion, strain, etc. [Ref.4]. Optical fibers sensors offer the potential for increased sensitivity as compared to more conventional technology and may be configured in arbitrary shapes. Additional advantages of lightweight and low cost construction, contribute to the fact that more than 60 different types of optical fiber sensors are now being investigated or are already in use.

These sensors range from simple on/off fluid level indicators to the more sophisticated interferometric configurations. The individual devices are usually either amplitude or phase (interferometric) sensors. In the amplitude case, the physical perturbation interacts with the fiber to directly modulate the intensity of the light in the fiber. The perturbation modulates the optical phase of the coherent light in the fiber; using an interferometric system, the optical phase modulation is converted to optical intensity modulation.

In Chapter II the theory of light propagation, phase modulation, conversion to intensity modulation, interferometric systems and gradient sensors will be discussed in detail.

B. PURPOSE OF STUDY

In 1977, the feasibility of a fiber optic acoustic sensor for underwater sound reception was demonstrated [Ref. 5 & 6]. Significant progess has been achieved since in the areas of enchancement of acousto-optic transduction mechanisms, component development and sensor packaging for the fiber optic sensor [Ref. 2 & 7].

A block diagram of a basic fiber optic interferometric system is shown in Figure 1.1. This system is an optical interferometer and has a laser source, input/output couplers, a sensor arm, a reference arm, photodetectors and a demodulation (signal processing) unit.

Taking advantage of the intrinsic dual path nature of this type of system, by using each arm as a separate sensor in a differential design, a fiber optic gradient hydrophone was developed and tested in an earlier phase of the present project [Ref. 8]. The geometric confriguration used is shown in Figure 1.2.

The aim of research described in this thesis was to package the fiber optic gradient interferometric system [Ref. 8 and 9], obtain sensitivity data in the laboratory, obtain sea trial data, and compare the results to those obtained with a conventional piezoelectric gradient hydrophone of the type currently used by the Navy in directional sonobouy applications.

C. FORMAT OF THE REPORT

The following topics are considered in Chapter II: the theoretical basis of the conventional gradient hydrophone operation, the calibration of gradient hydrophones, and the behavior of the interferometric type sensors used in this

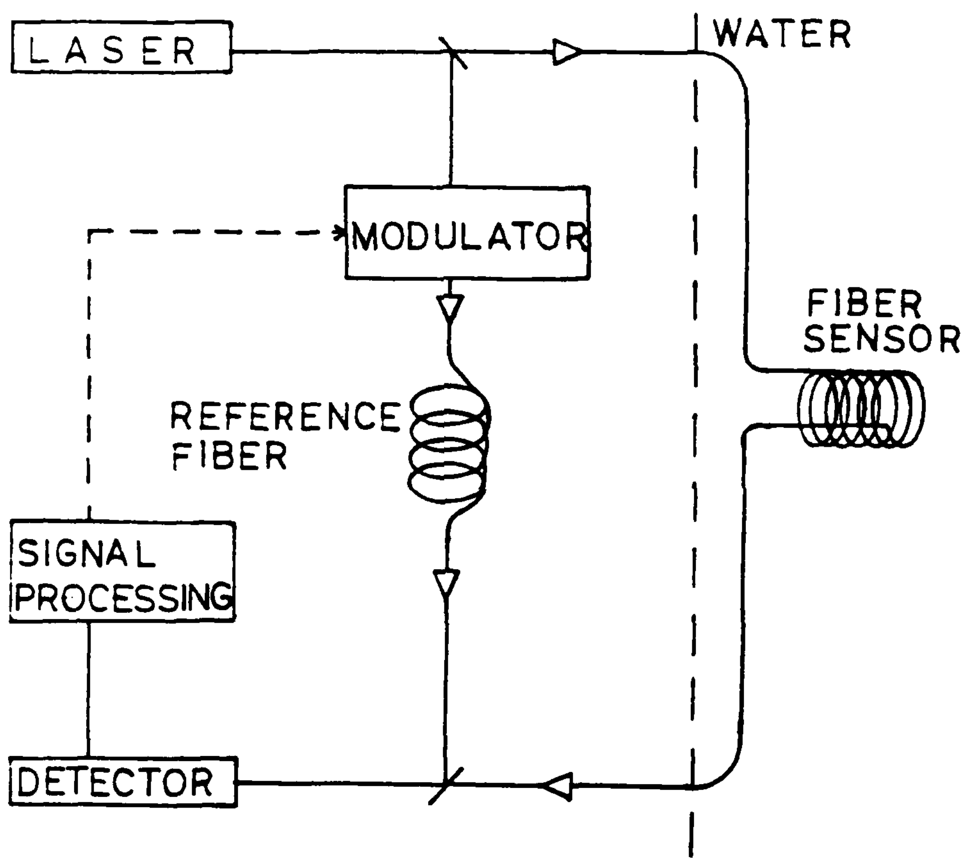

Figure 1.1 Fiber Optic Interferometric Hydrophone

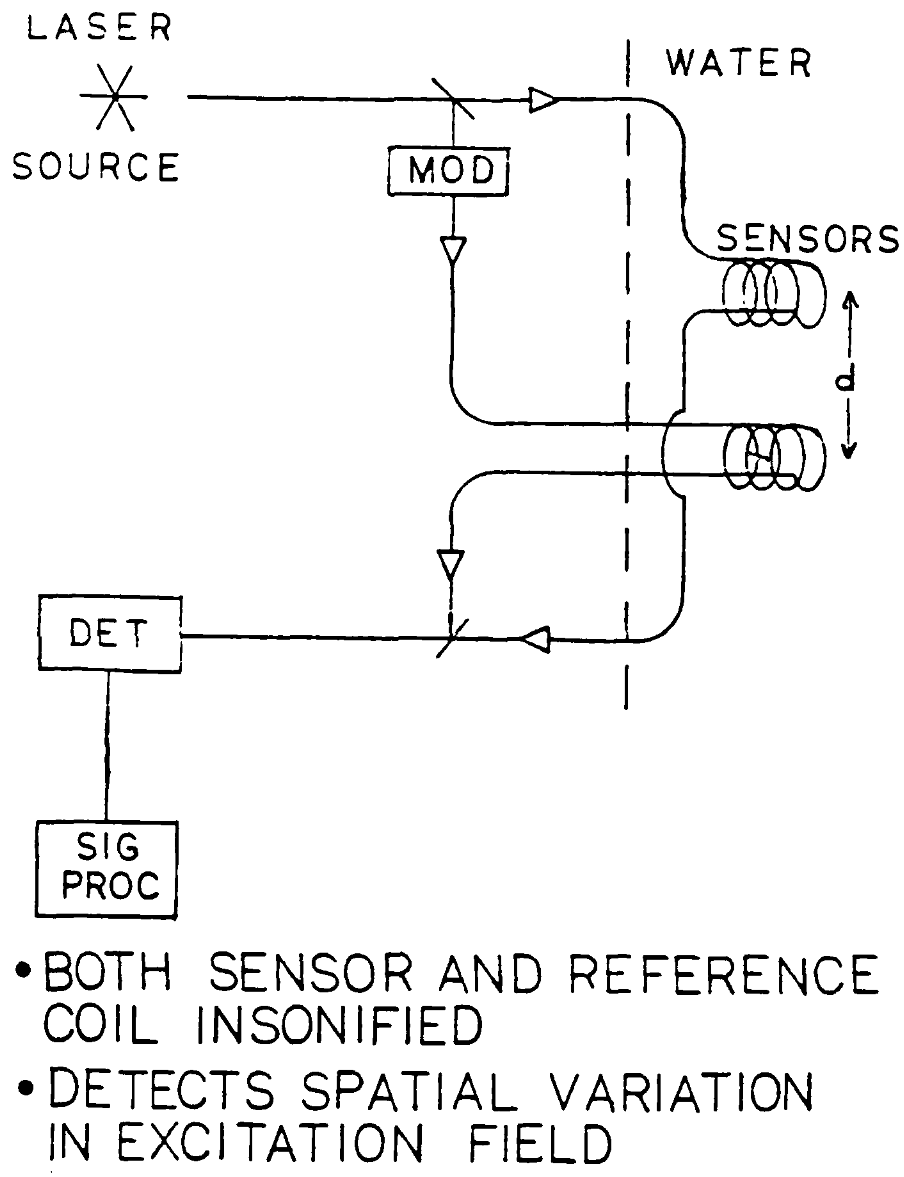

Figure 1.2 Fiber Optic Interferometric Gradient Hydrophone

study. Details of the construction of the fiber optic sensor systems, a calibrator for gradient hydrophones, and the sea trial apparatus are presented in Chapter III. Specifications of the instrumentation used for data acquisition, also are listed in Chapter III. The experimental procedures used to establish the characteristics of the system, data acquisition techniques, and the results of sensitivity measurements on individual and gradient hydrophones are discussed in Chapter IV. Analysis of the data and interpretation of the results are also presented in Chapter IV. Chapter V contains concluding remarks and recommendations for further work. Appendix A is a copy of the computer program used to gather and process interferometer data for the PZT and fiber optic gradient hydrophones. Appendix B lists data obtained for single element fiber optic hydrophones operating at He-Ne wavelength, i.e. 632.8 nanometers. Appendix C lists data obtained for a dual element 632.8 nm fiber optic gradient hydrophone. Appendix D contains data obtained in a sea trial of a piezoelectric DIFAR gradient hydrophone.

II. THEORY

A. CONVENTIONAL GRADIENT HYDROPHONE[1]

In many instances, information on the direction of incidence of an acoustic signal is required, in addition to its acoustic pressure level. Usually this is achieved by multiple hydrophones which are spatially distributed in a well defined fashion, e.g., a vertical or horizontal line array. The simplest of these directional arrays consists of a pair of omnidirectioal hydrophones that form a dipole sensor the output of which is the difference of the individual hydrophone outputs. The electrical output of a piezoelectric dipole pair is proportional to the pressure gradient of the sound field as described by Mills [Ref. 8]. Pressure gradient hydrophones have a dipole, or figure-eight, directivity pattern as sketched in Figure 2.1, hence they are bidirectional. Assuming the hydrophone size is small compared to the acoustic wavelength λ of the sound field, the dipole response when oriented at any angle θ relative to an incoming plane pressure wave is proportional to $\cos\theta$.

The fiber optic gradient hydrophone considered in this

---

[1]This chapter is a summary of the discussion presented by Mills in Ref. 8.

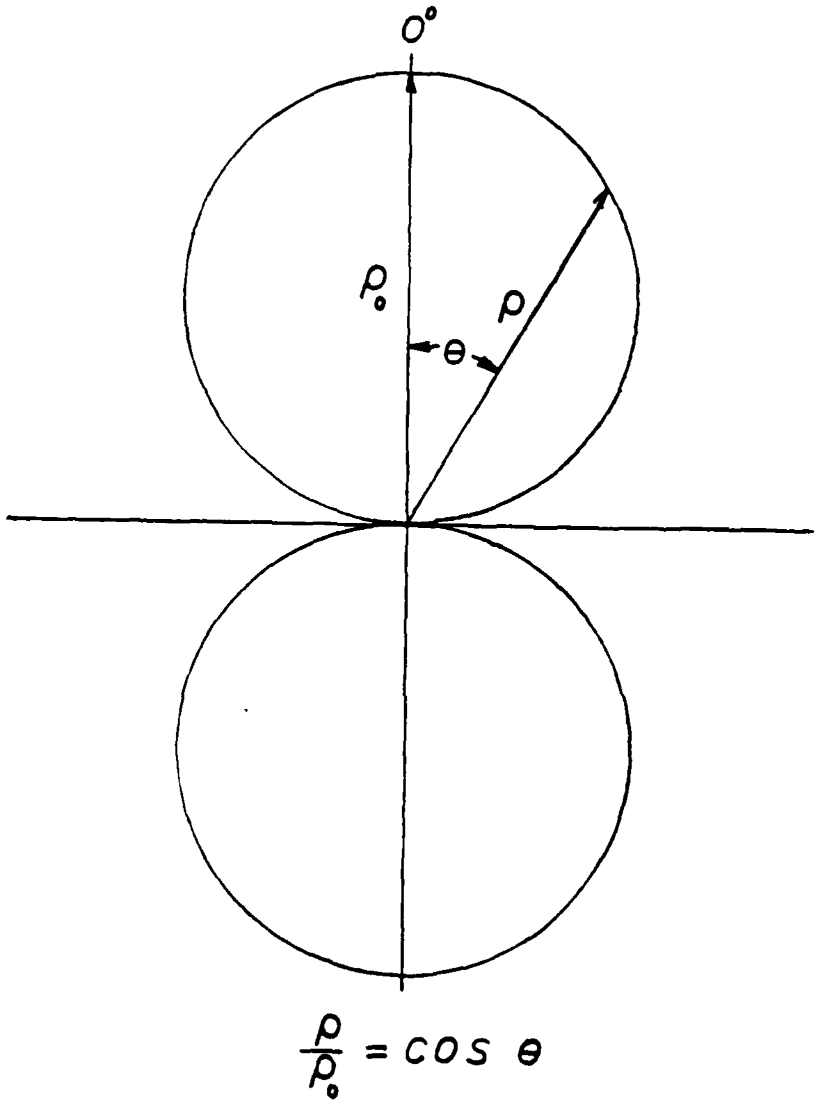

Figure 2.1 Directivity Pattern of Pressure Gradient Hydrophone

study is of this similar dipole type. Therefore, to illustrate its operation, assume two small pressure hydrophones are placed a small distance d apart, with $d \ll \lambda$, in a standing acoustic wave field P(x,t), as indicated in Figure 2.2. The dimensions of the two hydrophones are assumed to be much less than the wavelength of the acoustic field. The presence of the hydrophones is assumed to have a negligible influence on the sound field.

Consider the plane sinusoidal standing wave shown in Figure 2.3. The instantaneous acoustic pressure, P(x,t) is given by:

$$P(x,t) = P_o \sin[kx] e^{j\omega t} \qquad (2.1)$$

P_o is the peak acoustic pressure, k is the propagation wave number $k = 2\pi/\lambda$, x is the distance of one of the hydrophones from the pressure nodal point, ω is the angular frequency of the acoustic wave and t is time. Using the assumption sin kx = kx, for small values of kx, the equation can be written as:

$$P(x,t) = P_o\, kx e^{j\omega t} \qquad (2.2)$$

As indicated, both individual hydrophone are a distance $x = d/2$ from a standing wave pressure node (x = 0). The pressure difference, ΔP between these locations can then be expressed as:

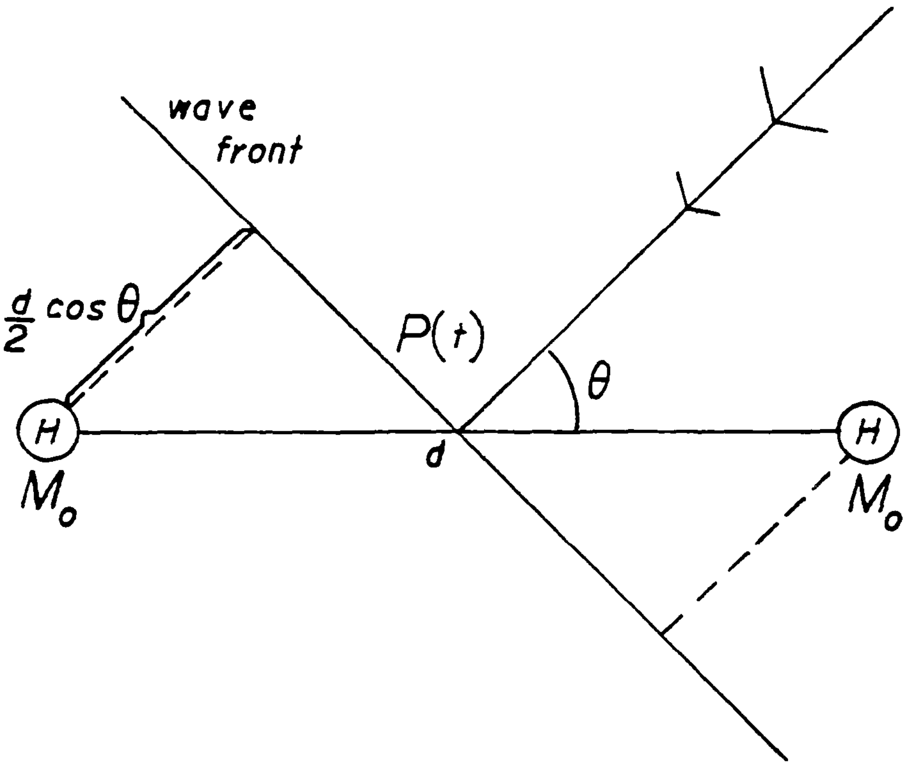

θ — angle of incidence

d — distance between hydrophones

M_o — free-field voltage sensitivity for individual hydrophone

Figure 2.2 Geometry Used in Deriving Sensing Characteristics of Acoustic Dipole (Pressure Gradient)

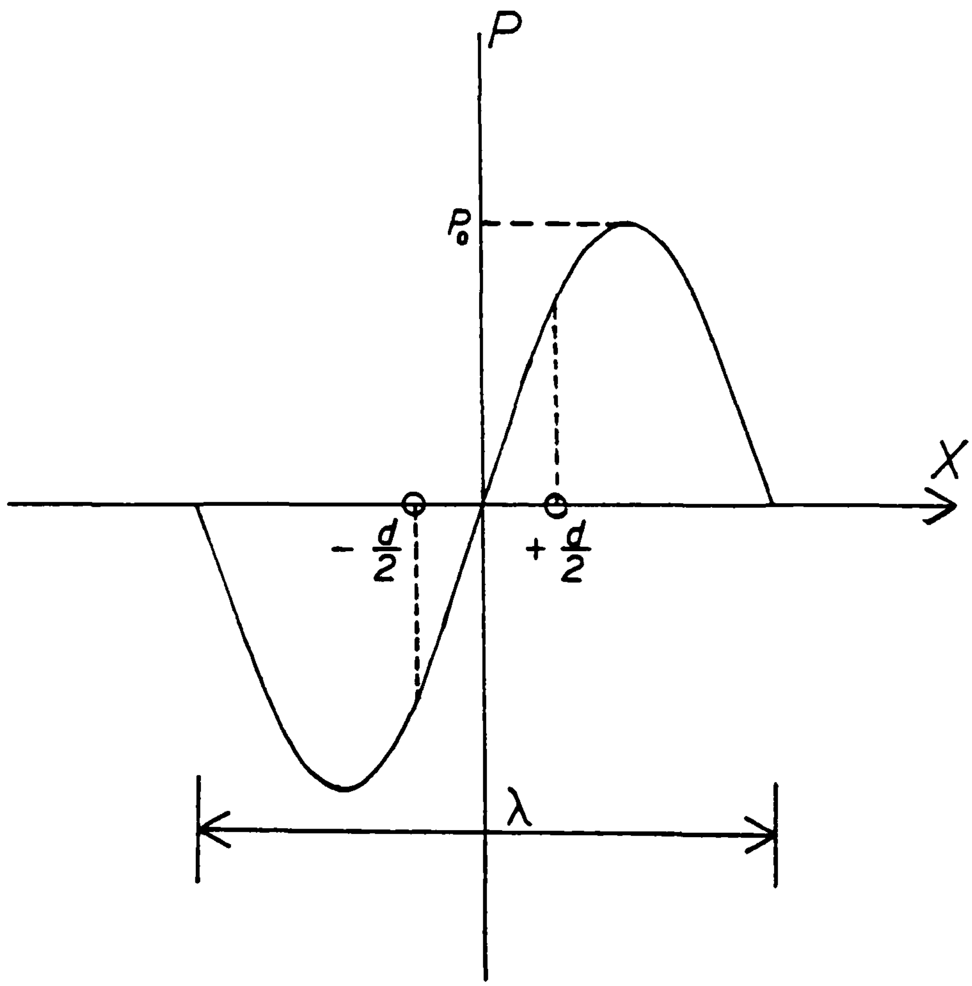

Figure 2.3 Pressure Distribution as Function of Distance from Null Pressure Point

$$\Delta P = P_{+d/2} - P_{-d/2} \qquad (2.3)$$

or

$$\Delta P = P_o \, kd \qquad (2.4)$$

When the individual hydrophones are equidistant from a pressure node, as assumed here, the pressure difference is a maximum. On the other hand, if the center of the pair is located at a pressure antinode, pressure difference is a minimum.

B. CALIBRATION OF GRADIENT HYDROPHONES

Usually in practice, pressure gradient hydrophones are calibrated in terms of pressure. The sensitivity of a pressure gradient hydrophone is usually given in terms of volts/micropascal (V/μPa), specified at particular frequency [Ref. 10]. Plane progressive waves are specified in the definition of free-field voltage sensitivity. Because of the difficulties in obtaining free-field conditions at low frequencies, in the present study a standing wave tube described in Chapter III Section A, was used.

According to Mills [Ref. 8], a free surface standing-wave tube system satisfies the following relationships in the ideal case (i.e., SWR = ∞):

$$p = p_o \sin kh \qquad (2.5)$$

$$u = (p_o/\rho c) \cos kh \qquad (2.6)$$

$$p/u = \rho c \tan kh \qquad (2.7)$$

here h is the distance from the air-water interface. Its is assumed that the hydrophones have negligible effect on the standing wave pattern.

In this report, fiber optic hydrophone free-field sensitivity is expressed in terms of microradian/micropascal (μrad/μPa). And rather than expressing gradient hydrophone sensitivity in terms of pressure sensitivity at a particular frequency the fiber optic gradient hydrophone sensitivity is expressed in μrad/μPa/cm. The procedures to obtain fiber optic hydrophone sensitivities are discussed in Chapter IV.

C. FIBER OPTIC ACOUSTIC SENSOR CONCEPTS

Laser light transmitted by optical fibers submerged in a liquid medium may be modulated (intensity or phase) by acoustic pressure variations. Only phase modulation of such an acousto-optic sensor system will be considered here. A detailed discussion of the theory of phase modulation is presented by Davis, et al [Ref. 7].

When an external pressure field (ΔP) is applied to the optical fiber it changes the fiber's physical characteristics. Changes can occur in the core radius, core length, and the optical indices of refraction in the core and cladding [Ref. 5 and Ref. 6]. The pressure induced changes of index and of length cause an optical phase shift $\Delta\phi$ given by:

$$\Delta \phi = nk_o \ell [(1/n)(dn/dP) + (1/\ell)(d\ell/dP)] P \qquad (2.8)$$

where n is the optical index of refraction of the core, k_o is the propagation constant of light in the fiber, P is the acoustic pressure and ℓ is the length of the fiber subject to the pressure. The pressure-induced length change $(d\ell/dP)$ is the dominant factor at low frequencies for a free or mandrel wound fiber.

Using a single frequency laser source, the time variation of the electric field vector of the lightwave may be expressed as:

$$\bar{E}(t) = \bar{E}_o \exp\{j[\omega_o t + A \sin(\omega_s t)]\} \qquad (2.9)$$

where ω_o is the angular frequency of the coherent laser source, ω_s is the angular frequency of the sound field and A is the phase shift amplitude.

To detect such phase modulation interferometric techniques must be employed. The laser light is first split and then sent through both the sensor fiber and reference fiber, these form the interferometric system, and are then recombined to give an intensity (amplitude) modulation prior to detection by the photodetectors. The total electric field at the photodetector may be expressed as:

$$\bar{E}_T = \bar{E}_1(t) + \bar{E}_2(t) \qquad (2.10)$$

$\bar{E}_1(t)$ is the electric field vector from the sensing arm and $\bar{E}_2(t)$ is the electric field vector from the reference arm (or for a gradient system, for the second sensing arm).

The intensity I(t) of the recombined beams is proportional to the magnitude of the square of $\bar{E}_T$. Neglecting terms that vary at angular frequency ω_o and $2\omega_o$, since they are undetectable by the photodetector, I(t) may be written as:

$$
\begin{aligned}
I(t) \; \alpha \; & E_1^2/2 + E_2^2/2 + \bar{E}_1 \cdot \bar{E}_2 \cos\phi J_o(A) \\
& + 2\bar{E}_1 \cdot \bar{E}_2 \sin\phi J_1(A) \sin\omega_s t \\
& + 2\bar{E}_1 \cdot \bar{E}_2 \cos\phi J_2(A) \cos 2\omega_s t \\
& + 2\bar{E}_1 \cdot \bar{E}_2 \sin\phi J_3(A) \sin 3\omega_s t + \cdots \qquad (2.11)
\end{aligned}
$$

where $\bar{E}_1$ and $\bar{E}_2$ represent spatial vectors and make explicit the fact that the polarization directions may not be the same.

Thus, from equation (2.11), the resulting intensity function consists of a series of harmonics of the acoustic frequencies. The amplitude of each successive harmonic is a function of the acoustic pressure and varies as the Bessel function of corresponding order [Ref. 8].

These recombined variations of optical intensity are detected with photodetectors to produce an electrical signal. Thus the resulting photodetector current has components of the following form:

$$i(t) = i_o \cos\phi\{ J_o(kx) + 2\sum_{n=1}^{\infty} J_{2n}(kx) \cos[2n(\omega_m t)]\}$$

$$- i_o \sin\phi\{2\sum_{n=0}^{\infty} J_{2n+1}(kx) \sin[(2n+1)(\omega_m t)]\} \qquad (2.12)$$

where J_n is the Bessel function of order n, ϕ is a non acoustically induced phase shift (which itself may change due to changes in temperature, for example), $k = 2\pi/\lambda$ is the optical wave number in the fiber, and x is the amplitude of the acoustically induced optical path-length change.

III. EXPERIMENTAL APPARATUS

A. ACOUSTIC CALIBRATOR

In an earlier study [Ref. 8], an acoustic calibrator had been constructed to calibrate fiber optic gradient hydrophones. However, this could be used only with the axis of coils of the hydrophone aligned along the axis of the calibrator. Since the gradient hydrophone now being tested is a rigid structure with the individual hydrophone coils mounted 10 cm apart it was necessary to increase the diameter ot the calibrator tube. A rotating apparatus was needed to turn the gradient hydrophone to vary the angles of the hydrophone axis with respect to the acoustic wave vector inside the calibrator tube. The new tube is made of PVC 1120 Type 12454-B and is 25.4 cm in diameter and is 56.4 cm tall.

The calibrator tube is mounted around the face of the acoustic driver which is a USRD type J-11 projector [Ref. 10]. To compensate for the water column a hydrostatic collar with a valve is placed on the bottom of the projector assembly. The valve is opened and air is pumped into the equalizing chamber until the air pressure is equal to the water pressure on the face of the driver. This air pressure is measured by a water filled U tube manometer mounted next to the calibrator assembly. The complete assembly is shown in Figure 3.1.

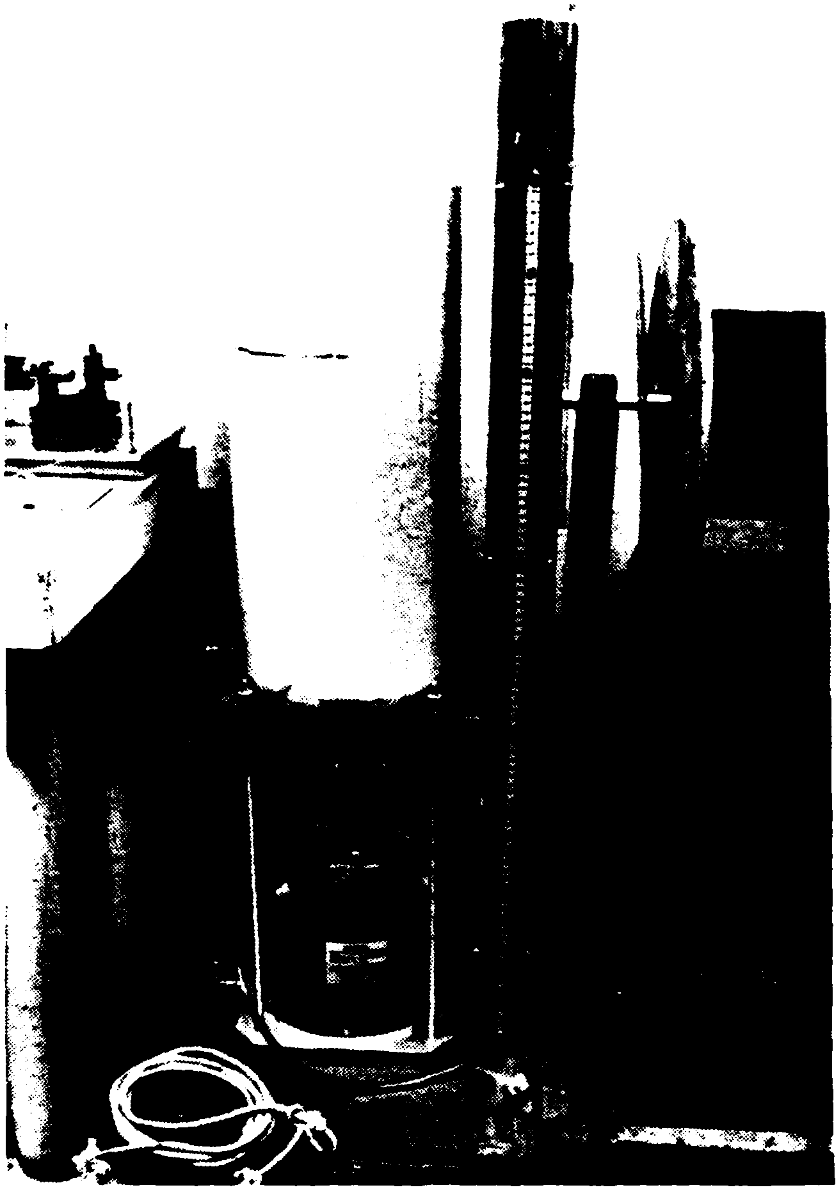

Figure 3.1 Acoustic Calibrator

B. 632.8 nm INTERFEROMETRIC SYSTEM

To test the feasibility of constructing and ruggedizing a gradient hydrophone for sea trial a laboratory Mach-Zehnder interferometric system, operating at 632.8 nm, was first constructed. As indicated in Figure 3.2, it consists of a Helium-Neon laser supplying laser light at wavelength 632.8 nm through a 2 X 2 input coupler which divides the laser light into the two fiber optic sensor arms. In one arm the laser light travels through two sections of the polarization controller [Ref. 11] and a sensor coil (hydrophone) to a 2 X 2 output coupler. In the second arm the light travels through one section of the polarization controller and is wound around a piezoelectric (PZT) cylinder and passes through the second hydrophone coil to the 2 X 2 output coupler. The coupler recombines, the two optical outputs of the individual hydrophone coils, thus converting phase modulation into amplitude modulation information. This amplitude modulated signal is transmitted by optical fiber to two photodetectors (photodiodes). These convert the recombined light into electrical signals which are monitored and recorded by the instrumentation package as described in Section G of this chapter. A photograph of this interferometer system without the gradient hydrophone is shown in Figure 3.3.

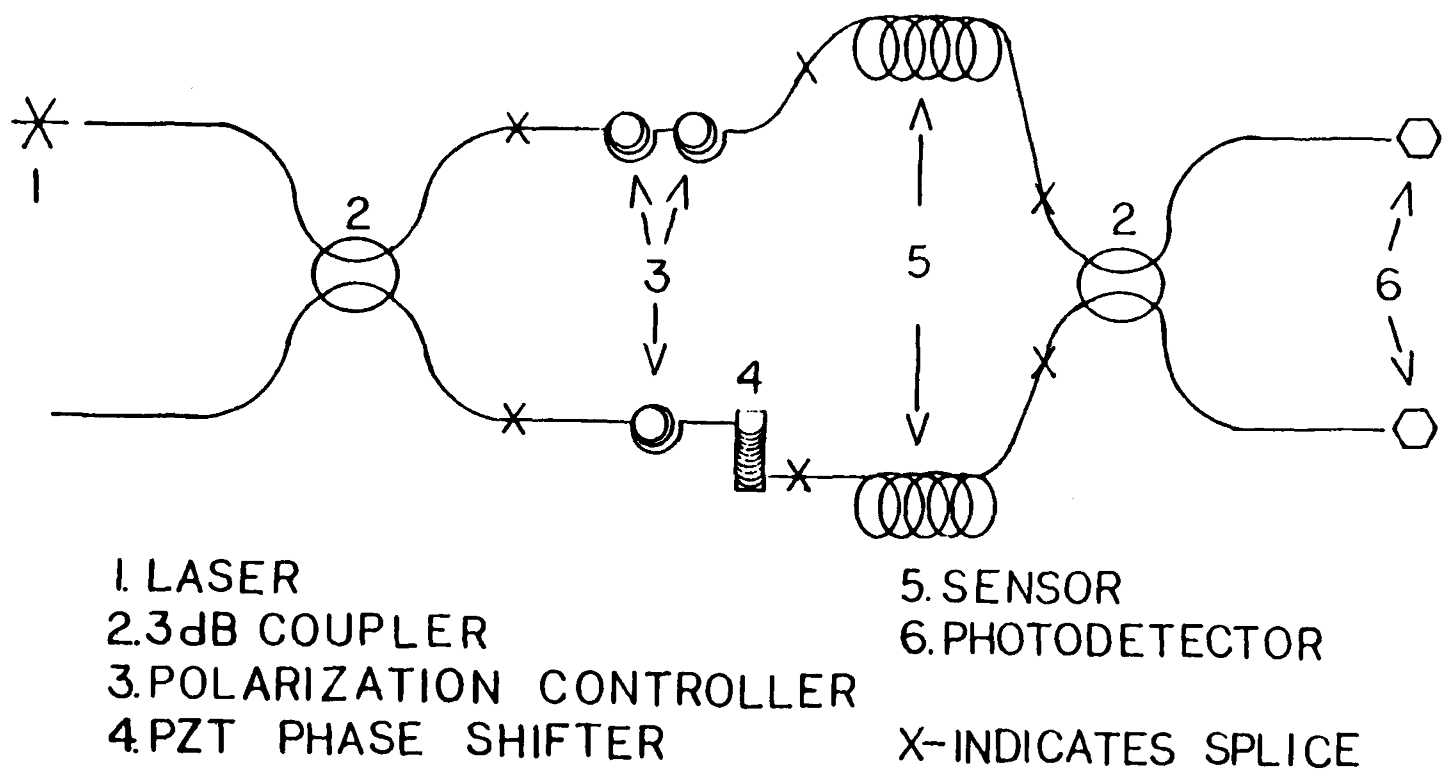

Figure 3.2 632.8 nm Mach-Zehnder Interferometer

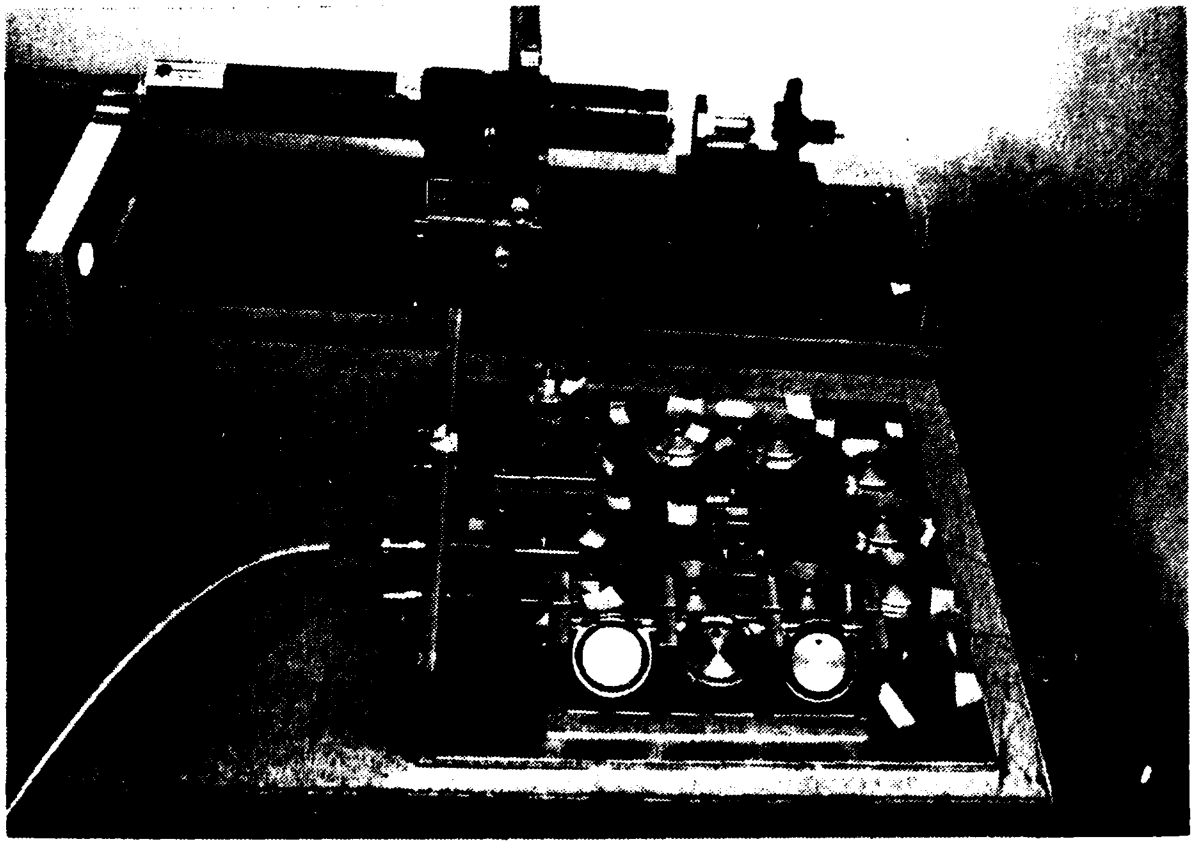

Figure 3.3 632.8 nm Interferometric System

1. Laser Source

The optical source used in the 632.8 nm interferometer system is an actively stabilized, single frequency, Helium-Neon laser. It is a Coherent Tropel Model 200. The specifications are as follows:

Output Power:	0.7 to 0.9 mW @ 0.6328 μm
Spatial Mode Structure:	TEM_{00}
Temporal Mode Structure:	Single Frequency
Polarization:	Linear
Beam Divergence (full angle):	1.3 degrees
Amplitude Noise:	(10Hz-10MHz) $\leq$0.2%(RMS)

Frequency Stability:
- Short Term: $\leq \pm$ 1 MHz drift per 5 minute interval (.002) PPM
- Long Term: Fundamental frequency varies by 5 MHz per degree Celsius ambient temperature change (.01 PPM).

2. Fiber Specifications

The fiber used in the 632.8 nm interferometer system is ITT Type T-1601. It is single-mode fiber optimized for a wavelength of 632.8 nm. Its construction and characteristics are shown in Figure 3.4. The specifications of the particular fiber used are as follows:

Fiber Ident.:	830420-401c
Preform No.:	EMT-22204B
Core Diameter:	3.8 μm
Outer Cladding Diameter:	75 μm

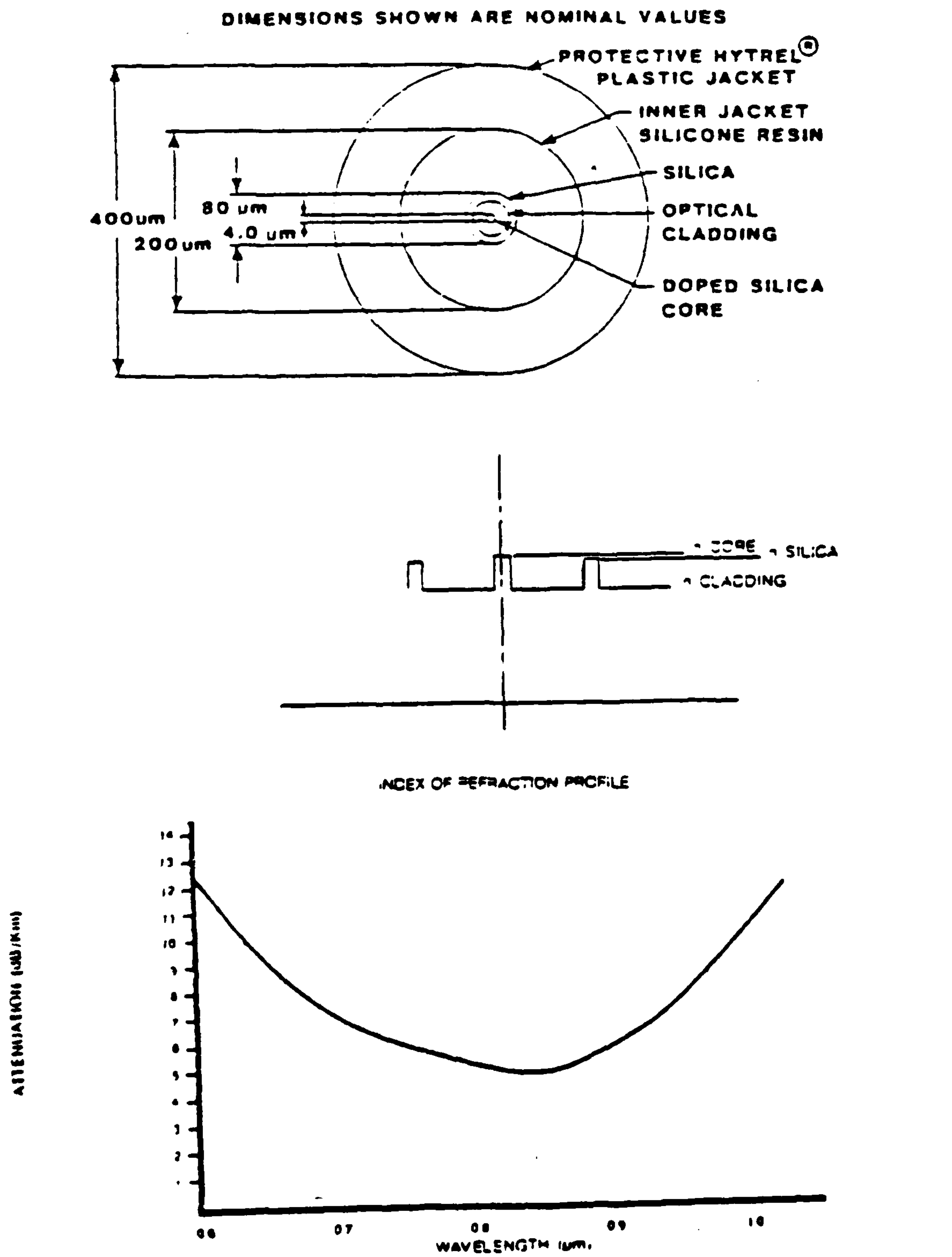

TYPICAL SPECTRAL ATTENUATION - SINGLE MODE OPTICAL FIBER
Figure 3.4 ITT Single-mode Fiber T-1601

Primary Sheath:	GE 615 Silicone
Secondary Sheath:	polyester Hytrel
Total Diameter:	406 μm
Attenuation:	6.55 dB/Km at 632.8 nm

D. Couplers

The purpose of a 3 dB coupler is to split the light equally into the arms of the interferometer or to recombine the light causing the light from the two arms to interfere in the output fibers and on the face of a photodetector. The particular 2 X 2 single-mode couplers used in the laboratory interferometer were manufactured by ITT. The specifications are as follows:

Serial Nos.:	JM-SM-164
Fiber No.:	830918-402b/EMC-41581B
Fabrication Date:	2/11/84
Excess Loss:	0.1 dB
Uniformity:	0.2 dB
Operating Wavelength:	632.8 nm

Serial Nos.:	JM-SM-165
Fiber No.:	830918-402b/EMC-41581B
Fabrication Date:	2/13/84
Excess Loss:	0.2 dB
Uniformity:	0.1 dB
Operating Wavelength:	632.8 nm

4. <u>Piezoelectric Phase Shifter</u>

The phase shifter consists of a lead zirconate-lead titanate (PZT) cylinder, Channel Industries Type 5500, around which the fiber is tightly wrapped. The cylinder is 7.[illegible] cm long by 3.8 cm outer diameter with wall thickness of 0.[illegible] cm. By wrapping 59 turns, corresponding to 7 m of fiber, on the PZT it was possible to produce a relatively large optical phase shift. The shifter has a sensitivity of [illegible] rad/volt. The calibration of the PZT is discussed in Chapter IV, Section A.

5. <u>Polarization Controller</u>

A polarization controller, as described by Lefevre [Ref. 11], was employed. This device is equivalent to fractional wave plates of classical optics. The controller [illegible] the stress birefringence induced by bending the fiber.

6. <u>Photodetectors</u>

The photodetectors used to detect the optical output [illegible] fiber from the interferometer are Clairex Type CLD-42 photodiodes. They are all silicon PN planar diodes with high linearity, low dark current and fast response. Their electrical characteristics are:

Active Area:	1.3 X 1.3 mm
Short Circuit Current:	35-70 μA
Open Circuit Voltage:	0.40 volts, typical
Dark Current:	1 nA

Junction Capacitance:	200 pF
Rise or Fall Time:	5 μsec
Temperature Coefficient:	$\pm$ 0.2%/°C, typical
Peak Spectral Response:	0.91 μm

C. 830 nm INTERFEROMETRIC SYSTEM

For the sea trial itself, a second interferometric system, again in a Mach-Zehnder confriguration as indicated in Figure 3.5 was constructed. It consists of two 830 nm diode lasers either one of which could be used to supply light. This goes through optical fiber to a 2 X 2 input coupler and splits the light into the two arms. The output side of each hydrophone goes to a 3 X 3 output coupler. The 3 X 3 coupler recombines the laser light and sends it out via three fiber leads. The two fibers used on the output side of the coupler go to two photodetectors (photodiodes) which convert the recombined light into electrical signals which are monitored and recorded by the instrumentation package as described in Section G of this chapter. A photograph of the system is shown in Figure 3.6.

1. Laser Source

The optical sources used in the 830 nm interferometer system are Mitsubishi Type FU-21LD AlGaAs/GaAS TJS (Transverse Junction Stripe) laser diodes. These were supplied with multi-mode fiber pigtails. These diodes emit light around 850 nm wavelength by applying forward current

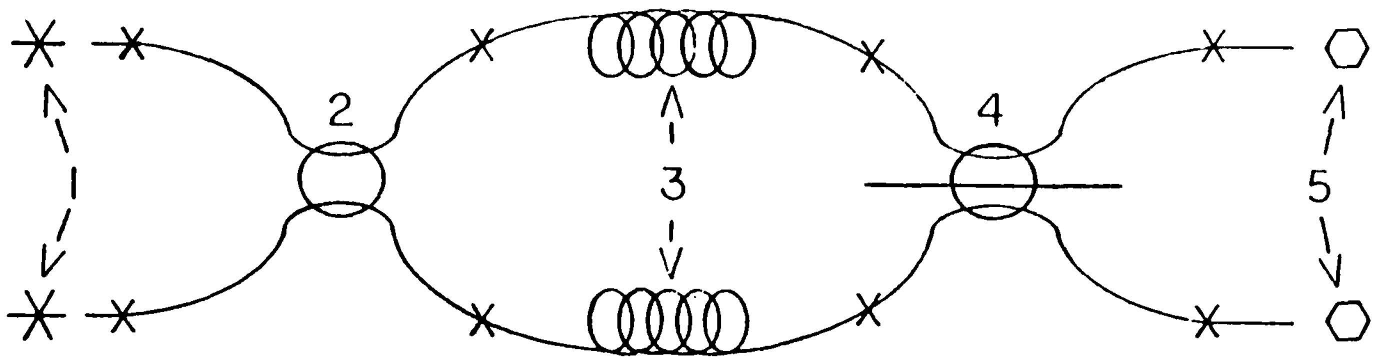

1. LASER
2. 2 X 2 3dB COUPLER
3. SENSOR
4. 3 X 3 3dB COUPLER
5. PHOTODETECTOR
X-INDICATES SPLICE

Figure 3.5 830 nm Mach-Zehnder Interferometer

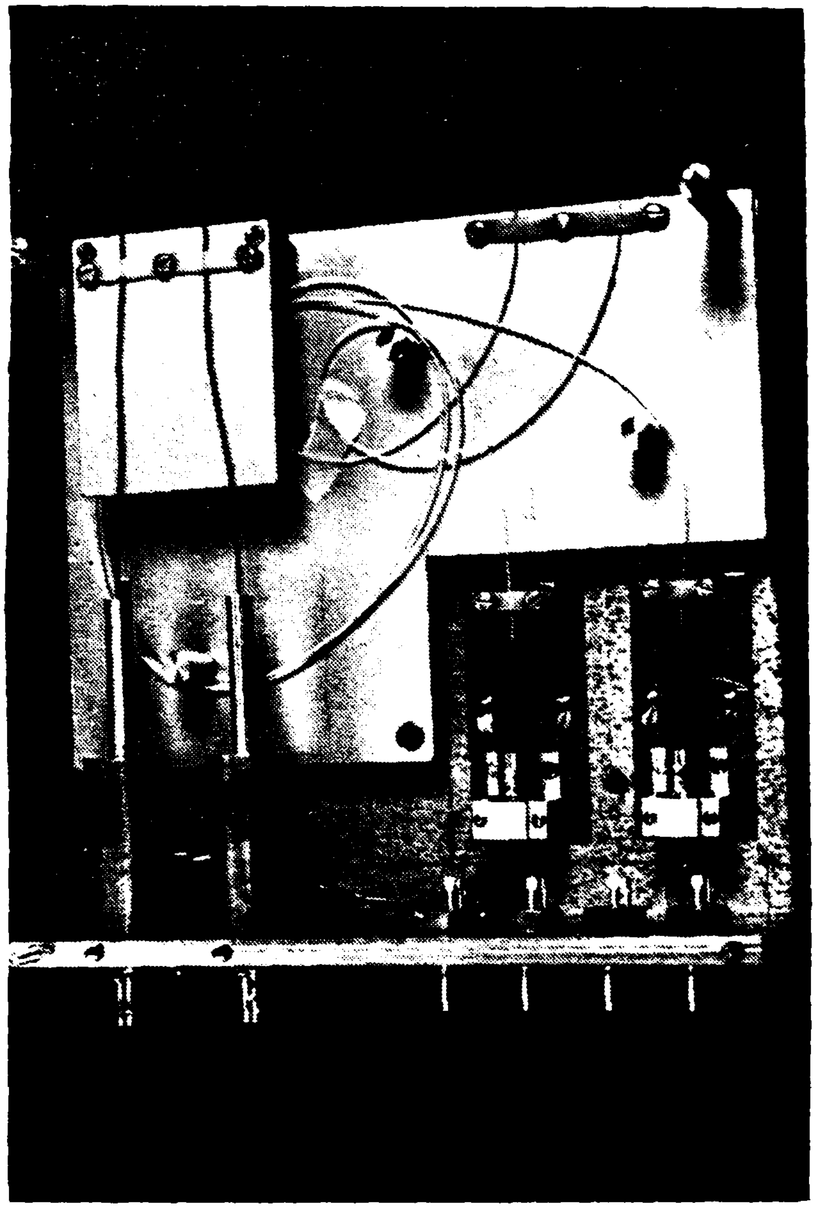

Figure 3.6 830 nm Interferometric System

exceeding threshold current. The laser output level can be monitored via a photodetector enclosed in the laser diode package. Some other features are: stable fundamental transverse mode oscillation, laser diode-fiber high coupling efficiency and long life hermetic seal. Each laser can operate under CW or pulse conditions according to input current, at case temperature up to 50°C. The specifications are as follows:

Serial Nos.:	54 and 66
Output Power:	3.2 mW
Fiber multi-mode:	GI Type 50 μm core
Fiber Numerical Aperture:	0.2
Lasing Wavelength:	795-905 nm, typical 850 nm
Threshold Current (CW):	30 mA typical, 50 mA max
Operating Current (CW):	55 mA typical, 90 mA max
Operationg Voltage (CW):	1.8 V typical
Light Input to Fiber (CW):	1.6 mW min, 3.2 mW typical

The diode lasers required a special power supply to control and monitor the output current supplied to them. A schematic of the power supply is shown in Figure 3.7. The diode lasers were tested and the optical power output was observed and recorded against the input current to verify the specifications. The results are shown graphically in Figures 3.8 and 3.9. No special effort was taken to control the temperature of the laser other than good heat sinking,

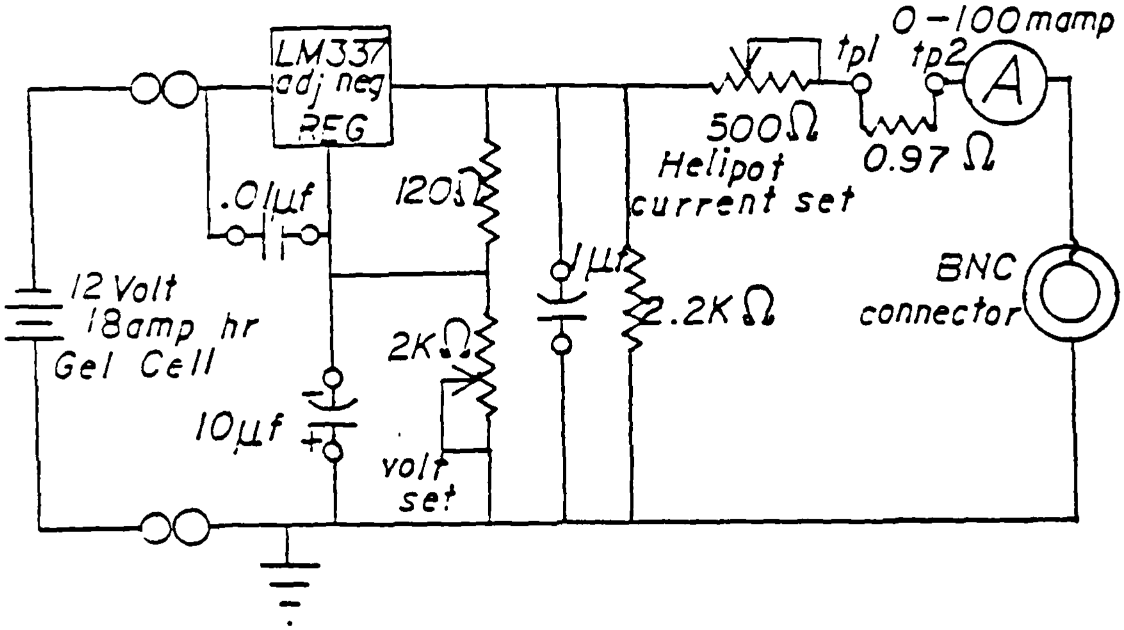

Figure 3.7 Laser Diode Power Supply

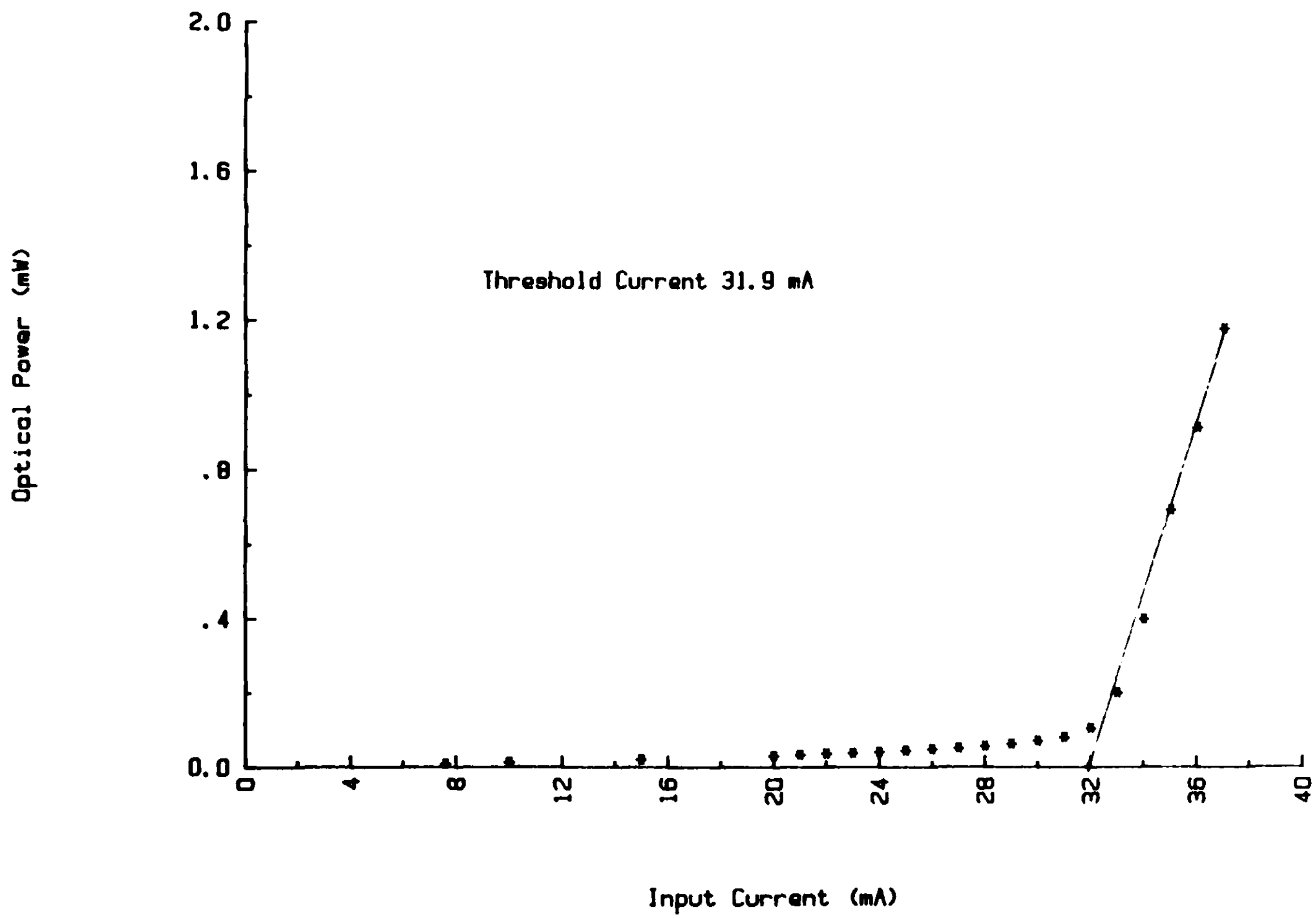

Figure 3.8 FU-21LD-54 Laser Diode Power Curve

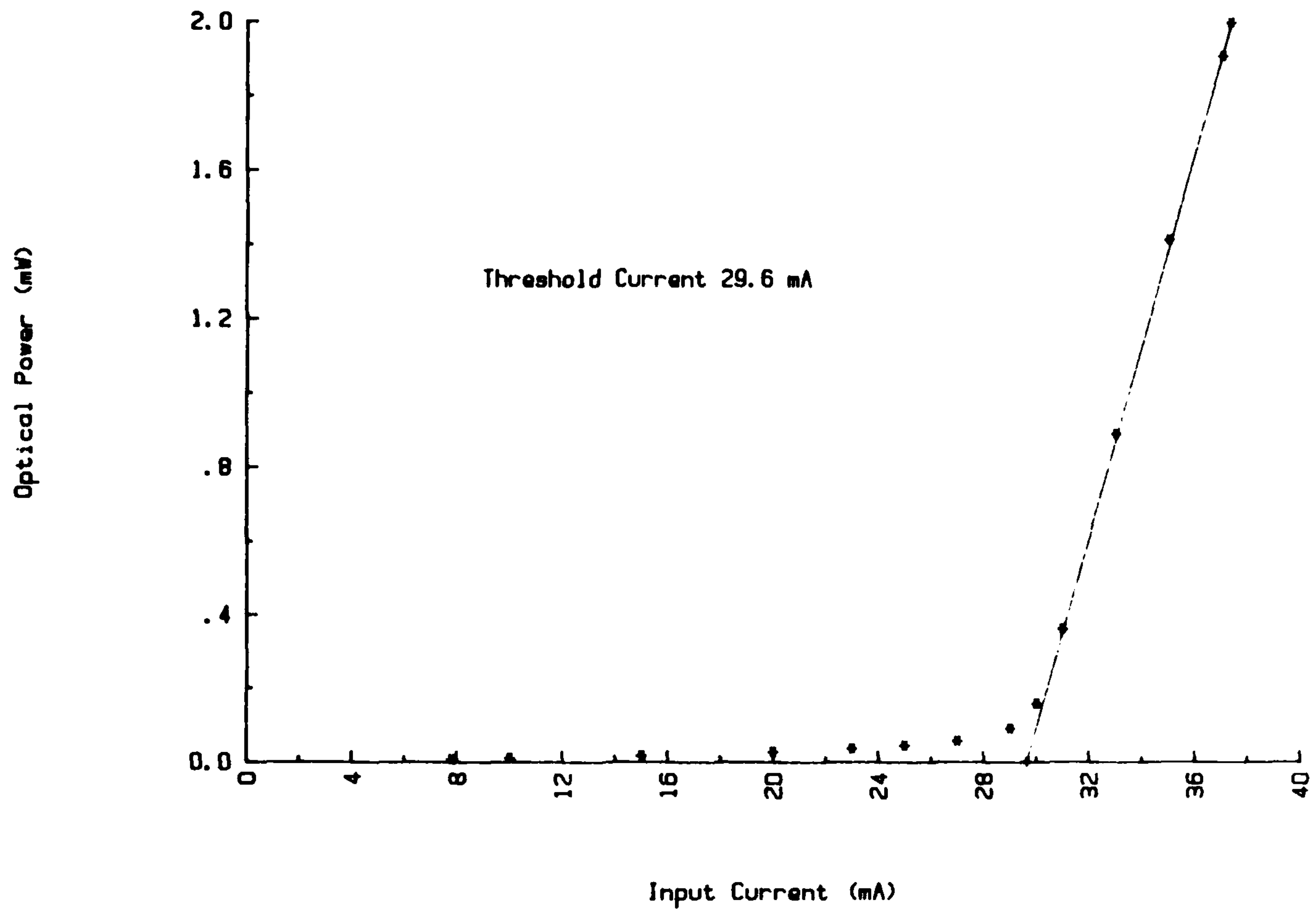

Figure 3.9 FU-21LD-66 Laser Diode Power Curve

it should be noted, that according to the manufacture, at a current of 40 mA, the light output changes at an average rate of 50 μW/°C between -20 °C and 50 °C).

2. Fiber Specifications

The optical fiber used was ITT single-mode fiber, type T-1601 optimized at 0.83 m. Specifications of the fiber are as follows:

Fiber Ident:	81092U-17Bic
Preform No.:	EMT-21972B
Numerical Aperture:	0.12
Core Diameter:	4.57 μm
Outer Cladding Diameter:	75 μm
Primary Sheath:	GE 615 Silicone
Secondary Sheath:	polyester Hytrel
Total Diameter:	406 μm
Attenuation:	2.07 dB/Km at 0.83 μm

Figure 3.4 is a sketch, provided by the manufacturer of the end of the fiber, with typical dimensions, approximate index of refraction profile and typical spectral attenuations.

The fiber from the 3 X 3 output coupler to the photodetectors is multi-mode and in a cable containing four optical fibers, manufactured by Fhalo Optical Division. The specifications are as follows:

Fiber Type:	A04X Series
Cable Diameter:	5.5 mm

Core Diameter:	50 μm
Clad Diameter:	125 μm
Buffer Diameter:	940 μm
Numerical Aperture:	0.2-0.22
Fiber Attenuation:	4.0-6.0 dB/km @ 0.82 μm
Optical Bandwidth:	200-800 MHzkm

7. Couplers

a. Coupler 2 X 2

A 2 X 2 ITT single-mode coupler was used for the input coupler. Its specifications are as follows:

Serial No.:	JM-SM-107
Fiber No.:	EMC 41556C/830427-401a
Fabrication Date:	6/02/83
Excess Loss:	0.1 dB
Uniformity:	0.2 dB
Operating Wavelength:	0.83 μm

b. Coupler 3 X 3

An ITT 3 X 3 single-mode coupler was used for the output coupler. Its specifications are as follows:

Serial No.	JM-SM3-58
Fiber No.:	EMC-41556C/830427-401b
Fabrication Date:	7/24/84
Excess Loss:	0.4 dB
Uniformity:	1.8 dB

Wavelength: 0.83 μm

4. Photodetectors

The photodetectors used to detect the optical output of the fiber from the interferometer are Clairex Type CLD-41 photodiodes. They are all silicon PN planar diodes with high linearity, low dark current and fast response. The electrical characteristics are as follows:

Active Area:	1.3 X 1.3 mm
Short Circuit Current:	min 6 to max 12 μA
Open Circuit Voltage:	0.40 volts typical
Dark Current:	1 nA
Junction Capacitance:	200 pF
Rise or Fall Time:	5 μsec
Temperature Coefficient:	+.2%/degree C typical
Peak Spectral Response:	0.91 μm

D. FIBER PREPARATION AND SPLICING

Both single-mode and multi-mode optical fibers were used in the experimental systems. The preparation for splicing is similar for both. The plastic coating over the glass fiber, usually Hytrel, must be removed by using a sharp razor blade. The blade is placed at a very small angle to the coating surface and the fiber is drawn to the blade to separate the plastic from the fiber. After most of the plastic is removed, the fiber is dipped into a bath of chromic acid. This turns the remaining plastic into a jelly [illegible] substance. The fiber is then dipped into distilled water and passed through a menthanol soaked tissue wiper.

To obtain a clean square end on the fiber it is then put into a fiber optic cleaving tool made by Thomas & Betts Corp. The clean square end is necessary to achieve a good splice. The ends of both must appear like A in Figure 3.10.

The fiber was spliced together using a Model PFS-200 [illegible] optical fiber splicer made by Power Technology Incorporated. After preparing the two fiber ends, they are placed into the splicer and mechanically, as well as optically aligned. The optical alignment of the two fibers is achieved by maximizing the laser light transmitted through the fiber cores at the output of the second fiber. Care must be taken to eliminate light transmitted through the cladding. This can be done by coating a section of the cladding of the output fiber with black paint. Then once the two fibers are aligned, one is moved in approximately 1 μm in the splicer to allow a small amount of glass to melt and achieve a good splice. The splicer has settings for Ramp Time, Arc Time and Arc Current and these must be determined experimently for each pair of fibers to be joined. For two single mode fibers of both 632.8 nm and 830 nm wavelength, it was experimently determined that a Ramp Time of 0.2 sec, Arc Time of 0.5 sec and Arc Current of 15 mA produced the best results. For single-mode to multi-mode fiber the settings were 0.1 sec, 0.4 sec and 14 mA respectively. If

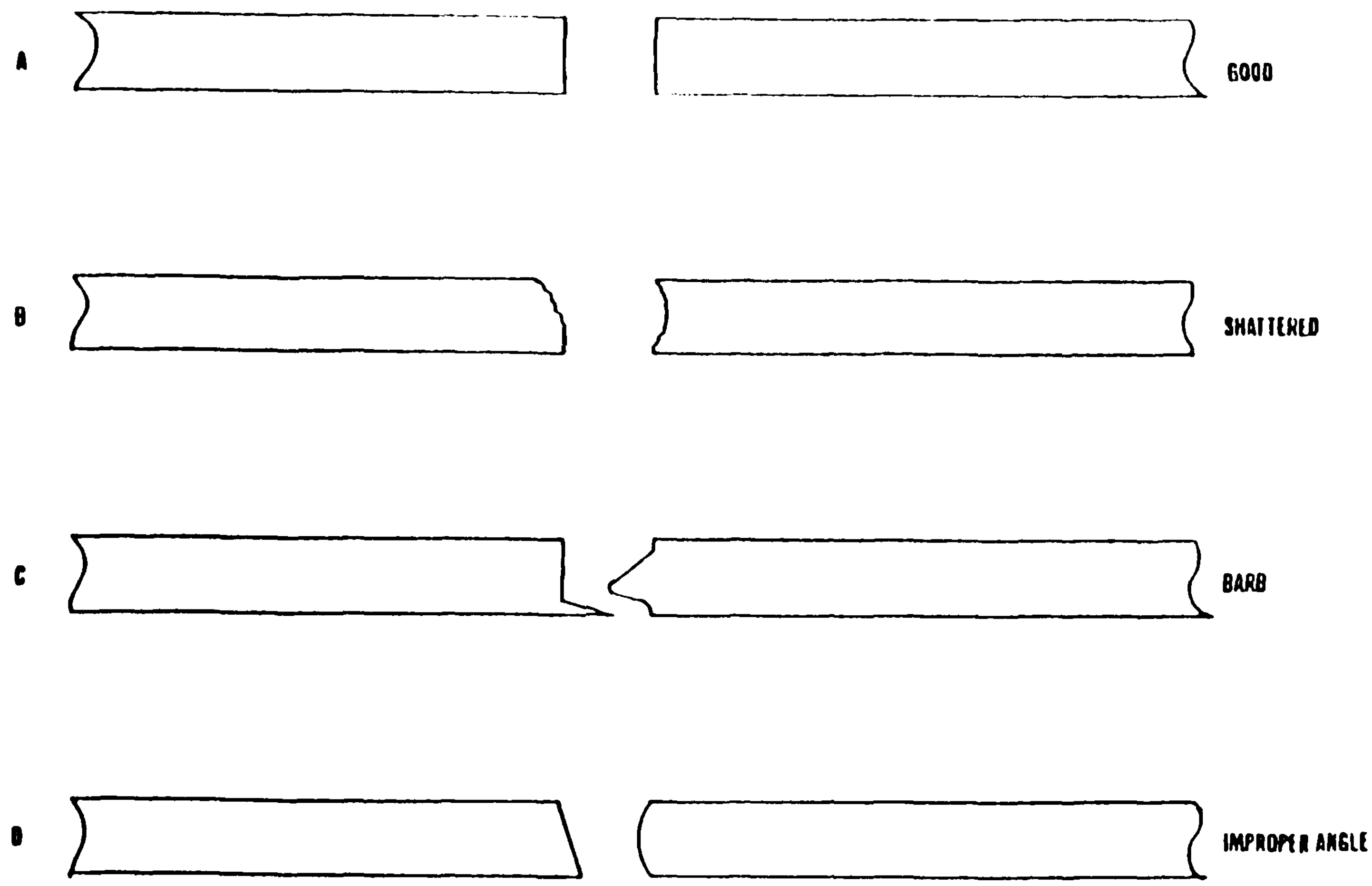

Figure 3.10 Representation of Proper and Improper Cleaves

the splice is to be successful the core-to-core alignment should be as shown in D of in Figure 3.11 and the measured light should remain nearly the same after fusion as it was before.

After the splice was made Scotch tape was placed over the splice to protect it from being broken by mechanical stresses. In later stages of development a splice protector manufactured by Sumitomo, Inc. was used. This consisted of a stainless steel rod, 6.35 cm in length with heat shrink tubing of a small diameter next to the rod and both covered by another piece of heat shrink tubing. This provides strength in the area of the splice and prevents bending/breaking.

I. MANDREL CONSTRUCTION

In the Mills experiment [Ref. 8], the fiber optic hydrophones consisted of loosely bundled coils. For the present experiment a design was needed to package the fiber optic gradient hydrophone for sea trial. The design used retained the toroidal coil shape [Ref.8] but an effort was made to put the coils on a mandrel in a way that allowed the acoustic signal to influence the fiber without degradedation of the sensitivity. The potting material used is a low viscosity epoxy, Stycast 1266[2].

Fabrication was begun by pouring epoxy into a mold that

----

[2]Stycast 1266 epoxy is made by Emerson and Cuming, Canton, MA 02021.

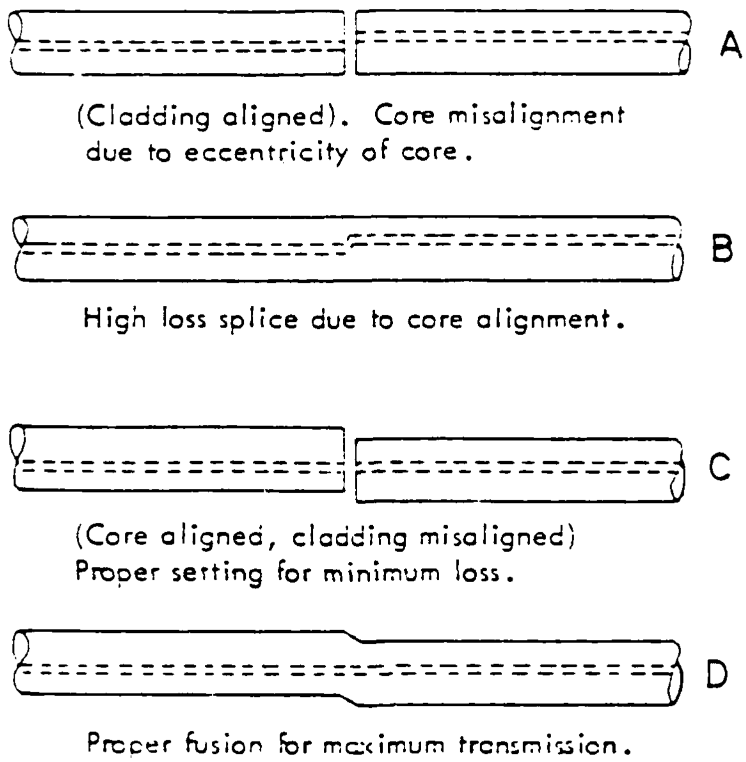

Figure 3.11 Representation of Proper and Improper Fuse Alignments

was [illegible] cm in diameter and 1.6 cm in height. It was allowed to harden at room temperature over a two day period. This epoxy casting was then machined into a bobbin shaped mandrel, with dimensions of 5.75 cm outer diameter, 1.42 cm in height with the groove 1.[illegible] cm in width and 0.20 cm in depth; as shown in Figure 3.12a. To facilitate winding, the mandrel was then [illegible] on a cylinder with a second mandrel. The second mandrel was used to hold the input and output leads of the [illegible]. The [illegible] with both mandrels was then mounted on a [illegible] of a small motor which rotated at 3 rpm. A thin layer of [illegible] was then brushed onto the first mandrel. The motor was turned on and the fiber was wound onto the mandrel to complete one layer of the sensor. A second and third layer of fiber were added in a similar manner. After all three layers were on the mandrel an outer coating of fiber was [illegible] the groove to the height of the wall of the mandrel, Figure 3.12b. Three layers of fiber were [illegible] to permit 10 meters of fiber to be wound on the [illegible]. Each mandrel has two meters of lead at each end. A photograph of a finished mandrel is shown in Figure 3.13.

C. GRADIENT SENSOR CONSTRUCTION

1. 632.8 nm Gradient Hydrophone

After both single hydrophone sensitivities were determined by experimental runs in the calibration tube, the two sensors were mounted 10 cm apart on an epoxy tube

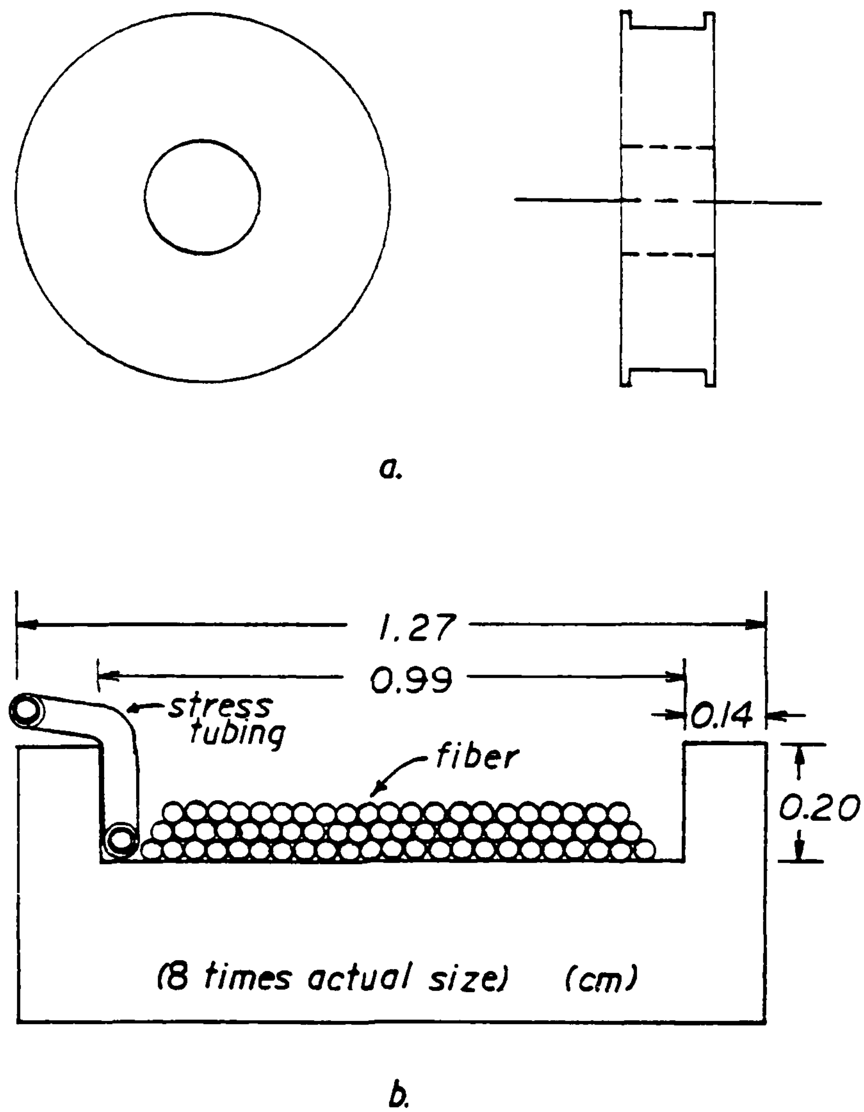

Figure 3.12 Cross Section of Fiber Optic Mandrel

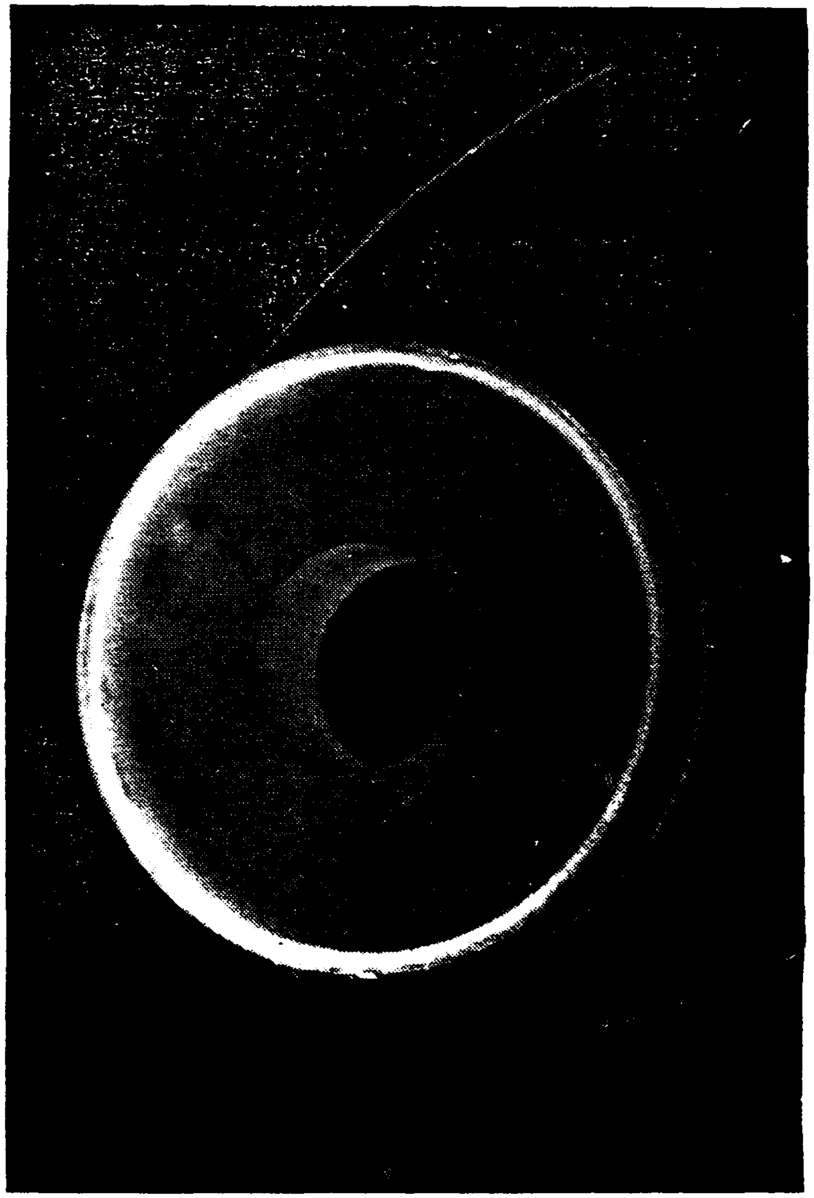

Figure 3.13 Fiber Optic Mandrel

1.54 cm in diameter. The optical fiber was run through a hole along the axis to an outlet at its center where the fiber was brought to the input/output couplers. This formed the sensor coil portion of the gradient hydrophone as shown in Figure 3.14.

C. 830 nm Gradient Hydrophone

After both single hydrophones were determined to have equal optical path lengths, 7 m in each arm to within 1 cm., they were fused to the input 2 X 2 coupler and output 3 X 3 coupler. Each individual hydrophone was wound on a teflon mandrel of 4.13 cm in outer diameter and 1.27 cm in thickness. The optical fiber was wound on the center part of the spindel which was 3.81 cm in diameter and 0.95 cm in width. These individual hydrophones were then mounted onto an aluminum T shaped bar, 10 cm apart, that accommodated both the input and output couplers on the top of T between the two hydrophones.

The optic fibers were then passed through the bottom part of the T into a short piece of tygon tubing. The 830 nm lasers multi-mode pigtails are fused to the single-mode fiber leads of the input coupler, one laser to each lead. The output fibers from the output coupler, which are single-mode, were fused to multi-mode fiber which went to the photodetectors. The entire hydrophone was dipped in a plastic coating material to protect the various fiber elements. The completed unit is shown in Figure 3.15.

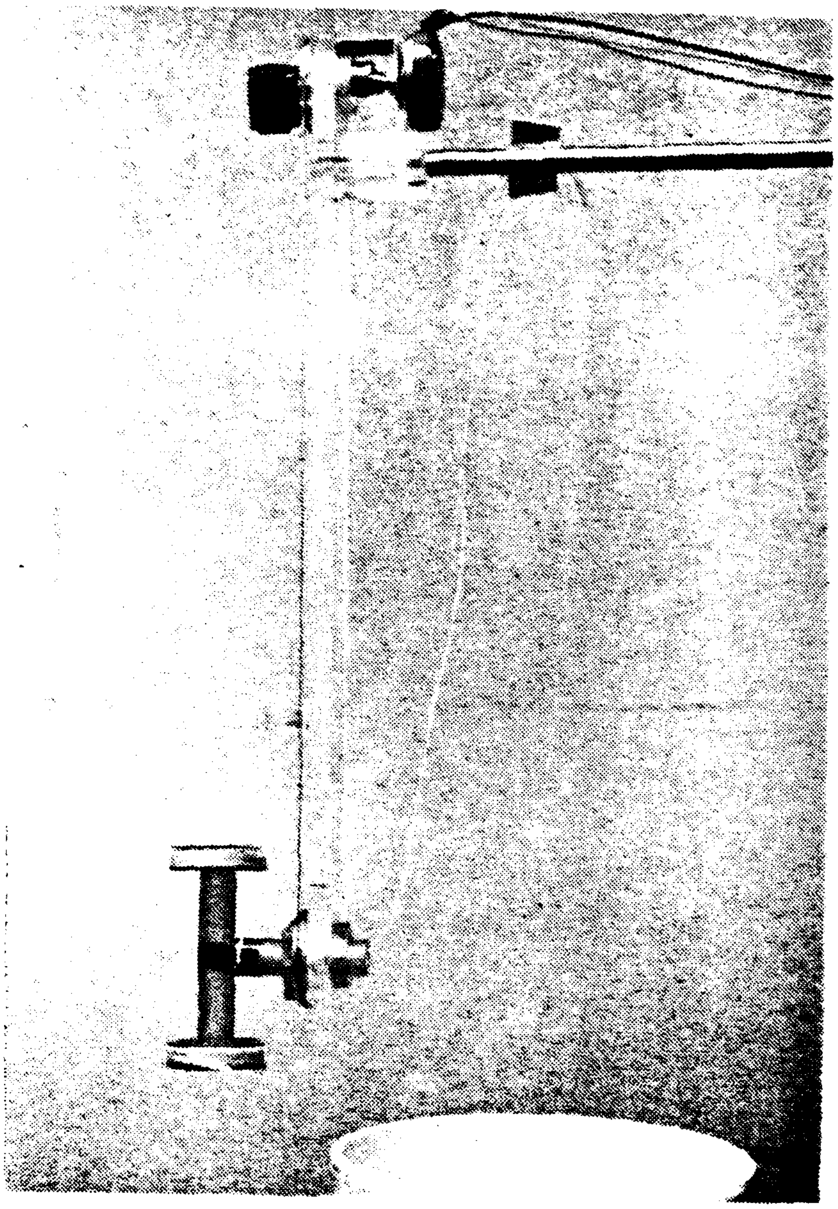

Figure 3.14 632.8 Gradient Hydrophone and Rotation Apparatus

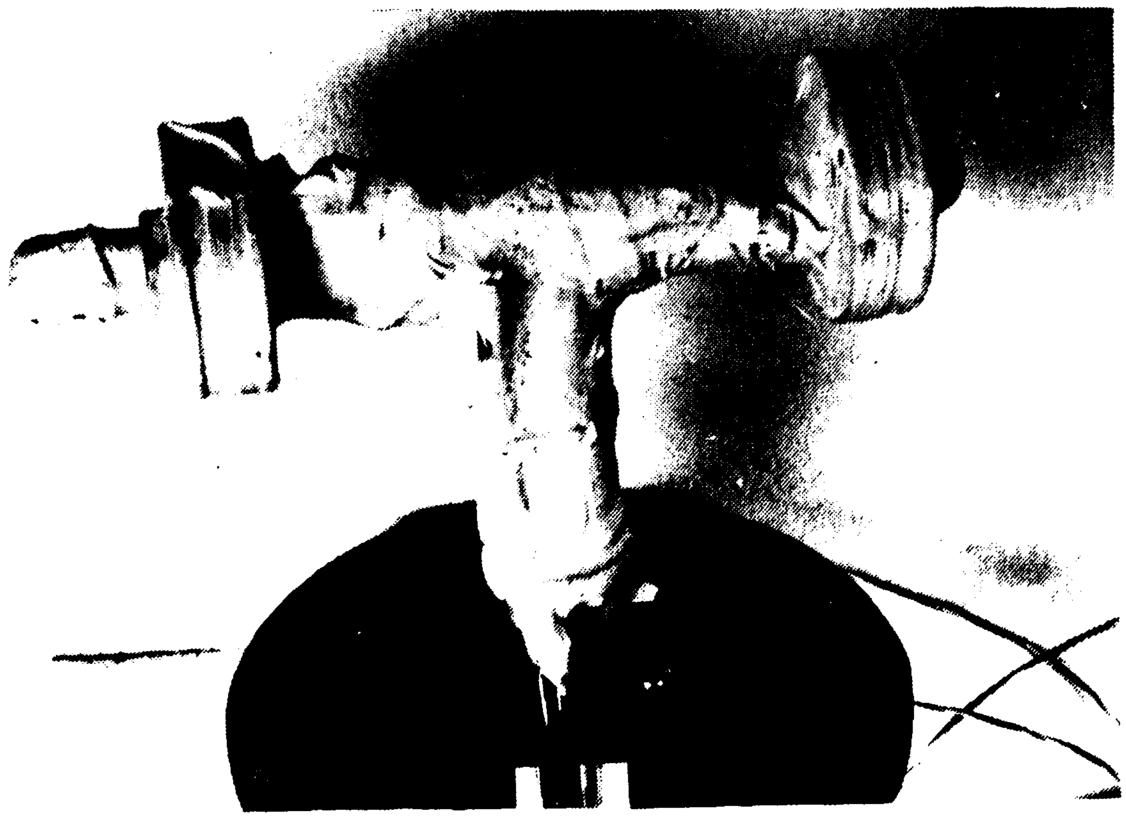

Figure 3.15 830 nm Gradient Hydrophone

E. INSTRUMENTATION AND DATA ACQUISITION SYSTEM

The instrumentation and data acquisition system used in both the laboratory and sea trial phases is shown in Figure 3.16. Computer data acquisition was used for portions of data taking using the program in Appendix A. The Hewlett-Packard 85F computer coordinates the peripherals, recorded and displayed the data, as shown in Figure 3.17. The following is a brief description of each instrumentation unit.

1. Computer HP-85F

The HP-85F is an eight bit microprocessor that utilizes BASIC computer language. The computer has as standard 16K bytes of read/write memory and 16K bytes of additional memory to give the system a total of 32K bytes. The computer has a 127 millimeter diagonal black and white electromagnetic CRT. A 32 character per line thermal printer/plotter is part of the unit. Programs or data may be stored on and read from magnetic tape cartridges. To interface with peripheral equipment, an I/O ROM and an interface card were added to provide HP-1B (IEEE standard 488-1975) instrumentation capabilities.

2. Synthesizer/Function Generator HP-3325A

The Hewlett-Packard model 3325A synthesizer/function generator can produce three kinds of waveforms sine, square and triangular. The frequency range for sine waveform is from 1 mircoHertz to 21 megaHertz, frequency resolution of 1 mircoHertz below 100 kiloHertz and 1 milliHertz above 100

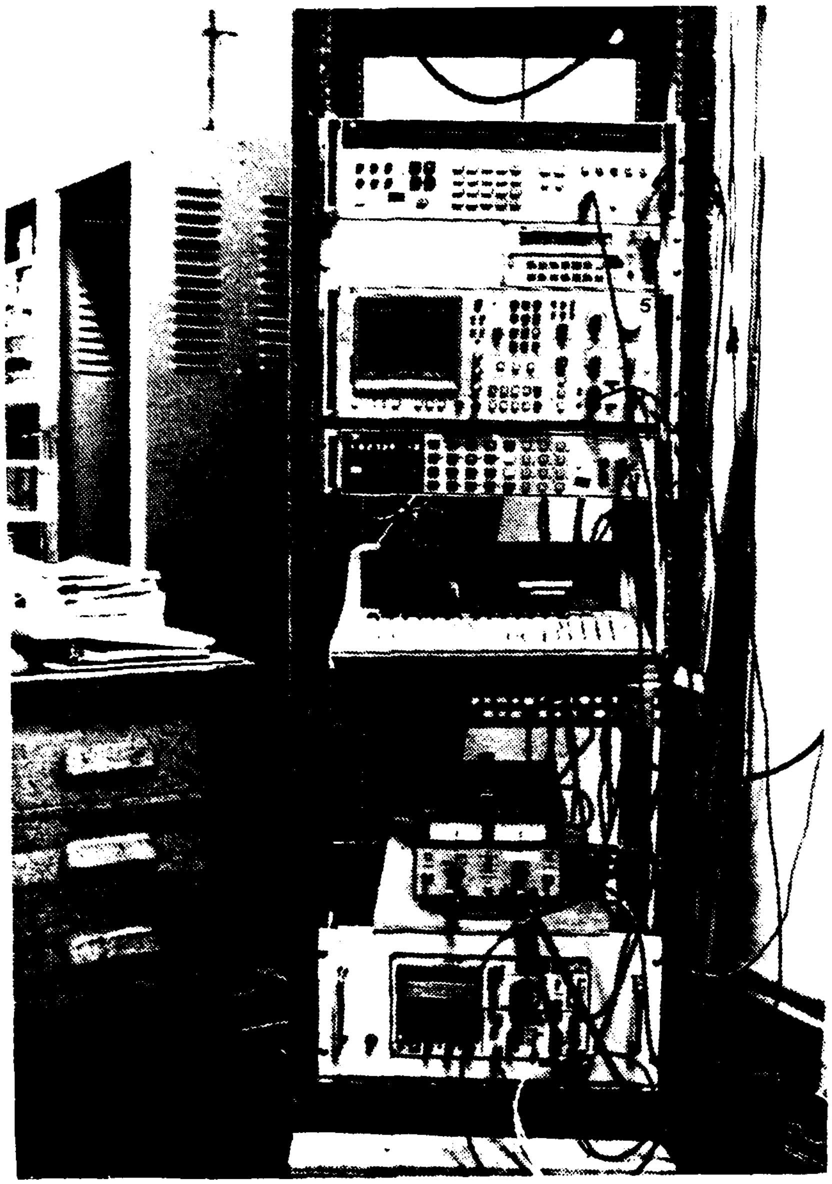

Figure 3.16 Instrumentation Package

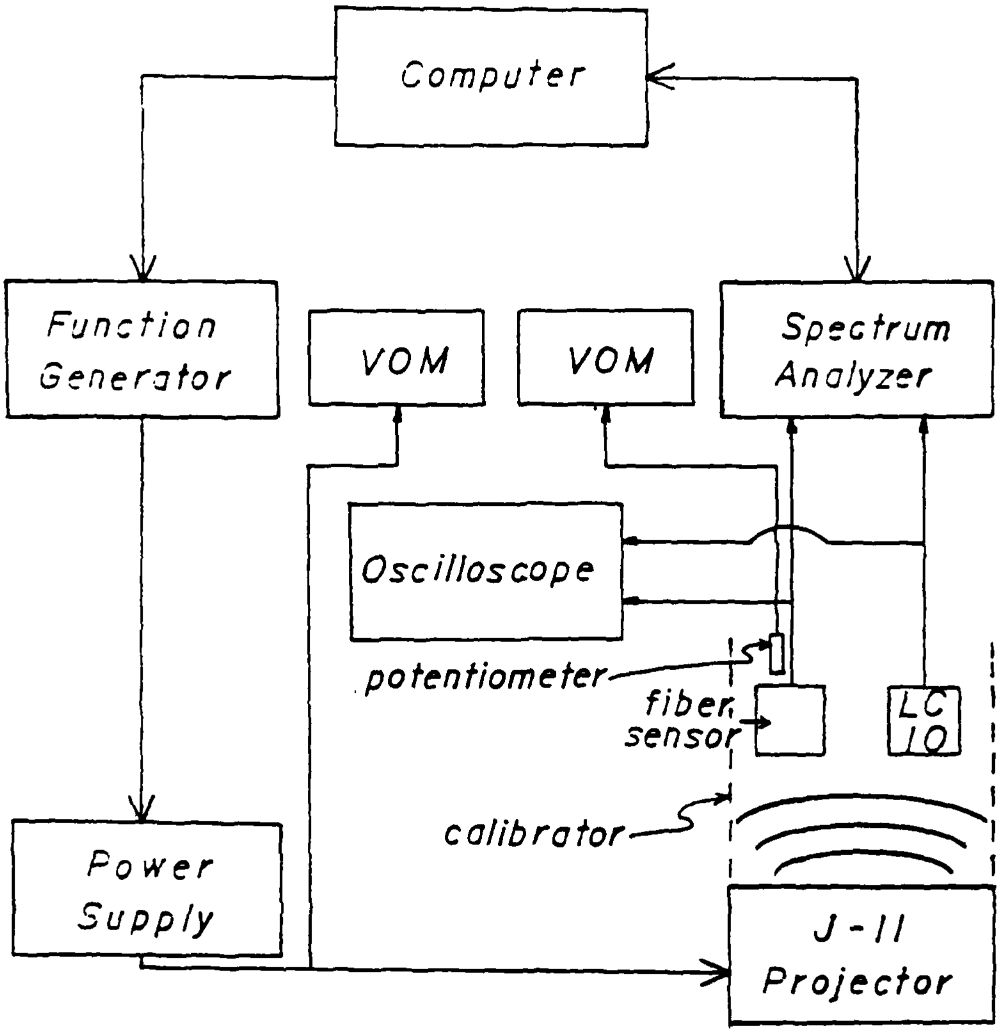

Figure 3.17 Block Diagram of Instrumentation System

kiloHertz with accuracy of $\pm$ 5X10^{-6} of selected value. The output amplitude is from 0 millivolts to 10 volts peak to peak into a 50 ohm load. This model is fully programable through a HP-1B connection. For this experiment sine waves of various frequency and amplitude were used.

3. <u>Spectrum Analyzer HP-3582A</u>

The Hewlett-Packard model 3582A is a dual channel spectrum analyzer. This instrument has a frequency range of 0.02 Hertz to 25,600 Hertz. The analyzer has a 11.9 by 9.6 cm CRT that can display two simultaneous information traces, plus four lines of alphanumeric data giving measurement confriguration and results. Frequency spans from 1 Hertz to 25,000 Hertz full scale allow flexibility in selecting the portion of the spectrum to be analyzed. Spans from 5 Hertz to 25,000 Hertz can be positioned anywhere within the frequency range of the instrument to provide excellent frequency resolution. The instrument's "front-end" sensitivity ranges can measure and analyze from 1 microvolt to 31.6 volts and has a dynamic range of 70 dB.

4. <u>Oscilloscope COS-5060</u>

The Kukisui model COS-5060 oscilloscope is a dual channel 60 MegaHertz instrument. Its vertical system provides calibrated deflection factors from 5 millivolts to 5 volts per division, with an accuracy of $\pm$ 3%. The horizontal system provides calibrated sweep speeds from 50 nanoseconds to 0.5 seconds per division. Trigger circuits enable stable triggering over the full bandwidth of the vertical system. This unit is used as a monitor of signal from the LC-10 and the optic fiber hydrophones only.

5. Digital Multimeter HP-3478A

The Hewlett-Packard model 3478A digital multimeter was used to monitor the potentiometer on the hand rotation device to obtain the approximate position of 632.8 nm gradient hydrophone during the laboratory phase. It was also used to monitor the resistance of the heliopot potentiometer on the rotating motor to give the approximate position of the hydrophone during the sea trail phase. The resistance measurement range is from 100 microohms sensitivity to 30 megaohms.

6. Bipolar Power Amplifier POW35-1A

The Kikusui model POW35-1A bipolar power amplifier was used to drive the J-11 projector in both the laboratory and sea trail experiments. It can supply power from -35 volts to +35 volts continuously at 1 ampere. The Kikusui will operate as a DC source, frequency response of slow 5 kiloHertz at ± 3 dB or frequency response of fast 30 kiloHertz at ± 3 dB. It has a 10 turn potentiometer with which to adjust output voltage gain.

7. Digital Multimeter HP-3456A

The Hewlett-Packard model 3456A digital voltmeter was used to monitor the voltage output of the J-11 projector during the laboratory and sea trail phases of the experiment. For AC r.m.s. voltage the voltmeter measurement range is from 0 to 10 volts ± 10 microvolts with 6 digit resolution and input impedance of 1 megaohm ± 0.5% shunted by < 75 picofarads.

8. Standard Hydrophone LC-10

An LC-10 hydrophone, (serial No. 2167 in calibrator and No. A695 in sea trial) was used as the standard hydrophone for sensitivity determinationa of the individual and gradient fiber optic hydrophones. Average free field voltage sensitivity for this hydrophone is specified by the manufacturer to be -209.2 dB re 1 volt/μPa.

9. Projector J-11

A J-11 projector was used as the sound source both in the laboratory and at sea for testing the hydrophones. Its operating range is from 20 Hertz to 12 kiloHertz. The maximum power above 100 Hertz is 200 watts. The efficiency for the J-11 is approximately -28 dB re ideal at 1 kiloHertz and the driving impedance is 23 ohms at 1 kiloHertz. The maximum depth allowed for operating the J-11 is 23 m. However, if the J-11 is operated below 100 Hertz the response characteristics change as a function of depth.

H. SEA TRIAL EXPERIMENTAL APPARATUS

The sea trial experimental apparatus was constructed for testing the directional properties of the fiber optic gradient hydrophone and for comparison with a standard DIFAR (directional) hydrophone. The apparatus was used to hold the J-11 projector, a rotating motor, a four channel pre-amplifier for the piezoelectric hyrophones and used to support the hydrophones themselves, as shown in Figure 3.18 a and b.

The sea trial apparatus was designed for use on the R/V Acañia. It consists of the J-11 projector and a watertight instrumentation package mounted on a rigid structure. The rigid structure is made of aluminum U channel that is 2.26 m in length and 0.122 m in width. It has two cross pieces of box aluminum bar that is 0.051 m X 0.051 m. One is 1.22 m in length and the other is 0.61 m in length. These are reinforced with a piece of aluminum bar welded below the box pieces which are used to support the J-11 projector. At the opposite end of the U channel is a rectangular plate used to support the watertight cannister which contains the rotating motor and the pre-amplifiers for the DIFAR phase, the 830 nm lasers, and the photodetectors for the fiber optic phase of the sea trials. To counteract the buoyancy caused by the watertight cannister and maintain the apparatus horizontal while submerged, counter balance weights of lead were added, 100 pounds. A detailed sketch of the top and side views of the apparatus is shown in Figure 3.19 a and b.

The center of the J-11 projector is suspended approximately 1.22 m below the aluminu m U channel and 1.69 m from the test hydrophones. The cannister holds the hydrophones

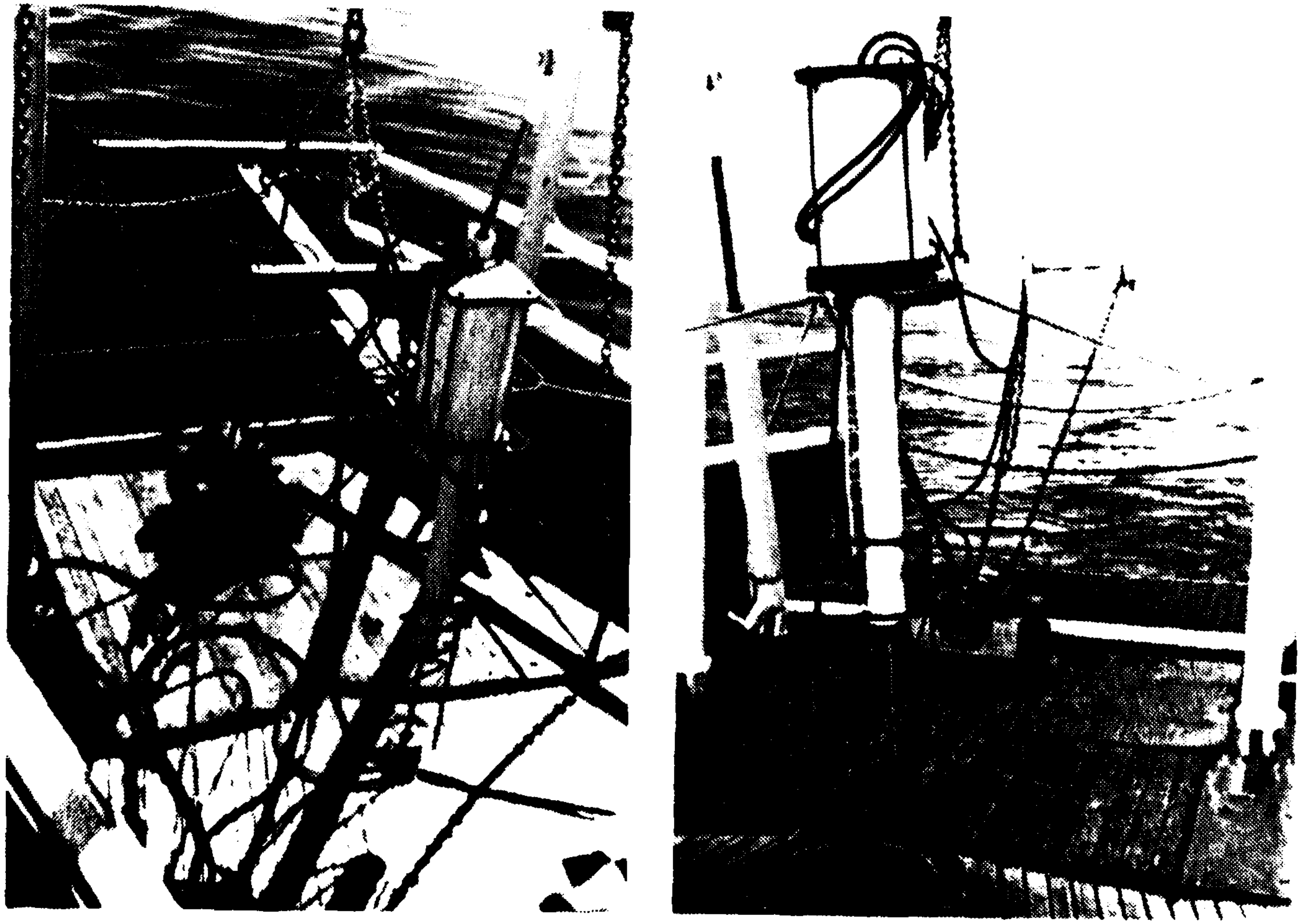

Figure 3.18 Sea Trial Apparatus

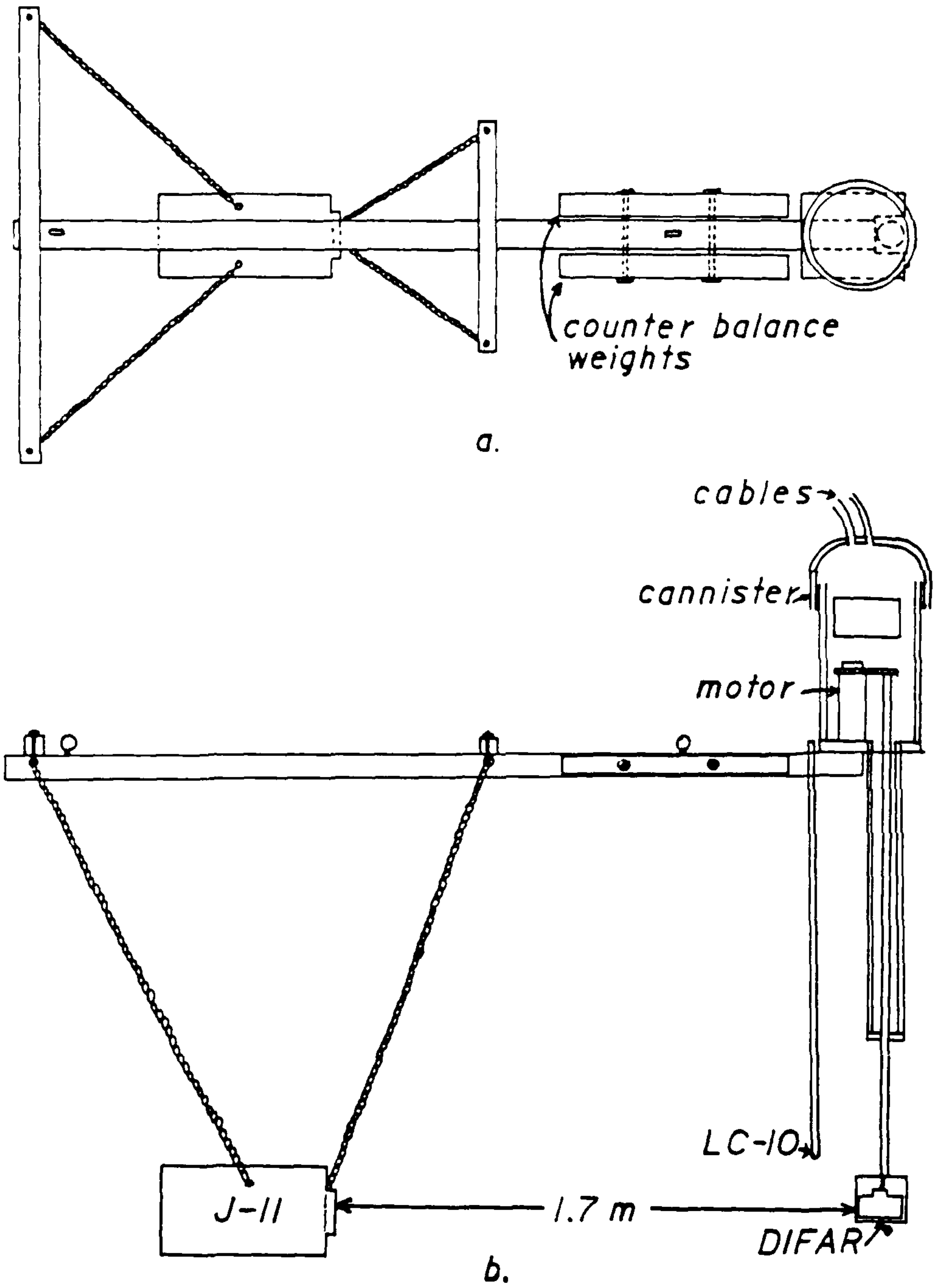

Figure 3.19 Sea Trial Apparatus

rigidly in place approximately 1.22 m below the aluminum U channel.

The motor is a 60 hertz 115 VAC Hurst synchronous motor, model GA, that has a 1 rpm rotation rate and can be used in the clockwise or counterclockwise direction. Attached to the motor is a precision potentiometer made by Helipot which has a value between 0 ohms to 10 kiloohms ± 5% corresponding to 360° rotation with linearity of ± 0.15 %.

The pre-amplifiers were used for the DIFAR hydrophone phase of the sea trail tests. It had four Burr-Brown OPA111 operational amplifiers to boost the signals from the omni, sine and cosine hydrophones of the DIFAR, a bender vane transducer, and for the reference LC-10 hydrophone. The circuit for this quad-amplifier system is shown in Figure 3.29.

A watertight cannister was designed and built to hold the rotating motor and the pre-amplifier electronics for the DIFAR phase, and, for the fiber optic phase, the rotating motor, the lasers and the photodetectors. The main section of the cannister was PVC Type 12454-B piping of 25.4 cm inner diameter and 45.1 cm in length. It had flat PVC plates, 2.5 cm thick, for upper and lower ends. Through the lower end two cables entered the cannister with O'ring watertight seals. At the lower end a 7.6 cm PVC 1120 ASTM D1785 piece of piping was glued into the plate. This allowed a stainless steel tube to be run from the motor to

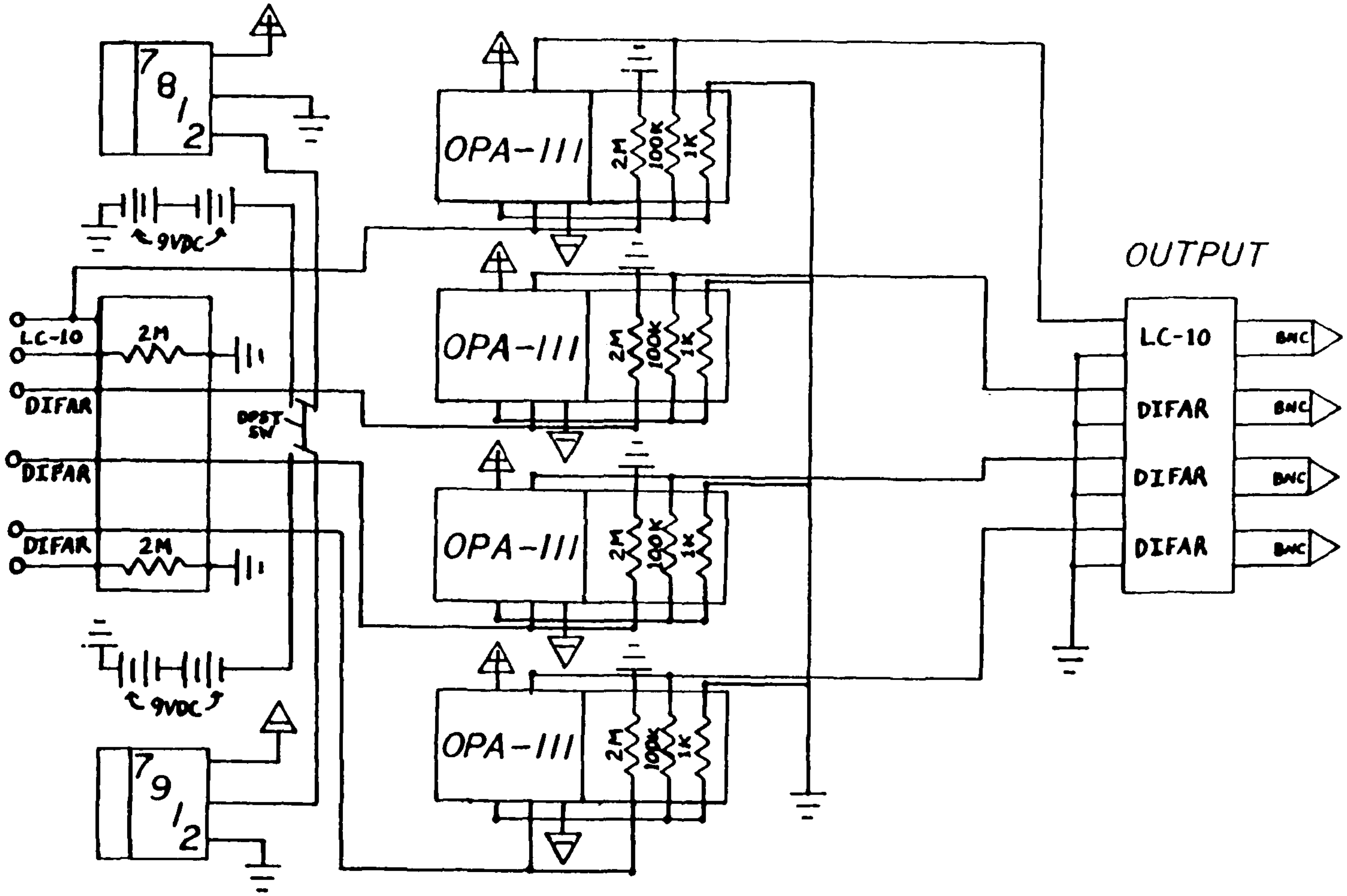

Figure 3.20 Quad-Amplifier Circuit

the hydrophones, maintaining the watertight integrity of the cannister while permitting rotation of the hydrophones. Maintaining the watertight integrity was accomplished by using a potting material and rubber tape at the bottom end of the steel tube and around the wires that entered. The steel tube can accommodate either wires or optical fibers.

IV. EXPERIMENTAL PROCEDURES AND RESULTS

A. INTERFEROMETER CHARACTERISTICS

Upon completing construction of the 632.8 nm interferometric system, shown in Figure 3.2, a test was conducted to check for proper operation. Detailed measurements were taken to determine the amplitude of the optical phase shift as a function of the drive voltage applied to the fiber wrapped piezoelectric cylinder in the reference arm of the interferometer. At the time of these tests only one sensor coil was included in the interferometer, i.e. refering to Figure 3.2, the sensor coil shown in the lower arm was not included.

A block diagram of the instrumentation used for gathering data with the system is shown in Figure 4.1. A sine wave of variable amplitude and frequency f was generated by the synthesizer/function generator HP-3325A and applied to the PZT. A HP-3582A spectrum analyzer and a COS-5060 Kikusui oscilloscope were used to monitor the output from one of the photodetectors.

Refering to equation (2.11), the AC portion of the photodetector signal is proportional to a sum of Bessel functions. To test the characteristics of the interferometer the piezoelectric cylinder is driven at a fixed frequency to examine the amplitudes of the fundamental and n^{th} order

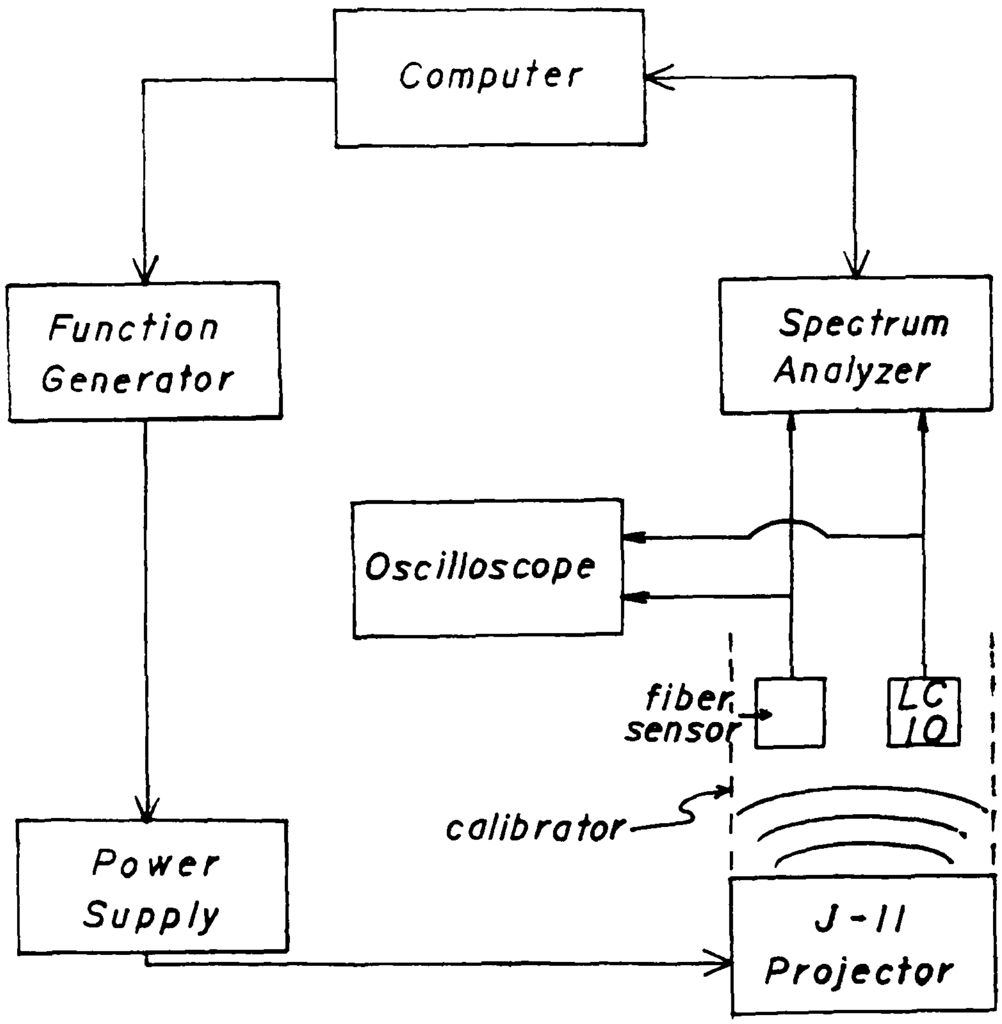

Figure 4.1 Block Diagram of Instrumentation System

harmonics as the voltage applied to the piezoelectric cylinder is increased.

Figure 4.2 shows the r.m.s. amplitude of the fundamental, 2nd and 3rd harmonics of the photodetector output as a function of the r.m.s. drive amplitude when the piezoelectric cylinder was driven at 1200 Hertz. This allows a comparison of the measured and theoretical maxima and minima of the Bessel functions. For example, the zero point of the fundamental for the Bessel function is 3.83 radians and the 2nd harmonic 5.14 radians. The ratio of the arguments of these zeroes is 1.34. Comparing the experimently determined piezoelectric drive voltage required to the zero the 2nd harmonic, 995 millivolts, to that of the fundamental, 735 millivolts, yields 1.35, which is within 0.7% of the theoretically predicted value. The sensitivity of the piezoelectric cylinder phase modulator at 1200 Hertz is the ratio argument of the zero of the Bessel function, 3.83 radians and the drive voltage at the zero of the fundamental, 735 millivolts, i.e. 5.21 rad/volts. Dividing this by the length of optical fiber wound on the cylinder, 7 meters, yields a modulator sensitivity of 0.744 rad/volt/m.

In Table I the voltages required to zero the fundamental of the voltage applied to the piezoelectric phase modulator are listed for the frequency range 100 to 2000 Hertz. As indicated in the graph shown in Figure 4.3, the piezoelectric sensitivity is relatively constant over this frequency

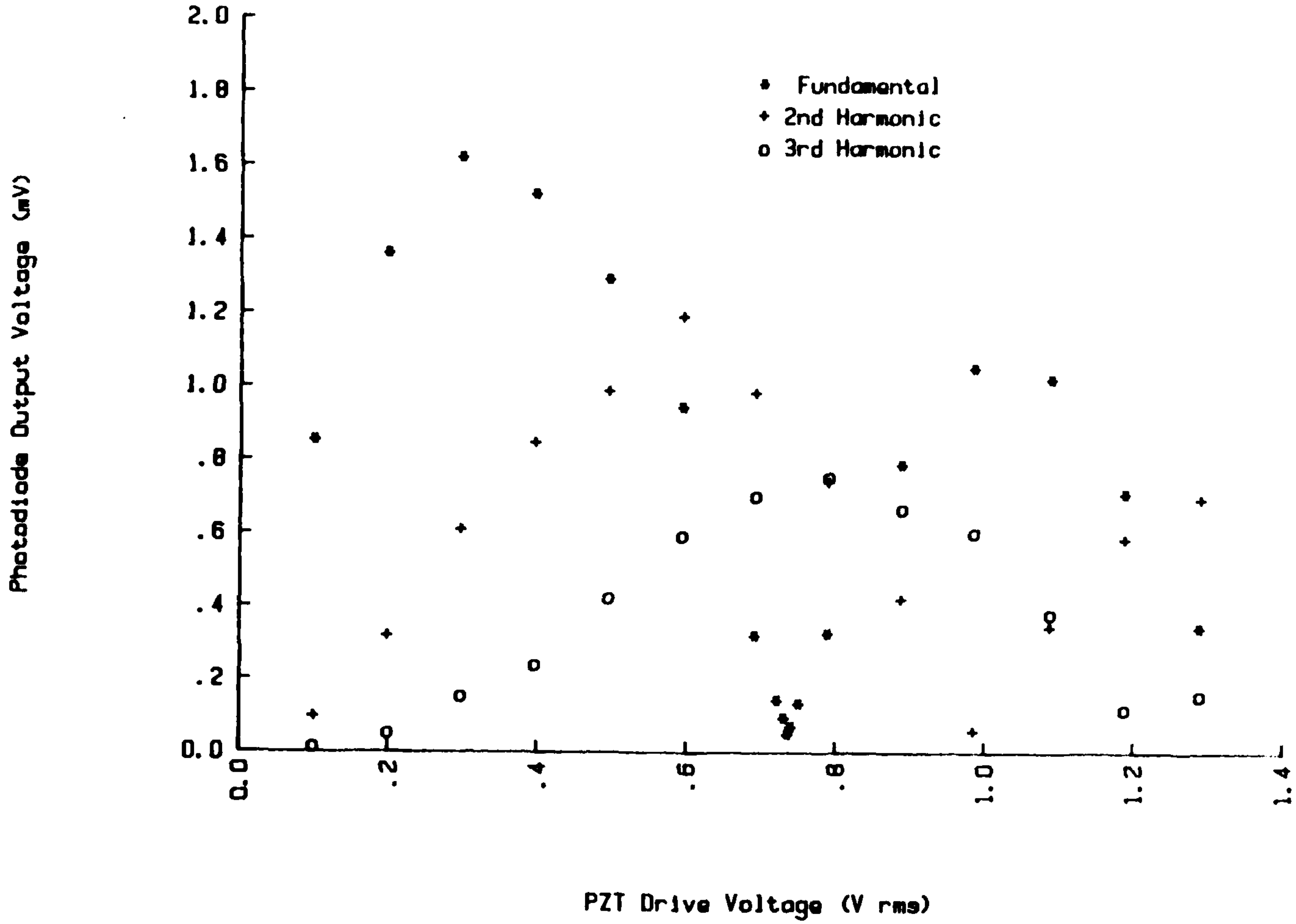

Figure 4.2 Piezoelectric Phase Modulator Response

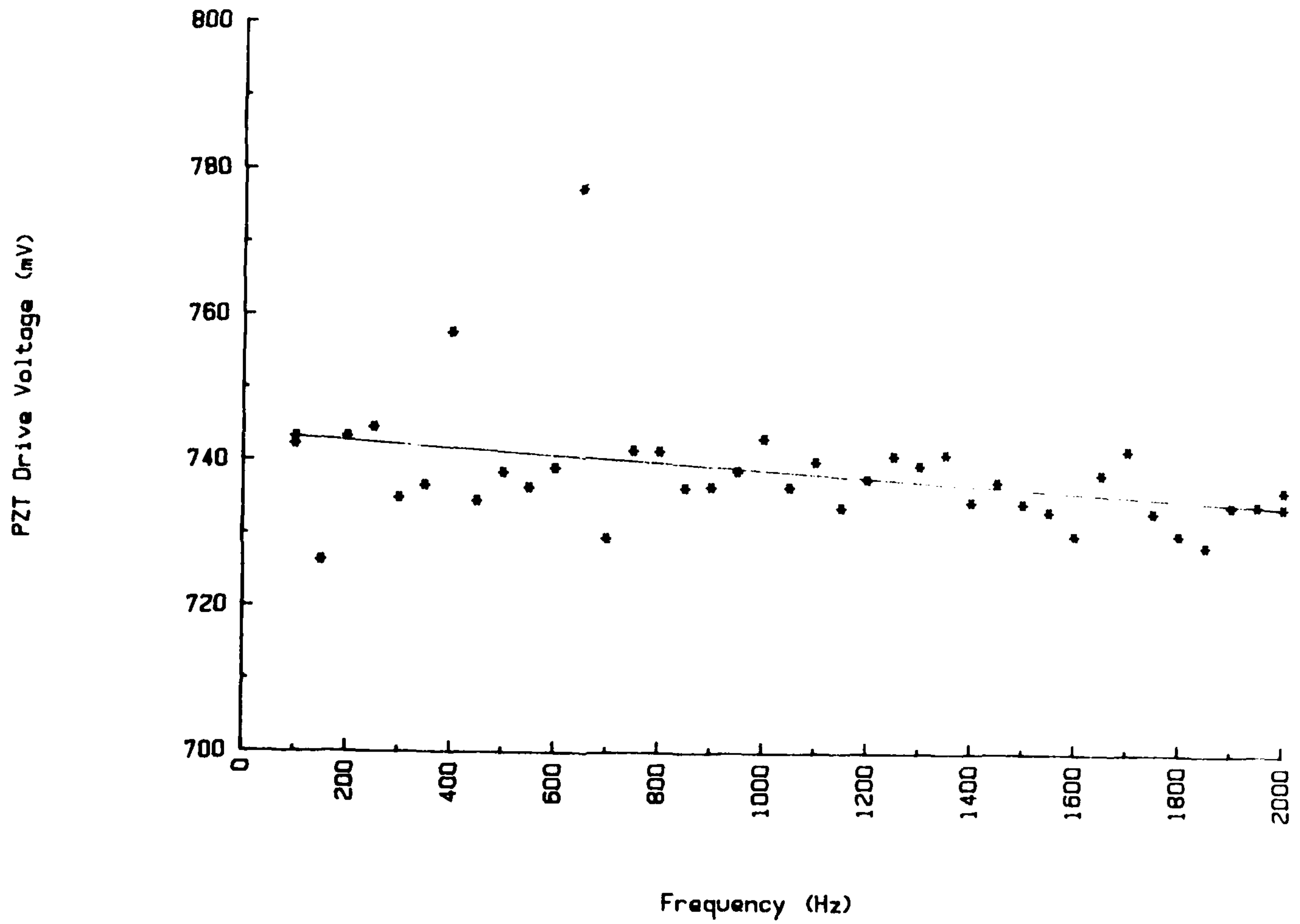

Figure 4.3 PZT Sensitivity Phase Modulator Frequency Response

TABLE I

Piezoelectric Sensitivity

Frequency (Hz)	Piezoelectric (mV)	Error %
100	742.3	0.03
150	726.3	1.68
200	743.3	0.15
250	744.6	0.92
300	734.9	0.82
350	736.7	1.48
400	757.6	6.09
450	743.5	0.24
500	738.5	1.75
550	736.4	0.66
600	739.1	1.04
650	777.3	5.95
700	729.4	1.45
750	741.5	0.03
800	741.4	0.33
850	736.3	0.03
900	736.5	0.19
950	738.7	0.47
1000	743.2	0.55
1050	736.5	0.60
1100	740.1	0.80
1150	733.8	0.66
1200	737.7	0.15
1250	740.9	0.58
1300	739.6	1.28
1350	741.2	1.56
1400	734.6	1.02
1450	737.3	0.62
1500	734.4	0.51
1550	733.3	0.89
1600	730.0	0.93
1650	738.4	0.15
1700	741.7	0.12
1750	733.2	0.17
1800	730.1	0.96
1850	728.6	1.47
1900	734.1	0.82
1950	734.2	0.69
2000	736.2	0.29

$PZT = 743.8 - (4.968 \times 10^{-3})\ f; \quad r = -0.336$

range. The data were least squares fit to a straight line yielding the following equation:

$$PZT = 743.8 - (4.963 \times 10^{-3})\ f \qquad (4.1)$$

where PZT is the voltage required to zero the fundamental, as listed in Table I, and f is the frequency. Therefore, the sensitivity ranges from 0.736 rad/volts/meter at 100 Hertz to 0.746 rad/volts/meter at 2000 Hertz. These interferometer characteristics are similar to those of the 830 nm system described by G. Mills [Ref. 8].

F. BESSEL FUNCTION RESPONSE

Absolute fiber sensitivity to acoustic pressure was determined by measuring the acoustic pressure required to null the interferometer output when the fiber hydrophone coil was submerged in the acoustic calibrator. As this process is quite tedious and time consuming a computer controlled data acquisition was devised. The calibrator acoustic pressure produced by the J-11 projector, was increased in amplitude while the outputs of the fiber optic and LC-10 hydrophones were monitored. Using the Bessel function theoretical curve as a basis, the zero of the fundamental of the fiber hydrophone output was approximated in the following manner. Since the output of the fiber optic hydrophone behaves like a sum of Bessel functions, equation (2.12), under computer control its fundamental was monitored, as the J-11 drive voltage was incrementally increased, to find the approximate peak amplitude of the fundamental. The computer approach employed was a five point parabolic least squares fit. A minimum of five amplitudes were required to run the least squares fit. The five points were obtained by determining a relative peak and using the two amplitudes on either side of it. The relative peak was determined by: first, an amplitude being less than the previous amplitude; second, taking the next amplitude which must be less than the previous two amplitudes.

The following general equation was used for the parabolic fit:

$$A(z) = az^2 + bz + c \tag{4.2}$$

where z was the J-11 drive voltage at each increment. The J-11 drive voltage (z_{max}), where the maximum for the fiber hydrophone occurs, was determined by taking the partial with respect to z:

$$\partial A(z)/\partial z|_{max} = 0 = 2az_{max} + b \tag{4.3}$$

giving

$$z_{max} = -b/2a \tag{4.4}$$

where a and b are coefficients for the least square fit of five measurements. To obtained the coefficients, the following series of equations were used:

$$\chi^2 = \sum_{i=-2}^{+2} \chi_i^2 = \sum_{i=-2}^{+2} [A(z_i) - A_i]^2 \tag{4.5}$$

where $x_i = x_0 + i\delta$ giving:

$$\chi_{-2} = 4\delta^2 a - 2\delta b + c - A_{-2} \tag{4.6}$$

$$\chi_{-1} = \delta^2 a - \delta b + c - A_{-1} \tag{4.7}$$

$$\chi_0 = c - A_0 \tag{4.8}$$

$$\chi_1 = \delta^2 a + \delta b + c - A_1 \tag{4.9}$$

$$\chi_2 = 4\delta^2 a + 2\delta b + c - A_2 \tag{4.10}$$

To find the values of the coefficients a, b and c at which χ^2 is a minimum, the following conditions mus hold:

$$\partial\chi^2/\partial a|_0 = 0 \tag{4.11}$$

$$\partial\chi^2/\partial b|_0 = 0 \tag{4.12}$$

$$\partial\chi^2/\partial c|_0 = 0 \tag{4.13}$$

Combining equations 4.5 through 4.12 generates the following relations:

$$34\delta^2 a + 10c = 4(A_{+2} + A_{-2}) + (A_{+1} + A_{-1}) \tag{4.14}$$

$$\delta b = [2(A_{+2} + A_{-2}) + A_{+1} - A_{-1}]/10 \tag{4.15}$$

$$20\delta^2 a + 10c = 2(A_{+2} + A_{-2} + A_{+1} + A_{-1} + A_0) \tag{4.16}$$

Subtracting (4.15) from (4.13) gives:

$$\delta^2 a = [2(A_{+2} + A_{-2} - A_0 - A_{+1} - A_{-1})]/14 \tag{4.17}$$

Using equations (4.14) and (4.16) to find the coefficients a and b, where δ is the J-11 drive voltage increment, gives z_{max} equation (4.3).

Since the Bessel function is approximately linear about the zero crossing, the output voltages were calculated for 10% and 5% less than and greater than the zero crossing voltage using the following equations:

$$X(1) = INT(1.873*z_{max}) \qquad (4.18)$$

$$X(2) = INT(1.977*z_{max}) \qquad (4.19)$$

$$X(3) = INT(2.185*z_{max}) \qquad (4.20)$$

$$X(4) = INT(2.289*z_{max}) \qquad (4.21)$$

Linear extrapolation of the calculated J-11 drive voltages was then performed to obtained the average, which is taken as the intercept. The LC-10 output voltages for the respective J-11 drive voltages were also linearly extrapolated to obtain the average LC-10 output voltage at the zero crossing.

C. CALIBRATOR CHARACTERISTICS

Upon completion of construction of the calibrator, as described in Chapter III Section A, its various resonance frequencies were determined. These were at 218 Hertz, 432 Hertz, 517 Hertz and 683 Hertz. At these resonance frequencies the positions of the various pressure maxima and minima were determined. These yielded values for the speed of sound at each frequency in the calibrator for a water depth of 49.6 cm as tabulated in Table II.

TABLE II

Calibrator Speed of Sound

Frequency (Hz)	Speed of Sound (cm/sec)
218	30,360
432	29,877
517	26,625
683	27,525

These values of sound speed yield an average speed of sound in the calibrator of c = 28,600 cm/sec ± 6.3%.

The standing wave pressure field within the calibrator was examined using the LC-10 standard hydrophone. Its output at 683 Hz, a function of depth is tabulated in Table III. The J-11 projector was driven at 700 mV. The LC-10 output vs the depth in the calibrator is shown graphically in Figure 4.4. Readings below 37.5 cm were not obtained since they were not needed for the gradient hydrophone sensitivity portion of the tests. Figures 4.5, 4.6 and 4.7 show the standing wave acoustic field at the resonant frequencies 517 Hz, 432 Hz and 218 Hz respectively.

TABLE III

Standing Wave Acoustic Field for 683 Hz

Depth (cm)	LC-10 (mV)
1	0.390
2	0.676
3	0.956
4	1.22
5	1.49
6	1.71
7	1.84
8	1.91
9	1.94
10	1.96
11	1.93
12	1.77
13	1.59
14	1.32
15	1.07
16	0.824
17	0.485
18	0.185
19	0.106
20	0.420
21	0.703
22	0.907
23	1.10
24	1.26
25	1.40
26	1.42
27	1.44
28	1.40
29	1.22
30	1.06
31	0.864
32	0.701
33	0.539
34	0.456
35	0.541
36	0.731
37	0.954
37.5	1.09

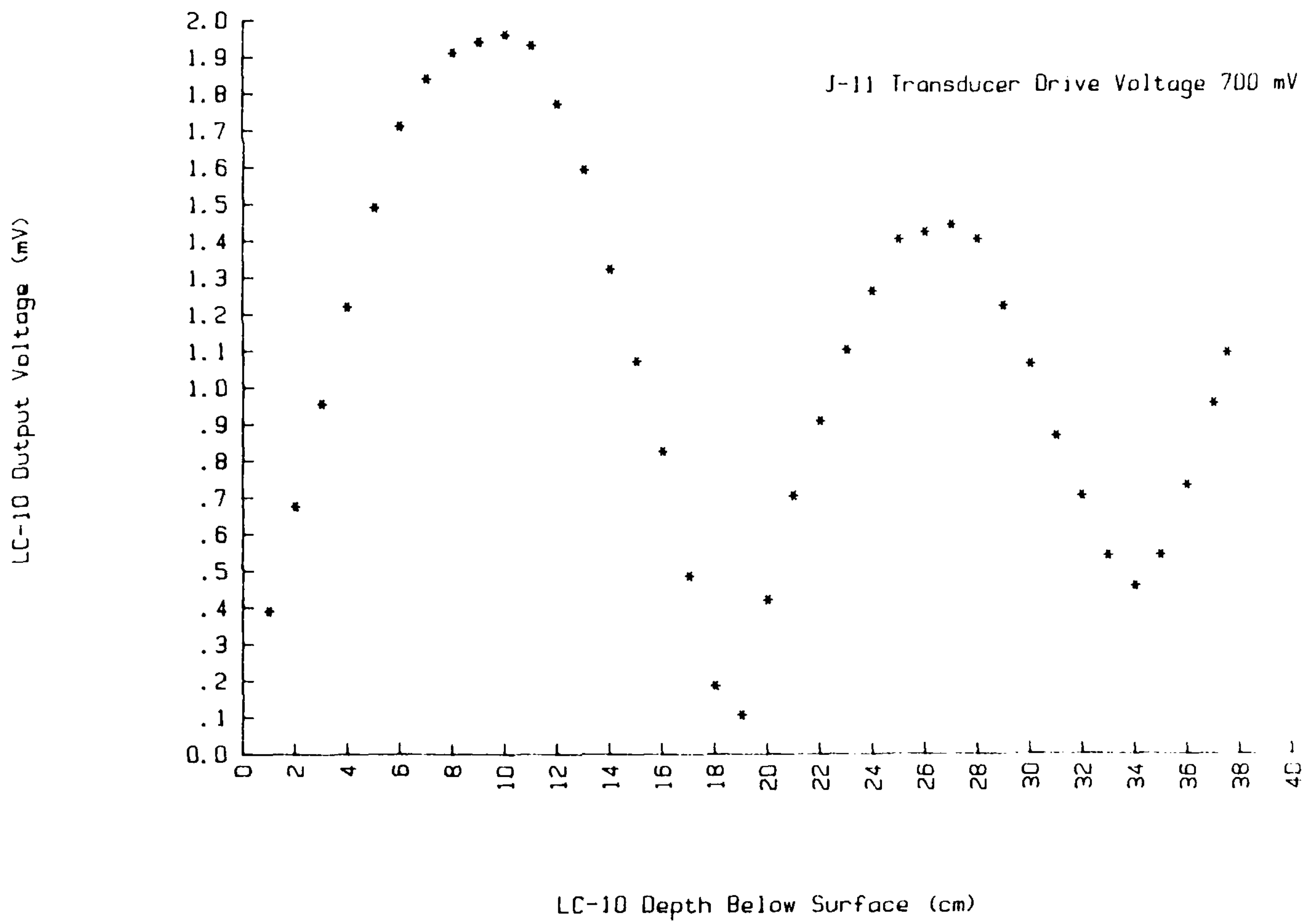

Figure 4.4 Standing Wave Acoustic Field for 683 (Hz)

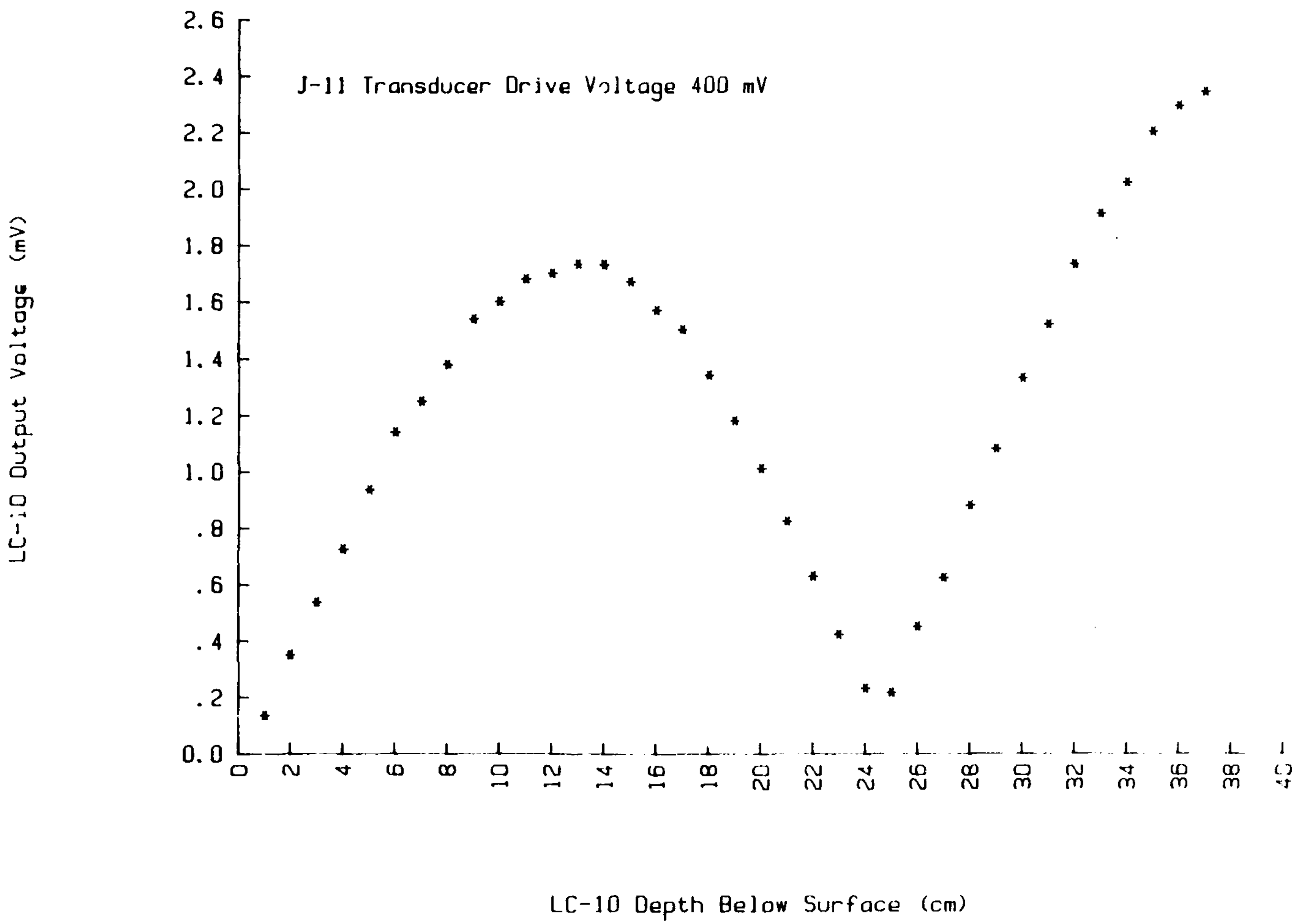

Figure 4.5 Standing Wave Acoustic Field for 517 (Hz)

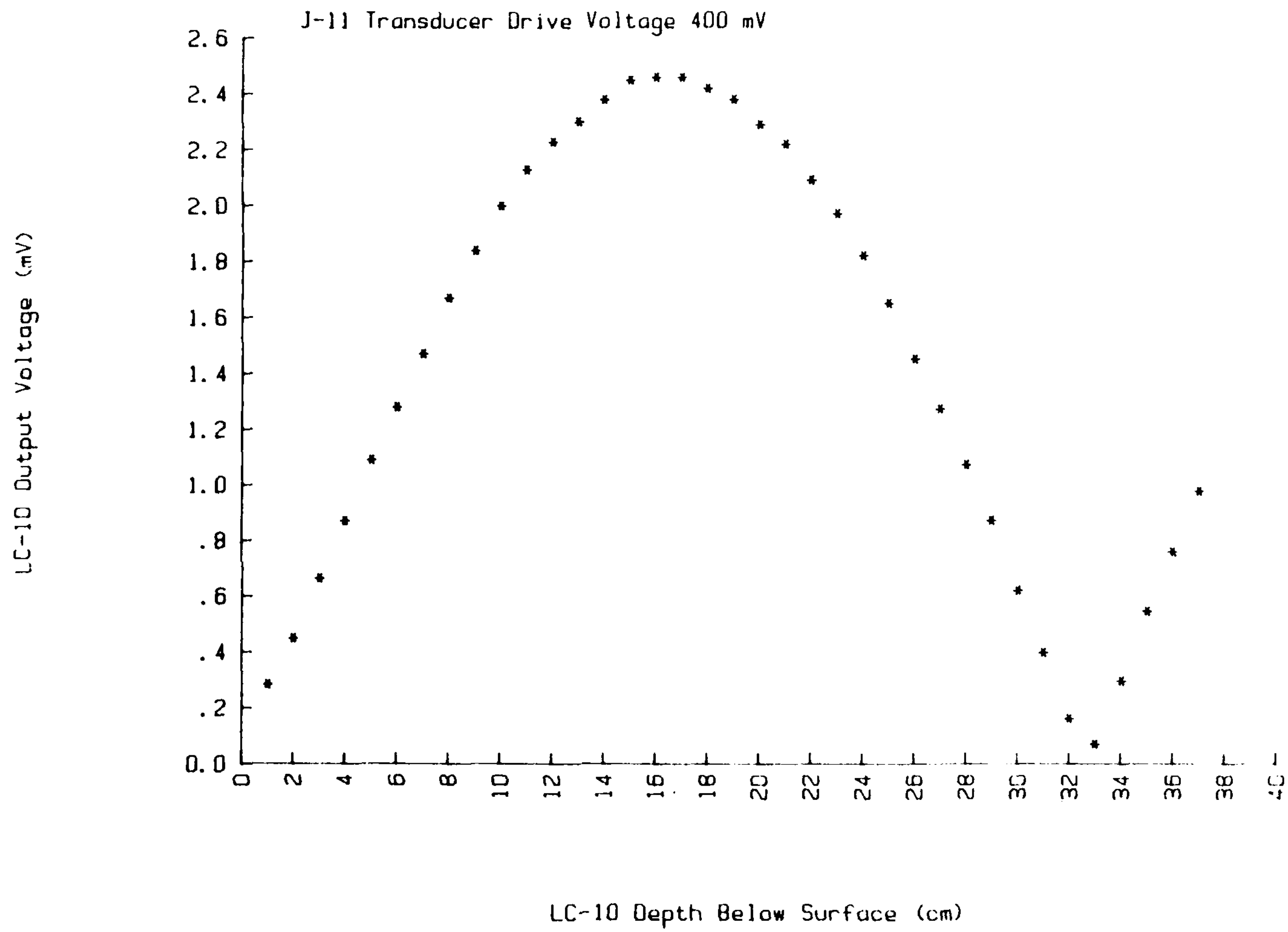

Figure 4.6 Standing Wave Acoustic Field for 432 (Hz)

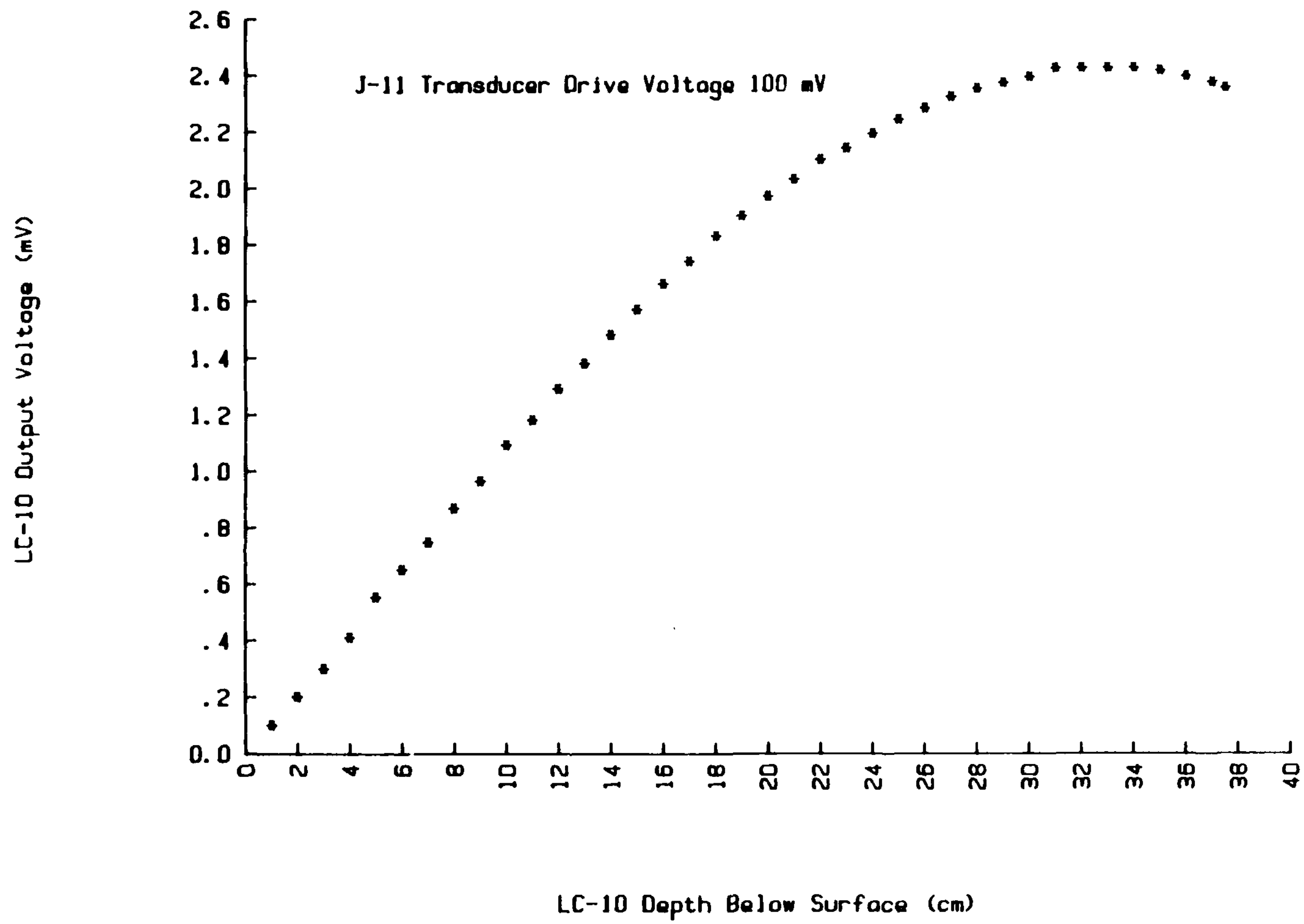

Figure 4.7 Standing Wave Acoustic Field for 218 (Hz)

D. INDIVIDUAL SENSOR SENSITIVITY

The individual 632.8 nm fiber optic hydrophone sensitivities for were determined in the calibrator described in Chapter III Section A. The sensitivity of hydrophone #2 was obtained while the interferometer contained only the one hydrophone coil in one arm and had a fiber wound piezoelectric (PZT) cylinder in the other arm. The hydrophone coil was positioned at the various pressure peaks at each of the four resonant frequencies. The computer program described in section B and listed in Appendix A was used to find the approximate LC-10 voltage output, i.e. the acoustic pressure, where the interferometer output nulled. The output of the photodiode was sent to the spectrum analyzer HP-3582A and to the oscilloscope Kikusui COS5060 so that the amplitude of its various frequencies component could be monitored and recorded by the computer. The instrumentation system used for the data acquisition is the same as shown in Figure 4.1.

After the initial computer data acquisition runs were completed, data also was obtained by hand at each calibrator resonance to determine as closely as possible the zero crossings of the fundamental and the 2^{nd} harmonic of the interferometer output. A graph of such data obtained at 517 Hz (with coil depth at 40.5 cm) is shown in Figure 4.8 and also listed in Appendix B. Computer controled data

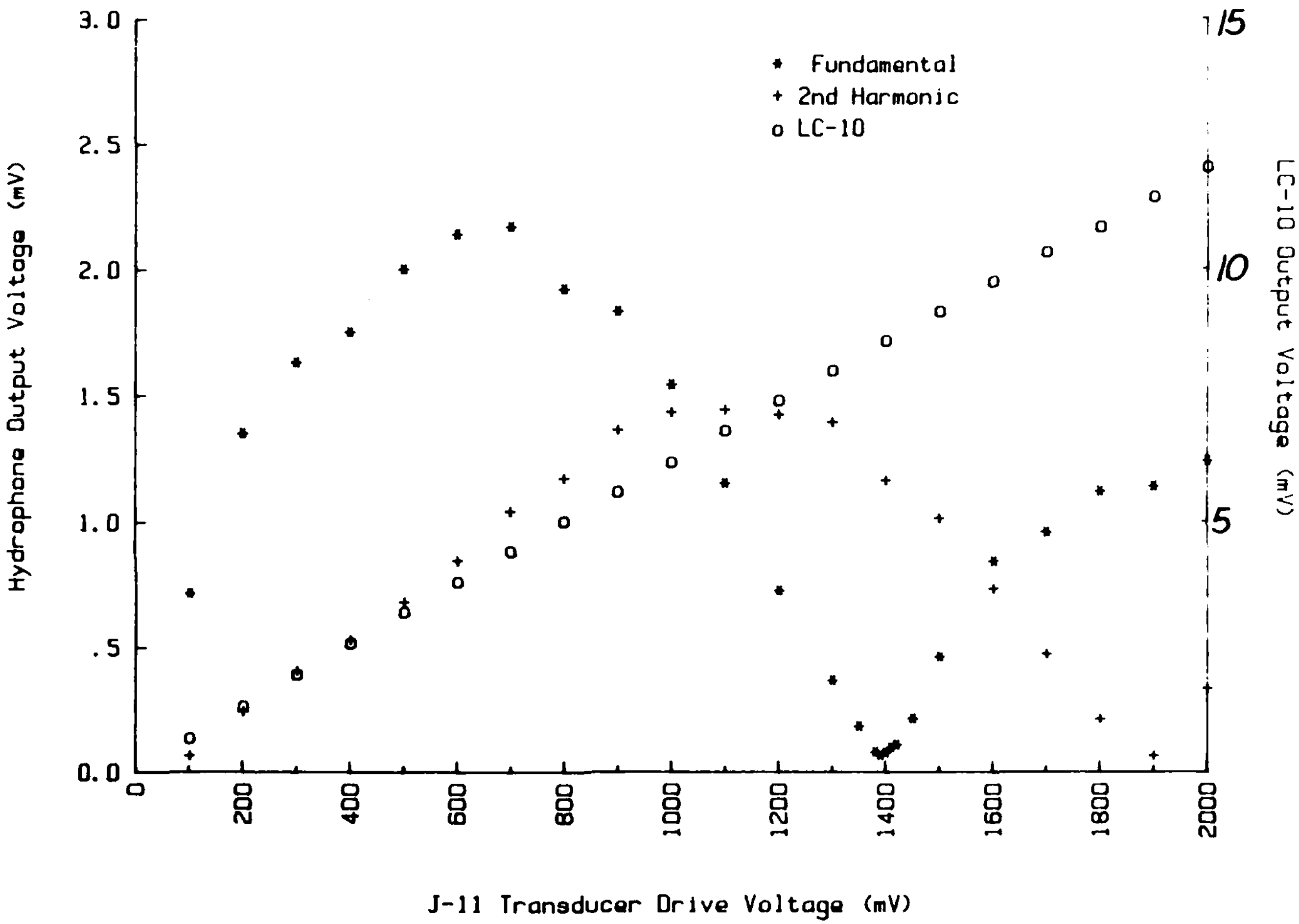

Figure 4.8 Single Hydrophone Sensitivity at 517 Hz

acquisition runs also were made at each calibrator resonant frequency to check the repeatability of the data.

The sensitivity of each fiber optic hydrophone was determined at the four resonant frequencies. Then a comparison was made of the fundamental and the 2nd harmonic behavior to that of the theoretical Bessel function characteristics of maxima and minima ratios. As Table IV shows the ratio data obtained on both fiber optic hydrophones #1 and #2 is within a few percent of the expected (theoretical) values for the Bessel function and independent of frequency.

TABLE IV

Bessel Function Ratio of Maxima & Minima

	Hydrophone 1		Hydrophone 2	
Frequency (Hz)	minima	maxima	minima	maxima
218	1.3981	1.6667	1.3298	1.5200
432	1.3495	1.6250	1.3350	1.6900
517	--	--	1.3525	1.6923
683	1.3440	1.7290	1.3758	1.6807

Bessel Function Theoretical Ratio of Minima - 1.3420

Maxima - 1.6576

After the sensitivity data was obtained for hydrophone #2, hydrophone #1 was installed into the arm with the PZT: making the system an interferometric gradient hydrophone.

The sensitivities obtained for both hydrophones #1 and #2 were different even though 10 m of fiber was wound on each mandrel. The difference could be due to the fact that a portion of the leads of hydrophone #2 were in the calibration tube during data acquisition for hydrophone #1. To determine if the presence of the leads of hydrophone #2 were baising the results of the sensitivity of hydrophone #1, all but a few centimeters were removed from the water and hydrophone #1 was set near a pressure maxima (9 cm) for 683 Hz. Hydrophone #2 was also tested in this manner to check for consistency of the sensitivity when it was the only hydrophone in the interferometer. The data obtained by hand for hydrophone #2, as the only hydrophone in the interferometer. was within 0.4% of that obtained when it was part of the gradient hydrophone at the resonant frequency of 683 Hz.

The LC-10 output voltage at the fundamental minimum which occurs at a optical phase shift of 3.83 radians and the known sensitivity of the LC-10 hydrophone are combined to determine the sensitivity of an individual fiber optic hydrophone using the following equation:

$$M_F = M_{LC-10} * 3.83 / V_{LC-10} \qquad (4.22)$$

where M_{LC-10} is the sensitivity of the LC-10 hydrophone in volts/μPa obtained from the manufacturer's specifications (Chapter 3 Section G.8), V_{LC-10} is the output voltage of the LC-10 at the fundamental minimum. M_F is the sensitivity of a fiber optic hydrophone. The sensitivities of the individual fiber optic hydrophones are indicated at the four calibrator resonant frequencies in Table V.

TABLE V

Individual Fiber Optic Hydrophone Sensitivity

Freq	Hydrophone 1: Depth of Hyd from surface boundary (cm)	Hydrophone 1: Nos. of runs	Hydrophone 1: Avg. M_F $\frac{\mu rad}{\mu Pa}$ 10^{-3}	Hydrophone 1: Std dev $\frac{\mu rad}{\mu Pa}$ 10^{-3}	Hydrophone 2: Depth of Hyd from surface boundary (cm)	Hydrophone 2: Nos. of runs	Hydrophone 2: Avg. M_F $\frac{\mu rad}{\mu Pa}$ 10^{-3}	Hydrophone 2: Std dev $\frac{\mu rad}{\mu Pa}$ 10^{-3}
218	33.0	6	10.24	0.68	33.6	2	11.96	0.29
218	34.5	4	10.93	0.60				
218	35.7	7	11.60	1.17				
432	15.5	10	12.24	1.44	17.8	1	11.60	---
432	16.5	5	13.92	0.60				
432	16.7	3	12.89	0.36				
517	13.5	3	15.57	0.15	40.5	2	13.44	2.26
517	14.5	3	17.25	0.22				
517	15.2	2	16.60	0.00				
683	9.0	4	14.76	0.29	8.5	3	10.89	0.59
683	9.5	2	15.90	2.00				
683	10.0	4	16.60	0.64				
683*	9.0	13	9.05	1.42	9.0	8	12.37	0.97
683**	9.0	1	10.54	---	9.0	1	11.60	---

* special set of data obtained while one fiber optic hydrophone was not immersed.

** special data obtained by hand to acquire the sensitivity of the fiber optic hydrophones as accurately as possible.

E. GRADIENT SENSOR SENSITIVITY

The two individual fiber optic hydrophones discussed in Section D were combined into a fiber optic gradient hydrophone as described in Chapter III Section F.1. The sensitivity of the gradient hydrophone was obtained at the

683 Hz calibrator resonant frequency. The gradient hydrophone was positioned so that one hydrophone was 5 cm above and one 5 cm below the pressure minima with the LC-10 reference hydrophone at the minima itself. The instrumentation system used is shown in Figure 4.9.

The J-11 projector drive voltage was increased, as in the individual hydrophone sensitivity data acquisition. until a zero crossing was located for the fundamental at a particular frequency. Since, the LC-10 output voltage at a pressure minima was very low it could not be used in computing the gradient hydrophone sensitivity directly. Therefore, the LC-10 hydrophone was moved to the maxima, 10 cm from the water surface, while the fiber optic gradient hydrophone remained centered at the minima.

The output voltage , V_{LC-10}, and the sensitivity, M_{LC-10}, of the LC-10 were used to find the pressure P_{rms} in the following equation:

$$P_{rms} = V_{LC-10}/M_{LC-10} \qquad (4.23)$$

The peak pressure P_o or P_{max} is calculated from the following equation:

$$P_o = \sqrt{2}\, P_{rms} \qquad (4.24)$$

The maximum pressure gradient ∇P is calculated from the following equation:

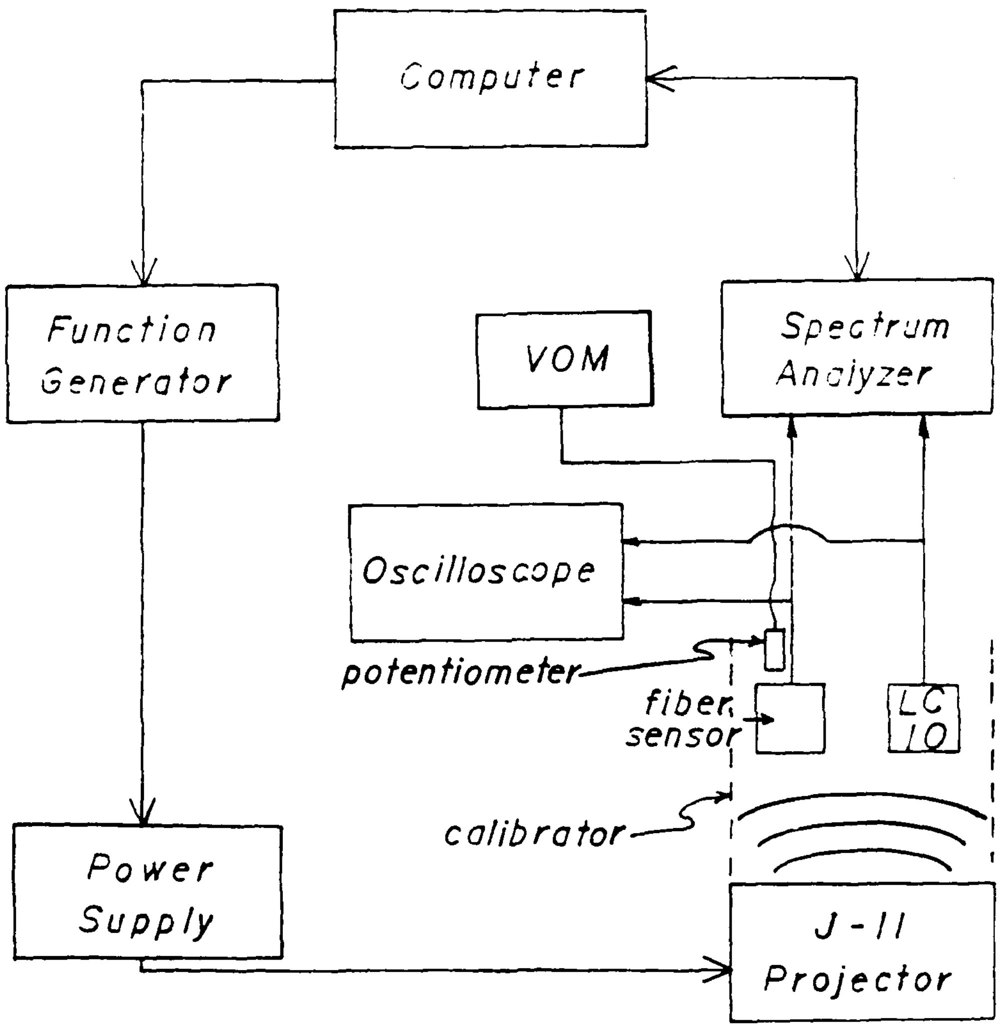

Figure 4.9 Block Diagram of Instrumentation System

$$\nabla P = kP_o \tag{4.25}$$

or

$$\nabla P = 2\pi P_o/\lambda \tag{4.26}$$

where $k = 2\pi/\lambda$ is the wave number and λ is the wavelength of the resonant sound in the calibration tube.

The sensitivity of the gradient hydrophone can be calculated directly by using the following equation:

$$M_{GH} = 3.83/\nabla P \tag{4.27}$$

where M_{GH} is the directly calculated sensitivity of the fiber optic gradient hydrophone and 3.83 is the phase shift in radians when the pressure gradient is sufficient to null the amplitude of the fundamental interferometer response. The units of the fiber optic gradient hydrophone sensitivity are μrad/μPa/cm.

The fiber optic gradient hydrophone sensitivity is calculated indirectly by using the sensitivities of both individual hydrophones in the following equation:

$$M_{ID} = (\phi_1 - \phi_2)/\nabla P \tag{4.28}$$

where M_{ID} is the indirectly calculated gradient hydrophone sensitivity. ϕ_1 and ϕ_2 are the phase shifts in the individual hydrophones, respectively [Ref. 8].

The phase shifts can be calculated by using the pressure value and the sensitivities of each individual hydrophone:

$$\phi_1 = P_+ * M_{H1} \quad (4.29)$$

and

$$\phi_2 = P_- * M_{H2} \quad (4.30)$$

where P_+ and P_- are the pressure amplitudes at the individual hydrophone location and M_{H1} and M_{H2} are the sensitivities of the respective individual hydrophones. The linear approximation at a pressure in the standing wave is:

$$P_{\pm} = \nabla P(d/2) \quad (4.31)$$

Substituting equations (4.30), (4.31) and (4.32) into (4.29) generates:

$$M_{ID} = P_{\pm} [M_{H1} + M_{H2}] / \nabla P \quad (4.32)$$

and substituting equation (4.27) into (4.33) generates:

$$M_{ID} = [M_{H1} + M_{H2}]/[2/\Delta x] \quad (4.33)$$

where $\Delta x = d = 10$ cm.

The directly calculated sensitivity for the 632.8 nm interferometric fiber optic gradient hydrophone at 687 Hz is:

$$M_{GH} = 0.097 \pm 0.011 \ \mu\text{rad}/\mu\text{Pa/cm}.$$

The average value used for V_{LC-10} was 12.46 ± 1.24 mv. The values used for M_{LC-10} and λ was 34.67×10^{-9} mV/μPa and 40.3 cm respectively.

The indirectly calculated sensitivity for the gradient hydrophone at 683 Hz is:

$$M_{ID} = 0.111 \pm 0.0075\ \mu rad/\mu Pa/cm.$$

The values used for the individual hydrophones M_{H1} and M_{H2} are $10.54 \times 10^{-3}\ \mu rad/\mu Pa$ and $11.60 \times 10^{-3}\ \mu rad/\mu Pa$ respectively. The agreement between M_{GH} and M_{ID} is well within experimental error.

The fiber optic gradient hydrophone was examined for its ability to determine a direction of the sound source as well as the acoustic level. Data was obtained for the directionality of the gradient hydrophone at a resonant frequency of 683 Hz in the calibration tube. The LC-10 reference hydrophone was placed at the pressure maximum (10 cm) and the fiber optic gradient hydrophone was centered at the pressure minimum (18 cm) and then rotated. For each orientation the J-11 drive voltage was adjusted to zero the fundamental component of the gradient hydrophone output. The data in Table VI indicates that the fiber optic gradient hydrophone produces the predicted directional dipole response, as shown in Figures 4.10 and 4.11 for separate rotation runs. The vertical position of the hydrophone in the calibration tube corresponds to 90° in the graph, Figure 4.12.

F. ANALYSIS

The material used for the mandrels in the 632.8 nm interferometric system, Stycast 1266 epoxy, was chosen for its low viscosity, machinability and the material

AD-A156 469 FIBER OPTIC GRADIENT HYDROPHONE CONSTRUCTION AND CALIBRATION FOR SEA TRIAL(U) NAVAL POSTGRADUATE SCHOOL MONTEREY CA G E MACDONALD MAR 85 2/2

UNCLASSIFIED F/G 17/1 NL

END
FILMED
DTIC

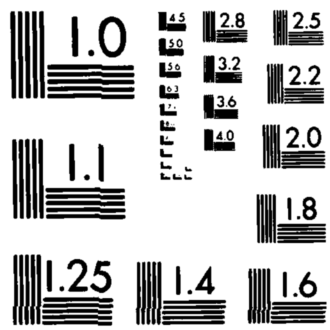

MICROCOPY RESOLUTION TEST CHART
NATIONAL BUREAU OF STANDARDS-1963-A

TABLE VI

Gradient Hydrophone Dipole Data

Position degrees	J-11 drive voltage (V)	LC-10 output voltage (mV)	$\frac{3.83*M_{LC-10}}{V_{LC-10}}$ rad/Pa X 10^{-3}
0	15.18	87.3	1.52
10	22.75	77.8	1.71
20	14.26	50.7	2.62
30	8.55	30.8	4.31
60	4.44	16.3	8.13
90	3.86	14.3	9.28
120	4.61	17.1	7.75
150	9.51	34.9	3.81
180	16.41	60.1	2.21
190	26.78	84.2	1.58
200	13.86	47.4	2.80
210	9.28	33.9	3.91
240	4.46	16.1	8.27
270	3.46	12.7	10.48
300	4.00	14.1	9.40
330	8.55	29.1	4.56

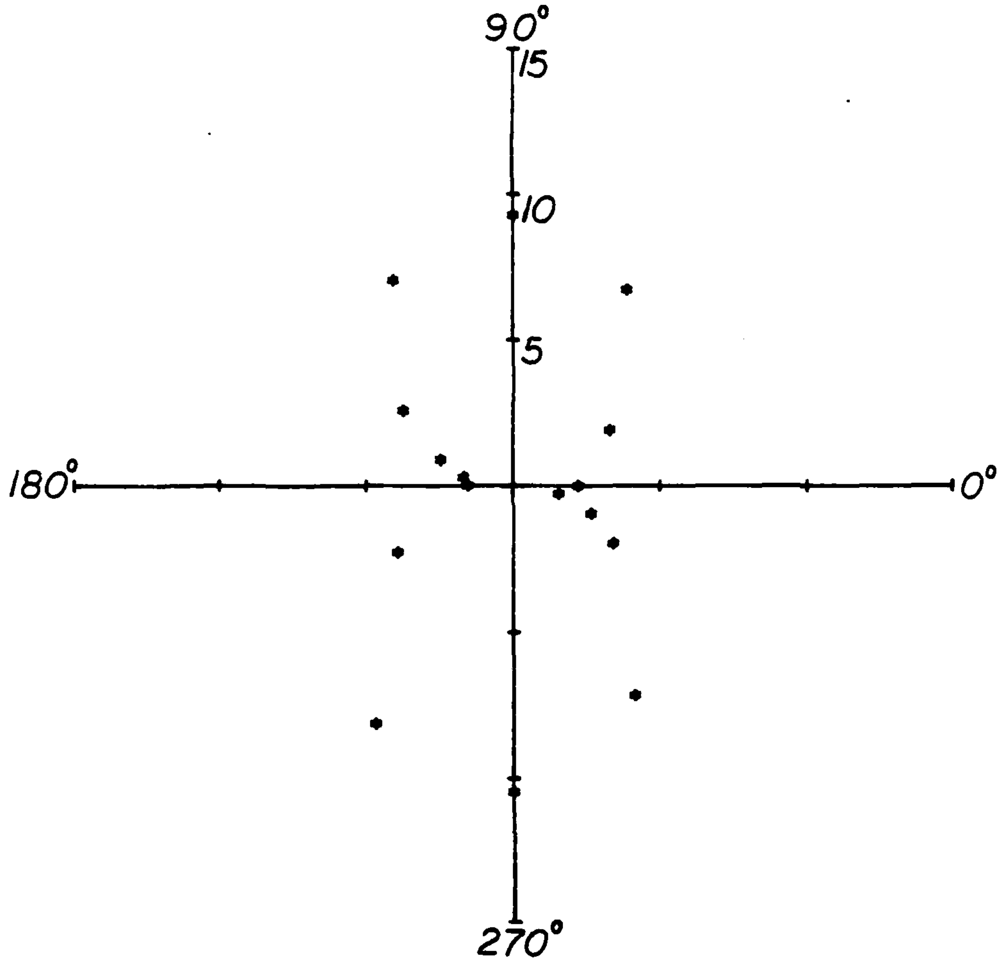

Figure 4.10 Fiber Optic Gradient Hydrophone
Directivity Pattern

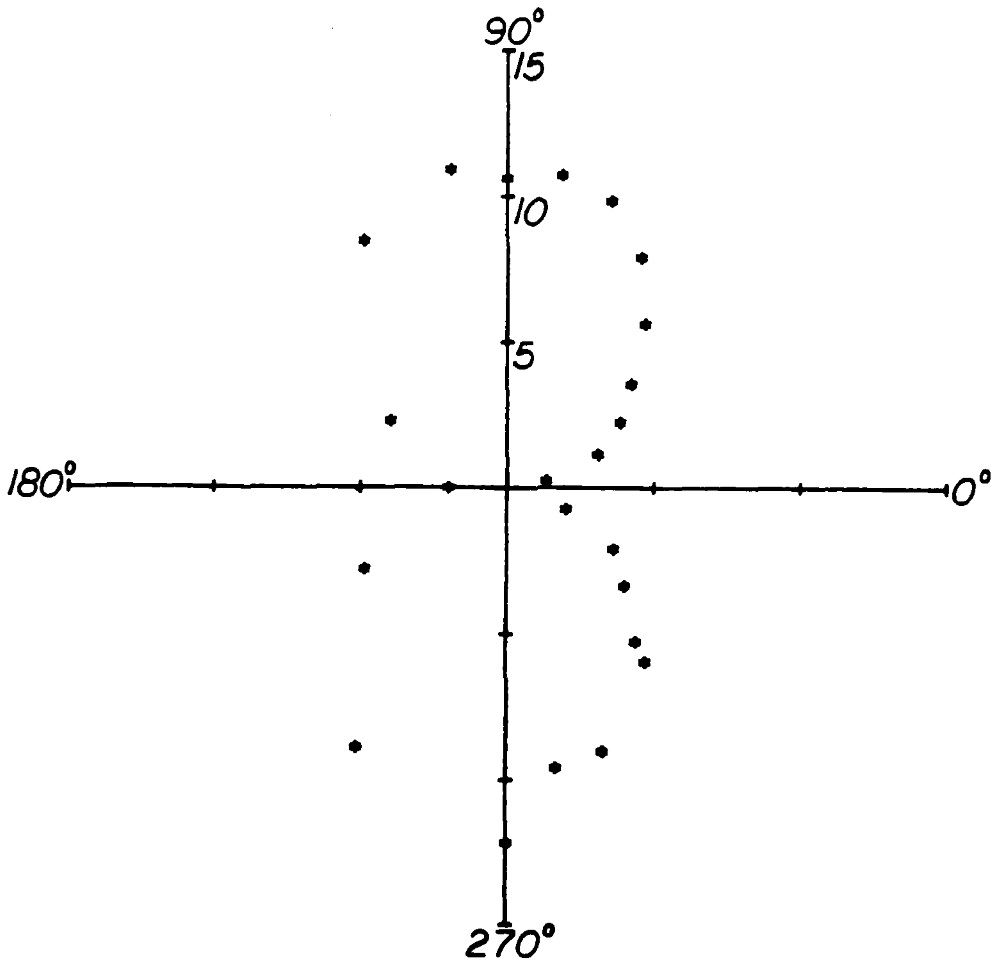

(X E-3 µrad/µPa)

Figure 4.11 Fiber Optic Gradient Hydrophone Directivity Pattern

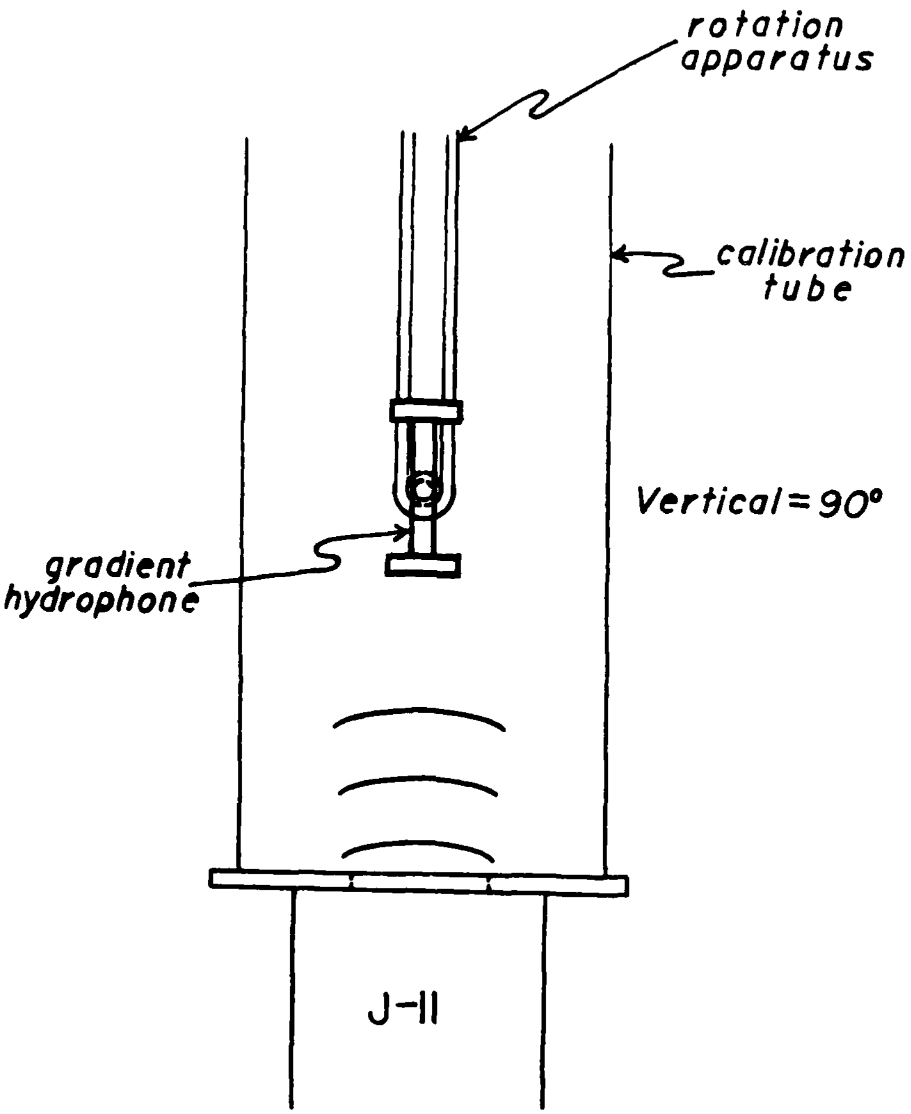

Figure 4.12 Fiber Optic Gradient Hydrophone Position in Calibrator

characteristics. The elastic moduli were determined by exciting the longitudinal, torsional and flexural resonances of the bar made of Stycast 1266 epoxy. These resonances were excited and detected electrodynamically using the technique of Barone and Giacommi [Ref. 13 and 14]. The longitudinal and flexural yielded a Young's modulus (E) of $3.23 \pm 0.10 \times 10^{-9}$ Pa. The torsional mode yielded a shear modulus (G) of 1.16×10^{9} Pa. The standard theory of isotropic elasticity yields from these values a Poisson's ratio (σ) of 0.392 and an average Bulk modulus (B) of 4.78×10^{9} Pa $\pm$ 6.5%.

From the definition of Bulk modulus,

$$B = \Delta P/(\Delta V/V) \tag{4.34}$$

one obtains

$$\Delta V/V = \Delta P/B = 3\Delta \ell/\ell \tag{4.35}$$

where $\Delta \ell$ is the change in any linear dimension ℓ. Therefore, the change in the length of the fiber ($\Delta \ell$) is obtained by rearranging equation (4.36):

$$\Delta \ell = \ell \Delta P/3B \tag{4.36}$$

For a pressure change of 1 Pa and a fiber length of 10 m, the change in length is 0.697 nm. The change in optical phase is calculated using the following equation:

$$\Delta\phi = 2\pi \Delta \ell / \lambda \tag{4.37}$$

The calculated change in phase of the light in the fiber imbedded in the epoxy material is 6.95 X 10^{-3} rad, for a wavelength λ of 632.8 nm. Therefore, the calculated sensitivity of the fiber imbedded in the epoxy material is 6.95 X 10^{-3} μrad/μPa. This value is within approximately 40% of the measured sensitivity for the individual hydrophones. However, this is assuming the fiber is uniformly surrounded by the epoxy. This is not the case, on one surface the epoxy material thickness is small. This may account for the difference between the measured and calculated sensitivities. This shows the epoxy to be an excellent material for ruggedness and support while not degrading the acoustic pressure signal.

Analysis of the single fiber optic hydrophone sensitivity can be compared to published data [Ref. 6 and 8]. From Table V, typical sensitivities are approximately 10^{-2} μrad/μPa for 10 m of fiber. This results in a sensitivity of 10^{-3} μrad/μPa/m which is consistent with earlier obtained results [Ref. 6 and 8]. This yields an increase in sensitivity over a standard directional hydrophone of approximately 14 dB [Ref. 12].

In Section E gradient hydrophone sensitivity was approximately 0.111 μrad/μPa/cm, which compares to Mills value of [Ref. 8].

Using the equipment built by Mills [Ref. 8], an exhaustive data acquisition program was conducted to check for depth dependency of the fiber optic hydrophones in the calibration tube. Appendix C gives a sample of the data taken for a sensitivity run in the short (15.24 cm) calibration tube. The frequency was varied from 100 to 2000 Hz in increments of 50 Hz with the J-11 drive and LC-10 output voltages recorded. The LC-10 output voltage was divided into the LC-10 sensitivity M_{LC-10} times 3.83 radians then plotted against the frequency, Figure 4.13.

This testing was conducted at several depths in the short calibration tube. The data showed no appreciable variation within experimental error other than the slight shifting of the hydrophone resonant frequency.

G. DIFAR SEA TRIAL ANALYSIS

An analysis of the DIFAR data obtained during the sea trial test compares to that published in [Ref. 12]. The DIFAR hydrophone[3] has three piezoelectric receivers encased in it. One is an omni-directional hydrophone. The other two (so called sine and cosine) are bender vane type gradient hydrophones. The sine and cosine each produce a dipole pattern, oriented at 90° to one another.

The sea trial was conducted aboard the R/V Acania in

---

[3]The bender vane transducer was made by Magnavox.

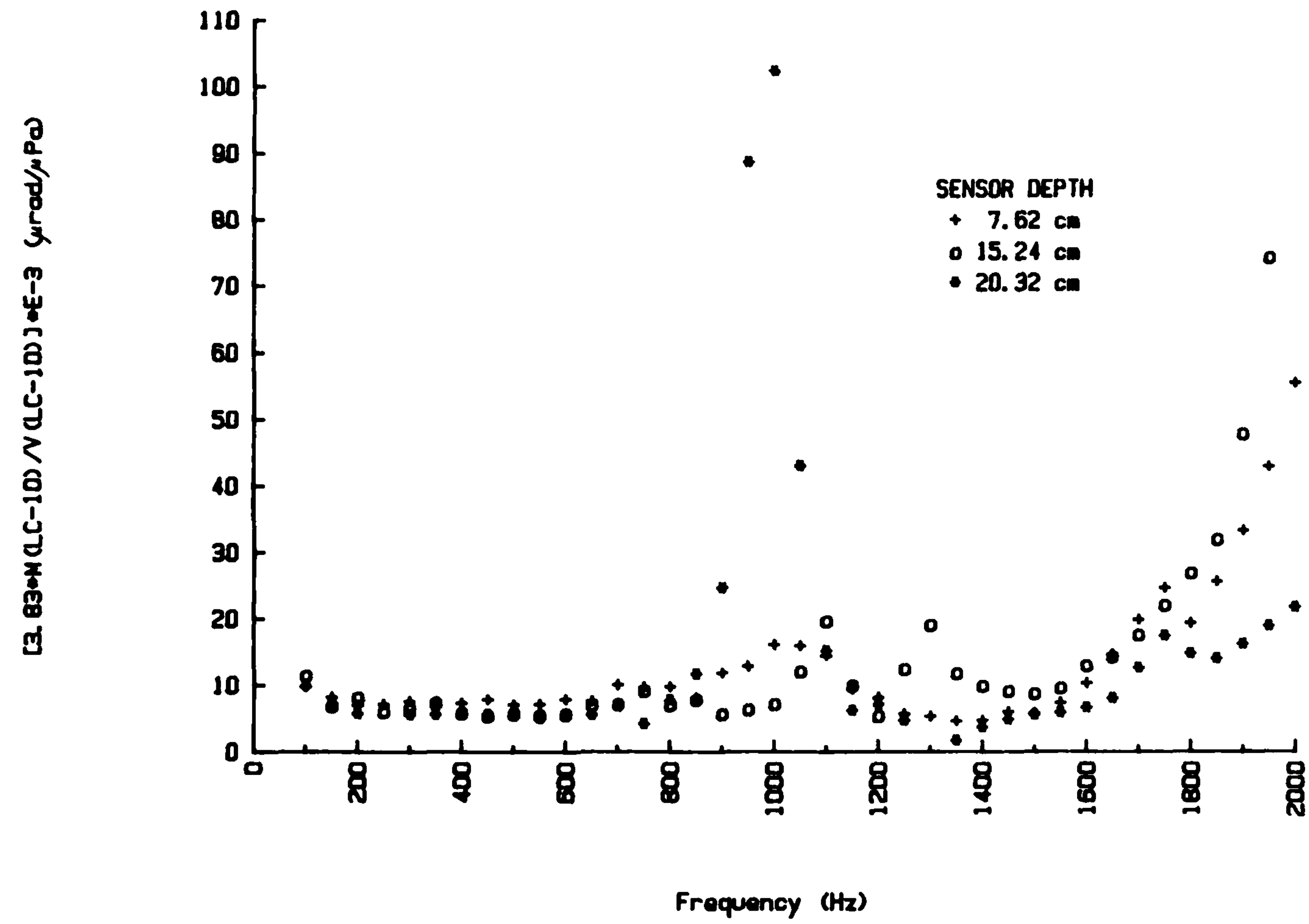

Figure 4.13 Depth Dependency

Monterey Bay, CA. The apparatus was lowered to a depth of 9 m at a location where the bottom was 100 m or greater. The DIFAR hydrophone was mounted on the sea trial apparatus described in Chapter III Section H. Figure 4.14 shows the instrumentation set up used for data acquisition. Appendix D contains a sample of the raw data obtained during the sea trial test.

Data acquisition was restricted to less than 360° for each part of the DIFAR hydrophone, to avoid tangling of the wires from the hydrophones. The system was turned clockwise and counter clockwise to prevent tangling. Figure 4.15 shows the cosine dipole pattern obtained from data at a frequency of 2000 Hz, drive voltage of 7.5 Vac and angle with respect to the J-11 projector. Figure 4.16 shows similar data for the sine dipole pattern at 2000 Hz and 7.0 Vac drive voltage. Figure 4.17 shows the omni data obtained at 500 Hz and 10.0 Vac yielding the expected circular pattern. Data was obtained for 250 Hz, 500 Hz, 1000 Hz and 2000 Hz for all three receivers in the DIFAR hydrophone. These tests established our ability to measure hydrophone characteristics in a sea environment.

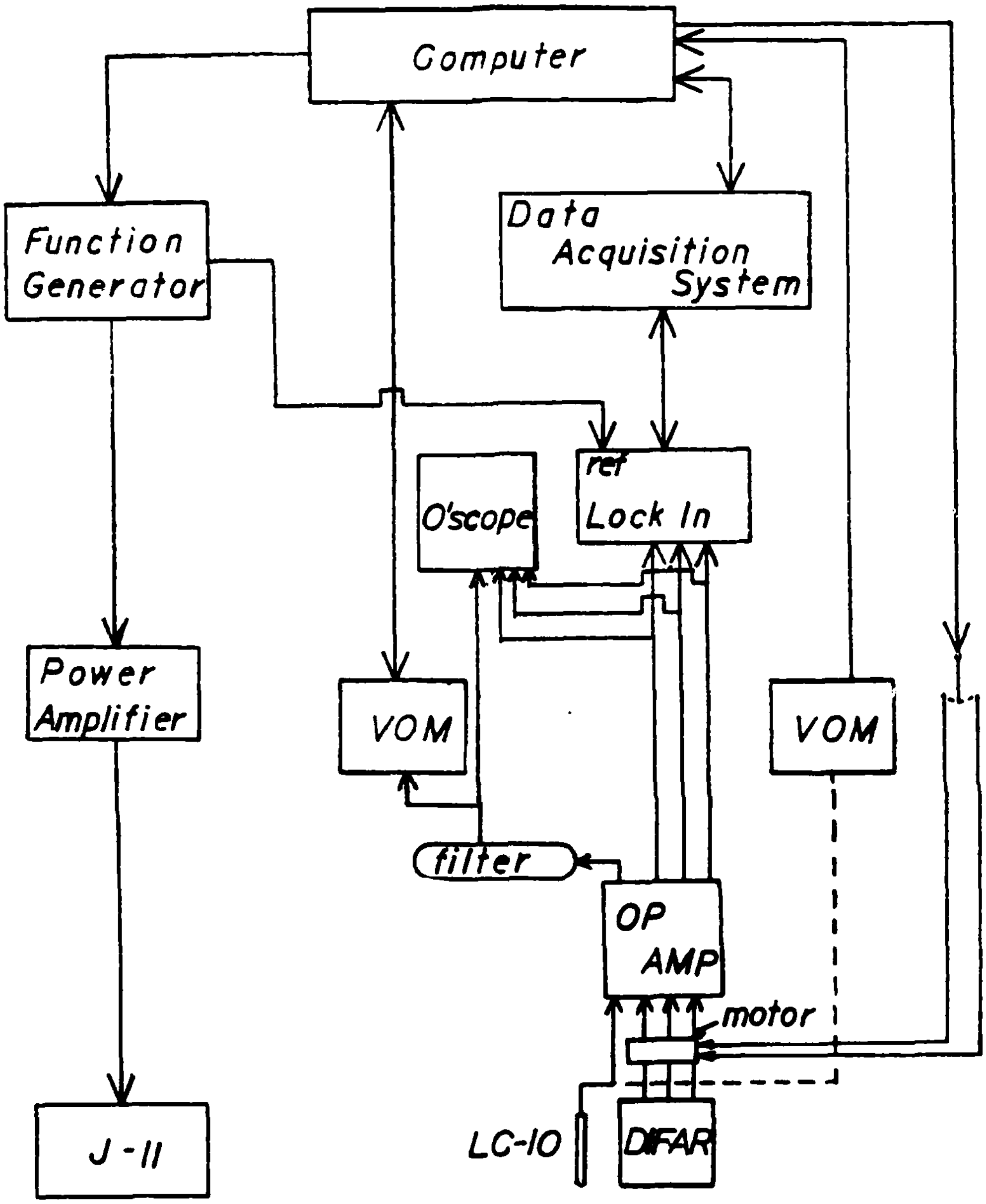

Figure 4.14 Block Diagram of Instrumentation Package

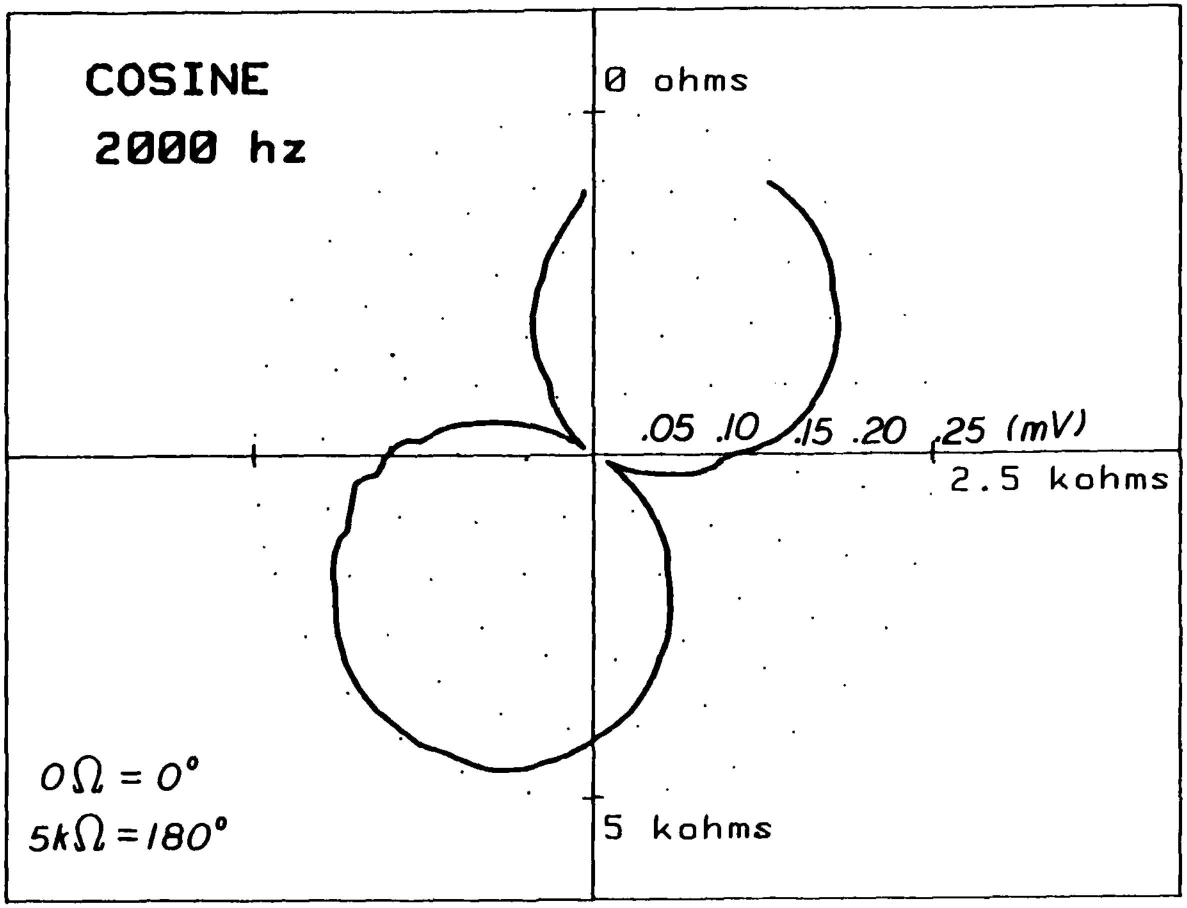

Figure 4.15 DIFAR Cosine Dipole Pattern

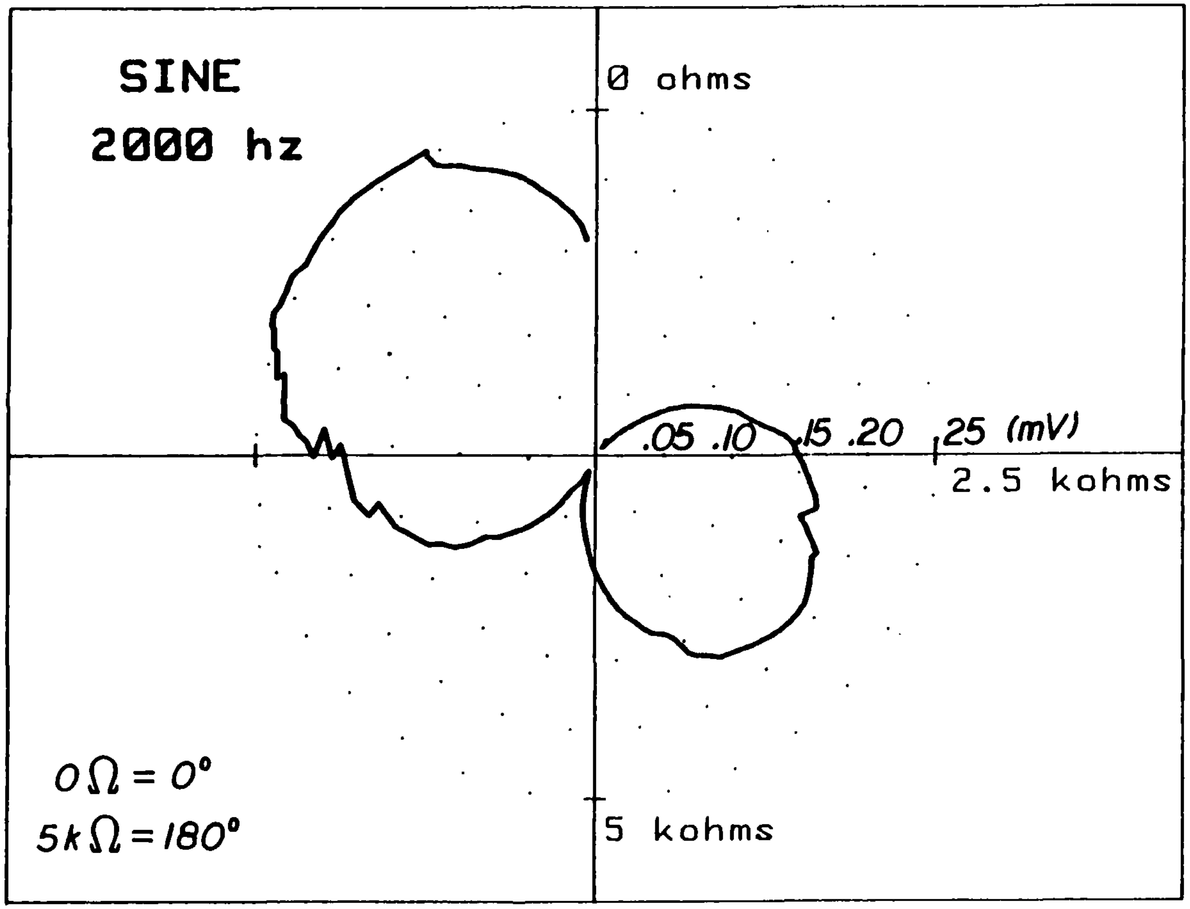

Figure 4.16 DIFAR Sine Dipole Pattern

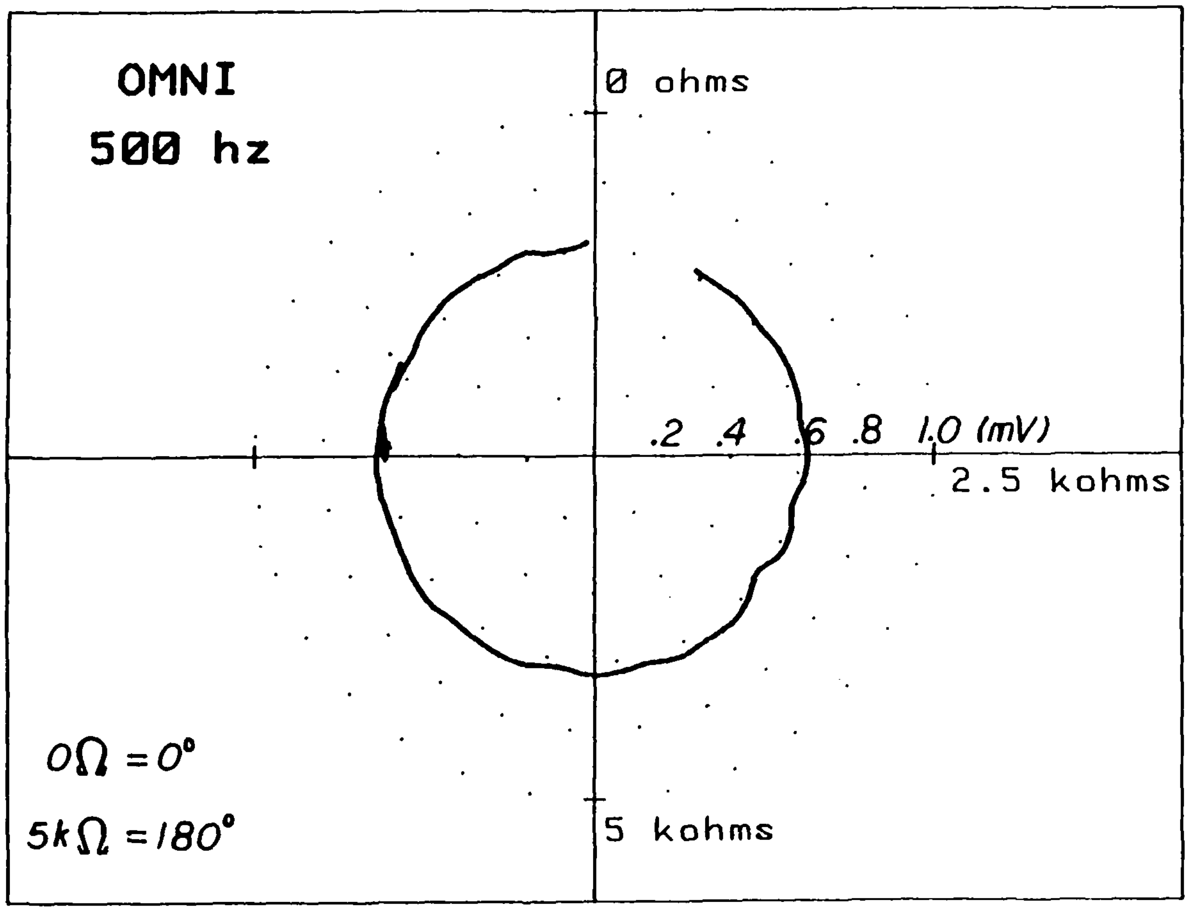

Figure 4.17 DIFAR Omni Dipole Pattern

V. CONCLUSIONS AND RECOMMENDATIONS

Fiber optic sensors have been under consideration, since 1977, for use as hydrophones with higher sensitivity than conventional piezoelectrics. Using sensing coils in both arms of a Mach-Zehnder interferometer, a fiber optic gradient hydrophone was tested and shown to be useable as a directional dipole hydrophone. The sensitivity of the interferometric fiber optic gradient hydrophone compares well with that of a conventional piezoelectric directional hydrophone presently used by the Navy.

The sensitivities of both the individual and gradient hydrophones compared well with earlier published values [Ref. 6 and 8]. This was proven in the laboratory using a calibration tube that allowed the gradient hydrophone to rotate 360°.

An experimental apparatus was designed and constructed that proved to be capable of conducting sea tests of conventional and fiber optic hydrophones. It supports an acoustic driver and hydrophones plus any required electronics, in a watertight cannister.

Further work is required to complete the study begun in this thesis project. This includes testing of the 830 nm dual diode laser gradient hydrophone constructed in this study. An alternative interferometric system should be constructed to decrease the number of fiber to fiber splices (fuses) required. The addition of a polarization controller within the interferometer is recommended, together with some form of passive stabilization. These improved versions of the gradient hydrophone interferometer systems should be tested and compared with DIFAR hydrophones, both in the laboratory and at sea.

APPENDIX A

DATA ACQUISITION PROGRAM

```
10 ! **************************************************
20 ! **************************************************
30 !
40 !
50 ! ****************  OPTICAL HYDROPHONE  ****************
60 ! ****************  COMPARISON  CALIB-  ****************
70 ! ****************   BRATION  PROGRAM   ****************
80 !
85 ! ****************  PROGRAM   "ZERO1C"  ****************
90 !
95 ! **************************************************
97 !
100 ! Revision 1 -  8 Jan 85
101 ! Revision 2 - 10 Jan 85
110 DIM R(150),A(150),X(4),Z(4),A7(64),A8(64),V(64),F(64)
120 INTEGER I,J,K,N
200 ! *** INITIALIZATION ******LIST 1010
204 CLEAR
205 !
210 DISP "This program controls a 3582 Spectrum Analyzer and
a 3325 Signal Source"
220 DISP "to measure the frequency response of a fiber
hydrophone"
230 DISP "by comparison with an LC-10"
240 DISP "Press CONT when ready to start"
250 PAUSE
260 CLEAR
290 !
300 ! Set Sensitivity
301 !
310 CLEAR
320 DISP " SENSITIVITY CODES"
330 DISP "2-30V  5-1000mV  8-30mV"
340 DISP "3-10V  6-300mV   9-10mV"
350 DISP "4- 3V  7-100mV  10- 3mV"
360 DISP " "
370 "Choose CH-A,CH-B Sens."
380 INPUT A1,B1
399 !
400 DISP "Enter initial and final frequencies and step size
in Hz"
410 INPUT F1,F2,F3
415 DISP " "
```

```
420 DISP "Enter maximum drive voltage in millivolts r.m.s."
430 INPUT A9
435 CLEAR
2440 N=INT((F2-F1)/F3)+1
445 IF N>64 THEN GOTO 5100
450 OUTPUT 717 ;"FU1AM1MR"
460 OUTPUT 711  ;"PRS"
470 OUTPUT 711  ;"AS";A1;"BS";B1;"MN1SP10"
480 OUTPUT 711  ;"MD3MP125NU4AV4"
490 OUTPUT 711  ;"SC1"
599 !
600 ! ********************* FREQ. LOOP *********************
601 !
610 FOR I=1 TO N
620 F(I)=F1+(I-1)*F3
630 OUTPUT 717  ;"FR",F(I),"HZ"
640 OUTPUT 711  ;"AD",F(I)
650 GOSUB 1000
660 NEXT I
670 GOTO 2000
999 !
1000 ! *************** BESSEL MAX SUBROUTINE ***************
1001 !
1003 PRINT " "
1006 PRINT "     ";F(I);" Hz DATA"
1007 PRINT " "
1010 PRINT "  J11(mV)     OUT(mV)"
1020 J=1 @ A(1)=D @ R(0)=0 @ R3=0
1030 OUTPUT 717  ;"AM",A(J),"MR"
1040 OUTPUT 711  ;"RE"
1050 WAIT 13000
1080 OUTPUT 711  ;"LMK"
1090 ENTER 711  ; R(J)
1100 PRINT USING 1110 ; A(J),R(J)*1000
1150 IF R(J)>R(J-1) THEN GOTO 1240
1160 IF J<5 THEN GOTO 1210
1170 IF J<N+1 THEN GOTO 1210
1180 IF R(J)>R(J-1) THEN GOTO 1260
1190 GOTO 1300
1210 A(J+1)=A(J)+D
1215 IF A(J+1)>=A9 THEN GOTO 5000
1220 J=J+1
1230 GOTO 1030
1240 IF R3>R(J) THEN GOTO 1260
1245 R3=R(J) @ N1=J @ A2=A(J)
1250 GOTO 1210
1260 PRINT "ERROR-Bessel function not working change drive
     amplitude increment"
1265 PRINT "For Frequency",F(I),"Hz"
1270 goto 660
```

```
1299 !
1300 ! Parabolic Fit
1301 !
1305 B5=(2*(R(N1+2)-R(N1-2))+R(N1+1)-R(N1-1))/10
1310 A4=(2*(R(N1+2)+R(N1-2)-R(N1))-R(N1+1)-R(N1-1))/14
1320 A0=A2-B5/(2*A4)*D
1330 X(1)=INT(1.873*A0)
1340 1(2)=INT(1.977*A0)
1350 X(3)=INT(2.185*A0)
1360 X(4)=INT(2.289*A0)
1399 !
1400 ! ****************** BESSEL  ZERO ******************
1401 X1,X2,Z1,Z2,X3=0
1402 !
1403 DISP " "
1404 DISP " Bessel Zero Loop ";F(I);"Hz"
1405 DISP " J11 at max =";A0;" mV"
1407 DISP " "
1408 DISP " J11(mV)   OUT(mV)  LC10(mV)"
1410 FOR K=1 TO 4
1420 OUTPUT 717  ;"AM";X(K);"MR"
1430 OUTPUT 711  ;"RE"
1440 WAIT 13000
1450 OUTPUT 711  ;"LMK"
1460 ENTER 711  ; Y(K)
1470 OUTPUT 711  ;"IM3AA0B1AV2NU2RE"
1480 WAIT 4500
1490 OUTPUT 711  ;"LMK"
1500 ENTER 711  ; Z(K)
1510 X1=X1+X(K)
1520 X2=X2+X(K)*X(K)
1530 X3=X3+X(K)*Z(K)
1540 Z1=Z1+Z(K)
1550 Z2=Z2+Z(K)*Z(K)
1560 OUTPUT 711  ;"IM1AA1AB0AV4NU4"
1570 DISP USING 1580 ; X(K),1000*Y(K),1000*Z(K)
1580 IMAGE 2X,5D,5X,2D.3D,4X,3D.D
1590 NEXT K
1600 ! Zero crossing calculation STORE "ZERO11"
1610 B=(Y(1)-Y(2))/(X(1)-X(2))
1620 C=Y(1)-B*X(1)
1630 A5=(-C)/B
1640 B=(Y(3)-Y(4))/(X(3)-X(4))
1650 C=Y(4)-B*X(4)
1660 A6=(-C)/B
1670 A7(I)=(A5+A6)/2
1680 A8(I)=(A5-A6)/(2*A7(I))
1700 ! LC-10 L. R. Interpolation
1710 ! V(LC-10)=M*A7 + P
1720 M=(X3-X1*Z1/4)/(X2-X1*X1/4)
```

```
1730 P=Z1/4-M*X1/4
1740 V(I)=M*A7(I)+P
1741 R2=(X3-X1*Z1/4)^2/((X2-X1*X1/4)*(Z2-Z1*Z1/4))
1742 R1=SQR(R2)
1750 DISP " "
1760 DISP "Fiber zero when drive"
1763 DISP A7(I);"mV +-";100*A8(I);"%"
1770 DISP "LC-10 zero  ";1000*V(I);"mV"
1780 DISP "r=";R1
1790 COPY
1800 RETURN
1999 !
2000 ! **************** OUTPUT AND DISPLAY ****************
2010 !
2020 PRINT "  Freq   J-11   LC-10   ERROR(%)"
2030 FOR I=1 TO N
2040 PRINT USING 2050 ; F(I),A7(I),1000*V(I),100*A8(I)
2050 IMAGE 2X,4D,2X,5D,2X,4D.D,4X,M3D.2D
2060 NEXT I
3000 END
4997 !
4998 ! ******************** ERROR TRAPS ********************
4999 !
5000 DISP "Required drive voltage exceeds ";a9;" mV"
5010 I=I+1 @ GOTO 620
5100 DISP "Program will only make measurements at 64
     frequencies"
5110 GOTO 400
6000 END
```

APPENDIX B

RAW DATA FOR SINGLE FIBER OPTIC HYDROPHONE AT 517 HZ

J-11 Drive Voltage (mV)	Fundamental (mV)	1^{st} Harmonic (mV)	LC-10 (mV)
100	0.717	0.065	0.646
200	1.35	0.243	1.29
300	1.63	0.406	1.92
400	1.75	0.530	2.55
500	2.00	0.680	3.17
600	2.14	0.844	3.77
700	2.17	1.04	4.38
800	1.92	1.17	4.97
900	1.83	1.36	5.56
1000	1.54	1.43	6.14
1100	1.15	1.44	6.76
1200	0.723	1.42	7.36
1300	0.364	1.39	7.95
1400	0.176	1.16	8.53
1500	0.460	1.01	9.12
1600	0.842	0.730	9.71
1700	0.957	0.470	10.3
1800	1.12	0.211	10.8
1900	1.14	0.064	11.4
2000	1.24	0.333	12.0
	Second Run of Data		
1500	0.407	0.959	9.12
1490	0.382	1.10	9.06
1480	0.343	1.10	9.01
1470	0.309	1.15	8.95
1460	0.266	1.08	8.89
1450	0.214	1.04	8.84
1440	0.189	1.05	8.78
1430	0.149	1.07	8.72
1420	0.110	1.16	8.65
1410	0.099	1.23	8.60
1400	0.078	1.34	8.54
1390	0.068	1.37	8.48
1380	0.081	1.50	8.42
1350	0.183	1.44	8.25
1300	0.398	1.48	7.95

J-11 Drive Voltage (mV)	Fundamental (mV)	1^{st} Harmonic (mV)	LC-10 (mV)
1200	0.830	1.72	7.36
1100	1.25	1.75	6.77
1000	1.60	1.73	6.16
900	2.05	1.66	5.58
800	2.20	1.49	4.97
700	2.34	1.28	4.38
600	2.23	1.10	3.77
500	2.33	0.969	3.16
400	2.04	0.751	2.54
300	1.98	0.550	1.91
200	1.58	0.316	1.28
100	0.787	0.084	0.647

Third Run

650	2.41	1.28	4.08
1390	0.135	1.90	8.47
1385	0.091	1.45	8.43
1380	0.114	1.49	8.40
1395	0.115	1.68	8.49
1390	0.069	1.55	8.46
1387	0.106	1.61	8.44
1392	0.103	1.67	8.47
1390	0.073	1.76	8.45

APPENDIX C

DEPTH DEPENDENCY DATA

Frequency (Hz)	J-11 drive voltage (mV)	LC-10 output voltage (mV)	% Error	$\frac{3.83 \cdot M_{LC-10}}{V_{LC-10}}$ µrad/µPa X 10^{-3}
100	1693	13.4	0.21	9.91
150	2120	19.0	5.18	6.99
200	2356	23.1	1.15	5.74
250	365	3.9	*322.31	34.05
300	2173	23.9	0.50	5.56
350	1941	22.1	1.51	5.61
400	1919	23.5	0.16	5.65
450	1705	23.8	0.61	5.58
500	1476	24.7	1.09	5.38
550	1112	26.3	0.85	5.05
600	679	24.7	0.93	5.38
650	533	24.0	0.10	5.53
700	1009	19.5	0.50	6.81
750	3387	31.7	2.24	4.19
800	3158	17.2	0.49	7.72
850	3395	11.4	1.30	11.65
900	2804	5.4	0.88	24.59
950	1539	1.5	2.16	88.53
1000	1340	1.3	1.06	102.15
1050	1256	3.1	10.31	42.84
1100	1511	8.8	0.36	15.09
1150	4773	21.5	0.26	6.18
1200	6127	18.8	1.43	7.06
1250	4328	28.6	4.38	4.64
1300	13150	87.8	*41.16	1.51
1350	18216	77.7	1.89	1.71
1400	11256	36.0	2.18	3.69
1450	10521	27.2	2.13	4.88
1500	10876	23.9	0.83	5.56
1550	11796	22.5	0.47	5.90
1600	11801	20.0	0.64	6.64
1650	10506	16.5	0.74	8.05
1700	8410	10.5	0.90	12.65
1750	10903	7.6	0.28	17.47
1800	9883	9.0	12.99	14.76
1850	8359	9.5	0.25	13.98
1900	8359	8.2	1.73	16.19
1950	6700	7.0	1.35	18.97
2000	5402	6.1	0.10	21.77

* Data has high % error therefore is discounted as true data

APPENDIX D

DIFAR SEA TRIAL DATA

Angle (degree)	Vpar X 10^{-1} (Vac)	Vdmm X 10^{-2} (Vac)
34	2.5855	2.5518
37	2.5800	2.5762
39	2.5759	2.5356
42	2.5614	2.3631
44	2.5430	2.2685
47	2.5152	2.3035
50	2.4811	2.4444
52	2.4463	2.5255
55	2.4053	2.5705
57	2.3487	2.5450
60	2.3044	2.4248
63	2.2463	2.3535
65	2.1829	2.2920
68	2.1207	2.2588
70	2.0603	2.2561
73	1.9841	2.3169
76	1.9018	2.4726
78	1.8226	2.5412
81	1.7338	2.4644
84	1.6397	2.5959
86	1.5378	2.4394
89	1.4508	2.2726
92	1.3580	2.2293
94	1.2579	2.4073
97	1.1667	2.5276
100	1.0614	2.3952
102	0.9529	2.4216
105	0.8445	2.4665
108	0.7432	2.5002
111	0.6283	2.4811
113	0.5103	2.3950
114	0.3910	2.4176
117	0.2769	2.8816
120	0.1597	2.1926
122	0.0654	2.3710
125	0.0656	2.4448
128	0.1632	2.4172
130	0.2641	2.2845
133	0.3305	2.5773
135	0.3953	2.5712

Angle (degree)	Vpar X 10^{-1} (Vac)	Vdmm X 10^{-2} (Vac)
138	0.5019	2.2253
140	0.6136	2.6355
143	0.6197	2.8091
147	0.6118	2.2455
151	0.7150	2.3271
153	0.8833	2.3936
154	1.0601	2.3988
156	1.1816	2.3392
159	1.2892	2.6026
164	1.3784	2.3678
164	1.5082	2.4604
166	1.6446	2.5369
169	1.7541	2.4270
172	1.8360	2.2392
174	1.9245	2.2375
177	1.9578	2.2886
179	2.0334	2.2792
182	2.1058	2.3618
185	2.1848	2.5467
187	2.2577	2.6160
190	2.3074	2.6118
192	2.3525	2.5841
196	2.4034	2.5713
199	2.4412	2.5535
200	2.4582	2.5307
204	2.4780	2.4681
206	2.4899	2.3146
208	2.4968	2.2189
211	2.5006	2.2212
216	2.4959	2.2982
217	2.4917	2.4848
219	2.4746	2.4809
221	2.4615	2.5169
224	2.4466	2.5603
227	2.4379	2.4671
231	2.4134	2.3593
233	2.3780	2.2976
235	2.3359	2.3100
237	2.2870	2.3595
240	2.2356	2.4043
242	2.1891	2.4694
247	2.1350	2.5000
250	2.0862	2.5400
252	2.0235	2.5616
254	1.8590	2.3225
259	1.7992	2.3441
261	1.7480	2.1585
263	1.6842	2.2635

Angle (degree)	Vpar X 10^{-1} (Vac)	Vdmm X 10^{-2} (Vac)
265	1.6061	2.4839
269	1.5249	2.5305
273	1.4551	2.5579
274	1.3735	2.5136
274	1.2953	2.3275
277	1.2037	2.1840
279	1.1103	2.1804
282	1.0043	2.2864
284	0.8929	2.4969
287	0.7956	2.5444
289	0.6875	2.5562
292	0.5774	2.4960
295	0.4654	2.3609
297	0.3623	2.3682
299	0.2495	2.4472
302	0.1347	2.5203
304	0.0364	2.5806
307	0.1016	2.6130
310	0.2158	2.4719
312	0.3325	2.2114
315	0.4497	2.1667
319	0.5540	2.2376
326	0.6620	2.4356
327	0.7702	2.5362
328	0.9475	2.4494
330	1.0429	2.3248
332	1.1364	2.2500
334	1.2390	2.3217
336	1.3294	2.4754
338	1.4261	2.4588
341	1.5142	2.5328
343	1.6001	2.5509
346	1.7350	2.3981
351	1.8793	2.3582
354	1.9975	2.4171
356	2.0864	2.3755
358	2.1438	2.5116

Cosine 1000B run

1. Spectrum Analyzer setting 250 mVac
2. Time Constant 1000 msec
3. J-11 Drive voltage 5 Vac

LIST OF REFERENCES

1. Barnoski, M. K., Fundamentals of Optical Fiber Communications, Academic Press, New York, 1981.

2. Bucaro, J. A., Lagakos, N., Cole J. H., and Giallorenzi, T. G., "fiber Optic Acoustic Transduction", Physical Acoustics Volume XVI, edited by Mason, W. P., Thurston, R. N., p. 385, Academic Press, New York, 1982.

3. Suematsu, Y. and Iga, K., Introduction to Optical Fiber Communications, John Wiley and Sons, New York, 1982.

4. Giallorenzi, T. G., Bucaro, J. A., Dandridge, A., Sigel, G. H., Cole, J. H., Rasleigh, S. C., and Priest, R. C., "Optical Fiber Sensor Technology", IEEE Journal of Quantum Electronics, v. QE-18, p. 626, 1982.

5. Bucaro, J. A., Dardy, H. D., and Carome, E. F., "Fiber-Optic Detection of Sound", Journal of the Acoustical Society of America, v. 62, p. 1302, 1977.

6. Cole, J. H., Johnson, R. L., and Bhuta, P. G., "Fiber-Optic Detection of Sound", Journal of the Acoustical Society of America, v. 62, p. 1136, 1977.

7. Davis, C. M., and others, Fiberoptic Sensor Technology Handbook, Dynamic Systems, Inc., McLean, Va., 1982.

8. Mills, G. B., Fiber Optic Gradient Hydrophone, Master's Thesis, Naval Postgraduate School, Monterey, Ca, 1984.

9. Mills, G. B., Garrett, S. L., and Carome, E. F., "Fiber Optic Gradient Hydrophone", Proceedings Society of Photo-Optical Instrumentation Engineers, v. 478, p.98, May 1984.

10. Underwater Electroacoustic Standard Transducer Catalogue, Underwater Sound Reference Detachment, Naval Research Laboratory, 1982.

11. Lefevre, H. C., "Single-Mode Fiber Fractional Wave Devices and Polarization Controllers", Electronics Letters, v. 16, p. 778, 1980.

12. Naval Research Laboratory Report 4360, Calibration of Magnavox Bender Vane Tranducers, by Underwater Sound Reference Division, May 1977.

13. Barone, A., and Gaicommi, A., Acustica, v. 4, p. 182, 1954.

14. Pollard, H. F., Sound Waves in Solids, Pion Limited, London, p. 151, 1977.

BIBLIOGRAPHY

Kinsler, L.E., Frey, A.P., Coppens, A.B., Sanders, J.V., Fundamentals of Acoustics, Wiley, New York, 1982.

Urick, M. H., Principles of Underwater Sound, McGraw-Hill, New York, 1975.

Weik, M. H., Communications Standard Dictionary, Van Nostrand Reinhold, New York, 1983.

INITIAL DISTRIBUTION LIST

		No. Copies
1.	Defense Technical Information Center Cameron Station Alexandra, VA 22314	2
2.	Library, Code 0142 Naval Postgraduate School Monterey, CA 93943	2
3.	Prof. E. F. Carome Department of Physics (code 61 Cm) Naval Postgraduate School Monterey, CA 93943	5
4.	Prof. S. L. Garrett Department of Physics (code 61 Gx) Naval Postgraduate School Monterey, CA 93943	6
5.	Dr. L. E. Hargrove Physics Division (code 412) Office of Naval Research 800 N. Quincey St. Arlington, VA 22217	1
6.	LT G. E. MacDonald PATWING ONE DET KADENA FPO Seattle 98770-0055	3
7.	Mr. & Mrs. G. E. MacDonald 5413 Inglewood Dr. Corpus Christi, TX 78415	1
8.	Dr. J. A. Bucaro Naval Research Laboratory Code 5130 Washington D.C. 20375	1
9.	CDR Robert Yelberton Naval Electronics Systems Command PDE 120-113 Washington D.C. 20363	1
10.	LCDR G. B. Mills 95 Osprey Dr. Groton, CT 06340	1

11. Manager ASWSP 2
PM-4
ATTN: Project Ariadne, CDR K. Evans & Dr. G Hetland
Dept. of Navy
Washington, D.C. 20362

12. LCDR J. Bulter 1
C/O Physics Dept. Code 61
Naval Postgraduate School
Monterey, CA 93943

13. LT P. Feldmann 1
C/O Physics Dept. Code 61
Naval Postgraduate School
Monterey, CA 93943

14. LCDR J. Long 1
Code 331
Naval Postgraduate School
Monterey, CA 93943

15. Prof. J. V. Sanders 1
Physics Department, Code 61Sd
Naval Postgraduate School
Monterey, CA 93943

16. Prof. R. N. Forrest 1
Code 71
Naval Postgraduate School
Monterey, CA 93943

END

FILMED

8-85

DTIC